UNIVERSITÀ DEGLI STUDI DI GENOVA

XXX Cycle

PhD in Clinical and Experimental Immunology

(PhD School in Biomedical Sciences)

IDENTIFICATION AND FUNCTIONAL CHARACTERISATION OF A NOVEL NKp44 SOLUBLE LIGAND

PhD student: Silvia Gaggero

Tutor: Prof. Claudia Cantoni

INDEX

1. INTRODUCTION

1.1. NATURAL KILLER CELLS

Natural Killer (NK) cells were first described in 1975 (1–3) and were named based on their description as cytolytic effector immune cells, which can rapidly induce the death of tumour and virus-infected cells in the absence of a prior specific immunization. NK cells are large granular cells classified as lymphocytes based on their morphology, surface markers, and origin from a Common Lymphoid Progenitor (CLP) (4–6). In particular, NK cells belong to the expanding family of Innate Lymphoid Cells (ILCs): based on their cytokine and transcription factor expression, NK cells are classified as ILC1, a group composed of T-bet-expressing cells, such as liver, thymic, and intraepithelial ILC1, able to release type 1 cytokines (7,8). Unlike T and B lymphocytes, NK cells components of the innate immune system because of the lack of antigen and clonal specificity and of long-lived memory. However, recent findings demonstrated that NK cells display some of the features typical of adaptive immunity, thus collocating them at the boundary between adaptive and innate immunity (9,10). NK cells can be found not only in the blood stream but also in lymphoid organs and in non-lymphoid peripheral tissues (5,11–14). The few reports of complete NK cell deficiencies in humans, resulting in uncontrollable fatal infections during childhood (15,16), support the notion of NK cell importance in host defence, especially in the early control against viral infection and in tumour immunosurveillance. Moreover, the presence of NK cells in other mammals and of NK cell orthologues in different vertebrates (i.e. fish, amphibians, and chicken) (17), as well as the particular role that NK cells exert in the uterus during pregnancy (18–20), argue for their importance and for their positive selection during evolution.

1.1.1. NK cell populations

NK cells constitute one of the three major lymphocyte subsets (i.e. B cells, T cells, and NK cells), since they represent approximately 10–15% of lymphocytes in peripheral blood. However, NK cells can also be found in lymphoid organs and non-lymphoid peripheral tissues (i.e. liver, lung, omentum, intestine, and placenta), where in the last years, an increasing number of unique and tissue-specific NK cell populations has been characterised (5,6,11–14).

$CD56^{bright}$ and $CD56^{dim}$ NK cell subsets

The first and better characterised NK cell subsets were those characterised by the $CD56^{bright}$ or $CD56^{dim}$ phenotype (4,6,21,22). CD56 is a glycoprotein belonging to Neural Cell Adhesion Molecule (NCAM) family, probably involved in mediating NK interactions with other cells, and was recently shown to be implicated in pathogen recognition (23). Early studies on NK cells described CD56 molecule as a marker

allowing the identification of mature NK cells, based on its cell surface density which correlates with the expression of other surface molecules responsible for the different phenotype, tissue localisation, and functions characterising $CD56^{bright}CD94/NKG2A^{+}CD16^{-}KIR^{-}$ and $CD56^{dim}CD94/NKG2A^{+/-}CD16^{+}KIR^{+}$ NK cell subsets (Fig. 1) (4,6,21,22). The different expression pattern of cell surface molecules involved in NK cell trafficking, suggests that $CD56^{bright}$ and $CD56^{dim}$ NK cells likely migrate to distinct sites *in vivo*: indeed, $CD56^{bright}$ NK cells represent only 10% of circulating NK cells, but they are enriched up to 90% in secondary lymphoid organs and in non-lymphoid tissues. Conversely, $CD56^{dim}$ NK cells largely predominate in peripheral blood and are poorly represented in other tissues (4,6,21,22). These differences result in the release of distinct cytokines, and in dissimilar cytotoxic and proliferating capabilities: in particular, up to recent years, the existence of a clear functional distinction between cytokine-releasing $CD56^{bright}$ and cytotoxic $CD56^{dim}$ NK cells was a general belief. However, recent studies showed that also $CD56^{dim}$ cells can release high amounts of cytokines but preferably upon contact with target cells, instead of in response to soluble factors as for $CD56^{bright}$ NK cells (24,25). Moreover, $CD56^{dim}$ and $CD56^{bright}$ NK cells display a different cytokine release kinetics, since interferon (IFN)-γ secretion by $CD56^{dim}$ NK cells occurs only at early times (2 to 4 h) upon cell stimulation, whereas IFN-γ release by $CD56^{bright}$ NK cells is more delayed (26).

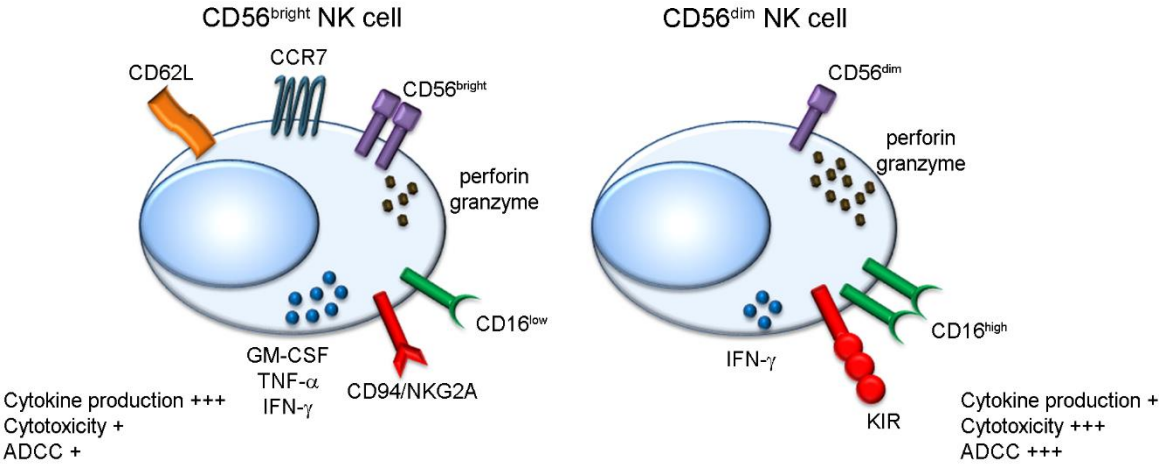

Figure 1. $CD56^{bright}$ and $CD56^{dim}$ NK cell subsets
Mature NK cells can be divided in two main cell subsets based on CD56 cell surface expression levels. Here the main surface markers, released cytokines, and effector functions of $CD56^{bright}$ and $CD56^{dim}$ NK cells are summarised. Adapted from (27).

Decidua-resident NK cells

Decidua-resident NK (dNK) cells are one of the most studied tissue-resident NK cell subsets: they derive from a $CD34^{+}$ progenitor in the uterus or from peripheral NK cells (pNK) acquiring the dNK cell phenotype ($CD56^{bright}CD16^{-}KIR^{+}$) when exposed to Transforming Growth Factor (TGF)-β, hypoxia, or demethylating agents. dNK cells represent up to 50-90% of lymphoid cells during the first trimester of pregnancy and are responsible for the production of cytokines, chemokines, and angiogenic factors (18–20). It is important to note that some activating NK cell receptors (NKp44, NKp46, DNAX Accessory

Molecule-1 (DNAM-1), and NKG2D) can recognise ligands expressed on human trophoblast: such interaction results in the triggering of cytokine release, but not in the induction of cytotoxic activity (28). Collectively, all dNK cell-derived soluble factors mediate key physiological processes required for successful pregnancy, such as regulating placentation and vascular remodelling of spiral arteries, and creating an immunosuppressive microenvironment able to allow the presence of a semi-allogeneic foetus. Importantly, dNK cells contribute to immunosuppression both through TGF-β release and through the interaction with decidual $CD14^+$ monocytes, able to induce the differentiation of regulatory T lymphocytes (Treg) (29). Interestingly, it has been shown that dNK cell dysfunction can be associated to unsuccessful pregnancy (18–20).

1.1.2. NK cell functions

Immunoregulatory functions

NK cells can regulate both innate and adaptive immune responses through the interaction with different immune cell types, including neutrophils, basophils, macrophages, Dendritic Cells (DCs), and T lymphocytes. Such immunoregulatory interactions, mediated by both cytokine secretion and cell-to-cell contacts, contribute to NK cell antimicrobial and anti-tumour functions (6,21,22,30).

In response to cytokines, $CD56^{bright}$ NK cells are primarily able to produce cytokines, such as IFN-γ, Tumour Necrosis Factor (TNF)-α, TNF-β, IL-10, IL-13, Granulocyte Macrophage-Colony Stimulating Factor (GM-CSF), and several chemokines. Since during infections NK cells are activated earlier than T cells, IFN-γ produced by NK cells is essential during the first phases of the immune response: IFN-γ is involved in macrophage activation, T cell polarization towards T_H1 response, and enhancement of antigen presentation through the up-regulation of Human Leukocyte Antigen (HLA) class I and class II molecules. NK cells also release chemokines, such as CXCL12, CCL3, CCL4, and CCL5, that recruit immune cells in the site of inflammation, whereas GM-CSF induces haematopoiesis and DC maturation (6,21,30).

One of the most studied NK cell interactions is the NK-DC bidirectional crosstalk that can occur in the periphery or in secondary lymphoid tissues, and results in DC-induced NK cell proliferation, NK cell-dependent DC maturation, and NK cell-mediated killing of immature DCs (iDCs) (30–33). DCs, undergoing maturation following antigen uptake, release cytokines that induce NK cell proliferation, cytotoxicity, and IFN-γ release. Both iDCs and mature DCs (mDCs) express ligands recognised by activating NK cell receptors, such as NKp30 and DNAM-1, and able to induce both IFN-γ secretion and killing of iDCs which failed to up-regulate HLA-I expression. This editing process allows the survival only of mDCs able to efficiently induce T_{H1} response (30–33).

As far as NK-neutrophil interaction is concerned, neutrophils can modulate NK cell survival, proliferation, cytotoxicity, and cytokine release; on the other hand, NK cells release IFN-γ and GM-CSF,

promoting neutrophil survival and Reactive Oxygen Species (ROS) production during early inflammation; moreover, NK cells can turn down neutrophil response by inducing apoptosis through an NKp46- and Fas-dependent mechanism (34,35). NK cells also interact with eosinophils: following direct contact with these cells, NK cells release higher IFN-γ amounts, kill tumour cells more efficiently, and promote adaptive immune responses through the DC editing process. In turn, NK cells induce the acquisition of an Antigen Presenting Cells (APC)-like phenotype in eosinophils that up-regulate HLA-I and -II molecules; however, NK cells can also kill eosinophils, suggesting a role for NK cells in dampening eosinophil-mediated immune response (36). The immunoregulatory role of NK cells has been investigated also in the context of NK-macrophage crosstalk. M1-polarised macrophages release IL-12, which stimulates IFN-γ production by NK cells and, in turn, NK cell-derived IFN-γ induces IL-12 release by macrophages. These effects are mediated both by cell-to-cell contact and by M1-derived IL-18. IL-12-activated NK cells acquire the ability to kill M0 unpolarised and M2-polarised macrophages: these cells, similarly to Tumour Associated Macrophages (TAMs), are unable to release IL-12, thus they do not activate NK cell functions (37).

NK cells can also interact with different non immune cell types: several studies analysed the interaction between Mesenchymal Stem Cells (MSCs) and NK cells. MSCs can inhibit NK cell proliferation through the release of soluble factors, whereas the impairment of NK cell-mediated cytotoxicity and cytokine release also requires cell-to-cell contact. It has been shown that both indoleamine 2,3-dioxygenase (IDO) and prostaglandin E2 (PGE2), expressed/produced by MSCs, are involved in the inhibition of NK cell proliferation, while PGE2 and soluble HLA-G play a role in the impairment of NK cell cytotoxicity. In addition, MSCs have been reported to inhibit the expression of NKp44, NKp30, and NKG2D activating receptors, thus affecting NK cell activation (38).

Cytotoxic activity

While $CD56^{bright}$ NK cells play an important immunoregulatory role, they are less effective mediators of cytotoxicity, as compared to $CD56^{dim}$ NK cells, which express higher levels of granzymes, perforin, CD16, and receptors involved in the induction of natural cytotoxicity. In the presence of target cells, NK cells can mediate two different types of cytotoxic activity: Antibody-Dependent Cell-mediated Cytotoxicity (ADCC) and natural cytotoxicity. ADCC is strictly dependent on CD16 receptor (FcγRIII), which binds the Fc portion of IgG on opsonised targets (4,6,21,22,24,27). Differently, natural cytotoxicity is finely tuned by a series of activating and inhibitory receptors expressed on NK cells and able to interact with their respective ligands on target cells. Early studies on NK cell functions suggested the ability of these cells to recognise and kill autologous cells lacking the expression of HLA-I, a class of self-molecules normally expressed on all human cells but often down-regulated by tumour and virus-infected cells in order to avoid T cell-mediated recognition. Following these observations, Kärre et al. proposed the “missing-self hypothesis”, according to which the absence of inhibitory signals

transduced by receptors recognising HLA-I molecules results in the induction of target cell killing (39). Subsequent studies revealed a more complex regulation, since the induction of NK cell cytotoxicity not only requires the absence or the partial loss of inhibitory signals, but also the transduction of activating signals (overcoming the inhibitory ones), mediated by the interaction of activating receptors with their respective ligands on target cells (25).

The main effector molecules involved in NK cell-mediated cytotoxicity are perforin and granzymes: perforin creates pores in the phospholipid bilayer of target cells, facilitating the entry of granzymes, a family of serine proteases located in cytolytic granules of cytotoxic T and NK cells. Granzyme B can mediate caspase cleavage and activation, resulting in the induction of cell death by apoptosis (40).

1.1.3. NK cell receptors

Activating and inhibitory receptors involved in the regulation of cytotoxic activity can be primarily divided in two classes based on their ligands: receptors recognising HLA-I molecules and receptors specific for non-HLA ligands.

HLA-I specific receptors

Killer Immunoglobulin-like Receptors (KIRs)

The most important HLA-I-specific receptors are Killer Immunoglobulin-like Receptors (KIRs), a family of highly polymorphic receptors recognising HLA-A, -B, and -C molecules (25,39,41). KIRs are sets of paired inhibitory (iKIRs) and activating (aKIRs) receptors characterised by either two (KIR2D) or three Ig-like (KIR3D) extracellular domains and a cytoplasmic tail that defines their functional properties. In particular, iKIRs display a long cytoplasmic tail (KIR2DL and KIR3DL) containing an Immunoreceptor Tyrosine-based Inhibition Motif (ITIM) sequence, whose phosphorylation upon receptor engagement results in the recruitment of phosphatases able to dampen early activation signals derived by activating receptors. aKIRs share the same structure of iKIRs, but are characterised by a short cytoplasmic tail (KIR2DS and KIR3DS) that associates with DNAX-activation protein (DAP) 12, an adaptor protein bearing Immunoreceptor Tyrosine-based Activation Motif (ITAM) sequences, necessary for the transduction of activating signals (25,42,43). KIRs allow NK cells to sense target cells with absent or reduced expression of HLA-I, therefore complementing T cell surveillance directed towards HLA-I-expressing cells: each KIR recognises epitopes shared within a group of HLA-I alleles; nevertheless, it has been observed that for many HLA-I alleles there is no corresponding KIR, while, on the other hand, some KIR ligands are still elusive, especially in the case of aKIR ligands (44–46). Curiously, KIRs do not necessarily recognise only HLA-I molecules: increasing evidence suggests that some aKIRs are also able to detect viral peptides, presented by HLA-I, and CpG oligodeoxynucleotides (ODNs): these

observations suggest that KIRs can act as sensors for changes in peptidome and microbial products during viral infection (45,47,48).

KIRs are clonally distributed within the NK cell population; indeed, NK cells can express one to eight different activating or inhibitory KIRs, depending on a stochastic process involving DNA silencing and DNA methylation of KIR genes (44,49,50). Since KIRs are clonally expressed on NK cells, and KIR and HLA genes are independently inherited, not all NK cells display an inhibitory receptor recognising self-HLA-I molecules: this situation could potentially result in the presence of a subset of autoreactive NK cells. However, it has been observed that NK cells expressing inhibitory KIRs for self-HLA-I are more responsive than potentially autoreactive cells: this observation led to the concept of NK cell education or licensing (49,50).

NKG2 receptor family

NK cells are also able to assess the overall expression levels of HLA molecules through the interaction between receptors belonging to the NKG2 family and the non-classical HLA-I molecule HLA-E. HLA-E presents peptides deriving from the leader sequences of classical HLA-I molecules; therefore, its expression levels reflect those of all the other classical HLA-I molecules (51,52). NKG2 receptor family includes five molecules (i.e. NKG2A, NKG2B, NKG2C, NKG2E, and NKG2F) which can associate with CD94 to form heterodimeric C-type lectin receptors, and the NKG2D receptor, which does not associate with CD94 and does not recognise HLA-E. In the case of NKG2F, its interaction with HLA-E has not yet been demonstrated. Similar to KIRs, NKG2 receptor family includes both activating and inhibitory molecules: CD94/NKG2A and CD94/NKG2B are inhibitory receptors characterised by a long cytoplasmic tail containing an ITIM sequence responsible for the transduction of inhibitory signals. The activating counterparts display a short cytoplasmic portion and are coupled with DAP12 transducing molecule (52). The expansion of $NKG2C^{+}$ NK cells has been demonstrated in the blood of Cytomegalovirus (CMV)-infected patients: NKG2C receptor appears to play a key role in this process through the recognition of HLA-E molecules loaded with viral peptides (53).

Immunoglobulin-like Transcript 2 (ILT2) receptor

ILT2, also known as Leukocyte Ig-like Receptor (LIR)-1, is a member of a receptor family mainly expressed on myeloid cells: similar to CD94/NKG2A, ILT2 senses the overall HLA-I expression and transduces inhibitory signals upon recognition of the non classical HLA-I molecule HLA-G (51,54).

NK cell receptors specific for non HLA-I ligands

NK cells also express an array of receptors that do not recognise HLA-I molecules: this group includes activating receptors, such as CD16, NCRs (Natural Cytotoxicity Receptors), DNAM-1, NKG2D, NKp80, NTB-A (NK-T-B-antigen), and 2B4 (42), as well as inhibitory receptors, such as IRp60 (Inhibitory Receptor protein 60) (55).

CD16

CD16, also known as FcγRIII, is the low affinity receptor for the Fc portion of IgG: upon recognition of antigen-antibody complexes, signal transduction through the CD3ζ adaptor protein leads to the induction of ADCC. Since this process requires the presence of antibodies, it is induced only following activation of adaptive immunity and the subsequent production of IgG (6).

Natural Cytotoxicity Receptors (NCRs)

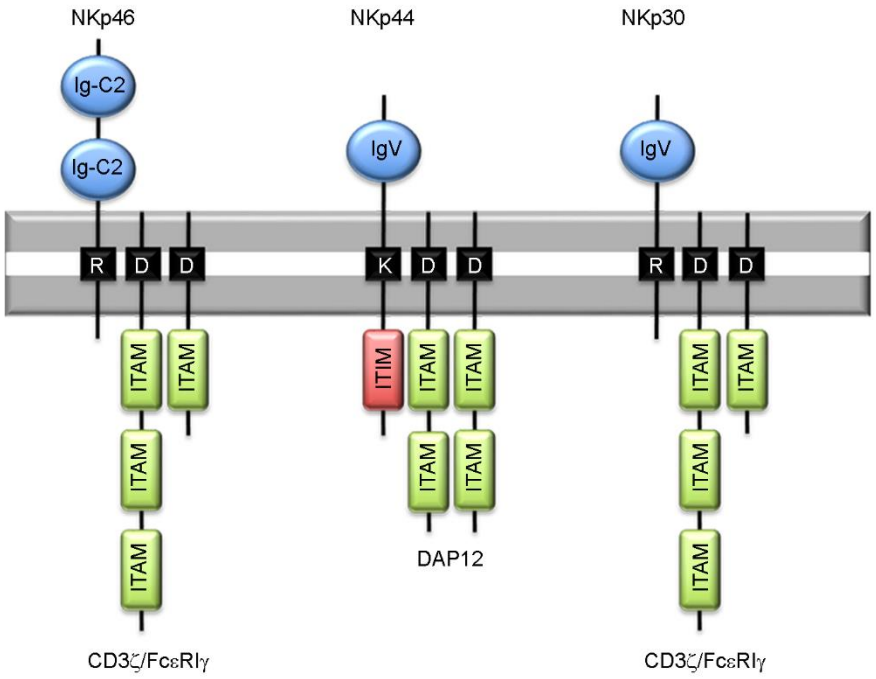

Figure 2. Schematic representation of NCR structure
For each receptor, the structure of the canonical isoform is represented together with the associated adaptor molecules. Ig domains are coloured in blue, activating ITAM in green, and inhibitory ITIM in red. The amino acids responsible for the association with adaptor molecules are indicated in the black boxes. Adapted from (56).

The NCR family includes three different receptors displaying similar functions (42,57), namely NKp46 (NCR1; CD335) (58,59), NKp44 (NCR2; CD336) (60,61), and NKp30 (NCR3; CD337) (62). NKp46 and NKp30 are expressed on both resting and activated NK cells, while NKp44 is expressed only upon IL-2-mediated NK cell activation. *Ncr1* gene is encoded within chromosome 19 (and its mouse orthologue on chromosome 7), while the genes coding for NKp44 and NKp30 are located on chromosome 6 (59,61,62). NCRs are type I transmembrane proteins belonging to the Ig superfamily, displaying one (NKp30 and NKp44) or two (NKp46) Ig-like domains that are responsible for ligand binding. NCRs associate with different ITAM-containing adaptor molecules able to transduce activating signals upon receptor engagement (Fig. 2) and can also form homodimeric structures with a disulfide bridge (63–66). A peculiar functional crosstalk among NCRs has been reported, since the engagement of one NCR appears to initiate both its own signal transduction cascade and the ones downstream of other NCRs

(67). Moreover, it was observed that NK cell activation is more efficient when different NCRs are activated, since target cells can express multiple NCR ligands.

NKp46

NKp46 is the only NCR that has an orthologue in other non-primate species, such as rat and mouse: this specific evolutionary conservation suggests that NKp46 could be the primary NCR involved in pathogen and tumour recognition (68,69). NKp46 displays two N-terminal C2-type Ig-like domains and associates with CD3ζ and the γ-chain of FcεRI through a positively charged Arg residue in the transmembrane domain (58,59). It has been shown that NKp46 can dimerize and that disruption of the dimer prevents ligand binding and receptor activating function (64).

NKp46 is expressed by all mature NK cells, in a small subset of T cells, and in some ILC populations, such as ILC3; nevertheless, it has been shown to be a more selective marker for NK cells and to better characterize them through species, as compared to CD56 (70). NKp46 expression can be down-modulated by exposure to L-kynurenine in the tumour microenvironment (TME) or by cortisol and methylprednisolone, while it is up-regulated in the presence of IFN-α, IL-2, and prolactin (71–73).

NKp30

NKp30 is characterised by an extracellular region containing one Ig domain and a proximal region rich in hydrophobic amino acids that could be involved in the interaction with its respective ligands. NKp30 ligand binding and signalling function are highly dependent on the integrity of the membrane-proximal stalk region (74). Six NKp30 isoforms have been identified: in particular, NKp30 a, b, and c isoforms display an extracellular V-type Ig domain, while d, e, and f isoforms encode for receptors characterised by a C2-type Ig domain lacking 25 amino acids (75). The transmembrane portion contains a positively charged residue (Arg) involved in the interaction with the signalling adaptor molecule CD3ζ (62). NKp30 splice variants also differ in the cytoplasmic region, since splice variations within exon 4 generate three different portions, resulting in either immunostimulatory or immunosuppressive functions. The d, e, and f isoforms have not been studied to date, in contrast to a, b, and c isoforms, whose differential expression and function have been examined in various settings (75–78).

NKp30 is expressed on all resting and activated mature NK cells, but can also be found on the surface of cord blood T cells upon IL-15 exposure (79), on endometrial epithelial cells after progesterone stimulation (80), and on $V\delta1^+$ T cells upon TCR engagement (81). NKp30, as well as NKp46, is down-modulated by cortisol and methylprednisolone, while it is increased in the presence of IFN-α, IL-2, and prolactin (71,72); by contrast, TGF-β has been shown to selectively down-regulate NKp30, but not NKp46 expression (82).

NKp44

NKp44 (60,61) is characterised by an extracellular Ig-like domain at the N-terminal that adopts a V-shaped conformation with a large positively charged groove on one face of the domain: this region could provide a binding site for yet unknown anionic ligand(s) on tumour cells (57,65). NKp44 also displays a 64 amino acid link region (stalk domain) containing 13 O- and 1 N-glycosylation predicted sites, a transmembrane domain, and a short intracellular tail. *Ncr2* gene comprises five exons, but two splice variants containing an additional exon have been reported (Fig. 3). NKp44RG1 (NKp44-3) variant has an additional exon that adds 35 amino acids to the protein but modifies the reading frame, resulting in a shorter cytoplasmic tail. The NKp44RG2 (NKp44-2) variant displays not only this additional exon, but also a 36 bp extension at the 5' of exon 4 encoding 12 additional amino acids (83). To date, no NKp44 gene has been mapped in the syntenic region of mouse chromosome 17, but an orthologue was found in various primate species (83,84), suggesting that NKp44 could be the last NCR gene appeared in phylogenesis. Only the NKp44-1 isoform contains in the cytoplasmic tail an ITIM sequence (EILYHTVA), which is absent in the other two isoforms due to alternative splicing. NKp44-1 isoform is more expressed by dNK than by pNK cells, and an increased expression of NKp44-2 and -3 isoforms in dNK cells has been shown to correlate with an increased risk of miscarriage (76,77). These observations may indicate that the ITIM sequence in NKp44-1 isoform could be involved in maintaining dNK cells in a status of tolerisation towards the semi-allogeneic foetus. NKp44 is coupled through a Lys residues in the transmembrane region to a dimer of the ITAM-containing adaptor molecule DAP12 for downstream signal transduction (60,61); the association between NKp44 and DAP12 is also essential for NKp44 surface expression.

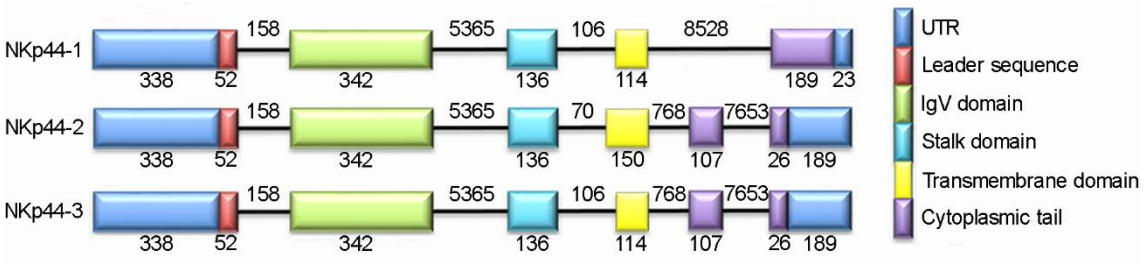

Figure 3. Schematic representation of NKp44 gene and its splice variants
For each splice variant, exon and intron lengths are specified; different colours represent various encoded domains as indicated. *Ncr2* exon lengths, but not intron lengths, are represented in scale with the real ones. Adapted from http://atlasgeneticsoncology.org

NKp44 is usually expressed by NK cells only upon activation with IL-2, IL-15, or IL-1β, but is constitutively expressed by dNK cells. NKp44 is also expressed by ILC3 NCR^+ cells, in which NKp44 engagement induces TNF production (85), and by pDCs, whose IFN-γ production is paradoxically inhibited upon NKp44-mediated stimulation (86). IL-2-induced up-regulation of NKp44 receptor on NK cells can be inhibited by prostaglandin E2 (PGE2), produced, for example, by Tumour-Associated Fibroblasts (TAFs) (87); a similar effect is also exerted by prednisolone (71).

NKG2D

NKG2D (CD314) is an activating C-type lectin receptor, constitutively expressed by all NK cells and by T cells and belonging to the NKG2 receptor family. It associates with DAP10 adaptor protein, containing a YINM sequence and involved in the transduction of activating signals upon interaction with its ligands (88–90). Infected and transformed cells usually activate stress responses, such as the DNA damage response, inducing the overexpression of NKG2D ligands, represented by Major Histocompatibilty Complex (MHC) class I Chain-related protein A and B (MICA/B) and UL16-Binding Proteins (ULBPs)-1/6 (88–90). MICA/B molecules are expressed by the gastrointestinal epithelium in normal conditions, and can be up-regulated in different cancers, including epithelial, lung, breast, kidney, ovary, prostate, colon tumours, and melanoma. They are transmembrane molecules containing the α1, α2, and α3 HLA-I-like domains, but neither associate with β2-microglobulin nor bind any peptide. ULBP-1, -2, and -3 are GPI-anchored surface molecules, whereas ULBP-4 contains a transmembrane domain and a cytoplasmic portion: ULBPs are expressed by both normal tissues and tumours and are characterised by α1 and α2 chains that resemble those of HLA-I molecules (88–92).

DNAM-1

DNAM-1 (CD226) is a transmembrane protein that can transduce activating signals through the phosphorylation of tyrosines in its cytoplasmic tail, resulting in the enhancement of cytotoxicity and cytokine production by NK cells. DNAM-1 is characterised by two extracellular Ig-like domains and a cytoplasmic portion containing three tyrosine residues. In addition to NK cells, also T cells, monocytes, and a small subset of B lymphocytes express this receptor (93,94). DNAM-1 binds two members of the nectin family: CD112 (Nectin-2) and CD155 (Poliovirus Receptor, PVR), two closely related molecules that are highly expressed on several tumour cell types (95). Nectins are widely expressed also on normal cells, including neurons, epithelial, endothelial cells, and fibroblasts; this implies that normal cells are protected against NK cell cytotoxicity by the expression of self HLA-I molecules (95,96). Based on DNAM-1 ligand expression levels, a remarkably heterogeneous tumour susceptibility to NK cell-mediated lysis among different patients was observed in different types of tumours, such as neuroblastoma and leukaemia (96). Interestingly, DNAM-1 ligands are also able to interact with TIGIT (T cell Immunoreceptor with Ig and ITIM domains) and CD96 inhibitory receptors: both receptors can be expressed on NK cells and bind PVR with a higher affinity than DNAM-1. Thus, TIGIT and CD96 can compete with DNAM-1 for ligand recognition, and can counterbalance DNAM-1-mediated NK cell activation (94,97,98).

IRp60

IRp60 (also known as CD300a or CMRF35-H9) is expressed by all NK cells and by other cell types, including T lymphocyte subsets, monocytes, and granulocytes. In NK cells, it has been shown to inhibit the cytotoxic activity induced by different activating NK receptors (55,99). IRp60 is a 60 kDa surface

molecule belonging to the Ig-superfamily, displaying one extracellular Ig-V domain and a cytoplasmic tail containing three classical and one non-classical ITIM motifs that are tyrosine phosphorylated upon receptor engagement. IRp60 is highly related to five CMRF35 proteins encoded in the same gene cluster on chromosome 17, where IRp60 gene is located; in particular, CMRF35-A (CD300c) shares high similarity with IRp60, but does not contain any ITIM in its intracellular portion and may thus display an activating function (55,100).

Recently, two ligands for IRp60 have been identified: this receptor is able to bind phosphatidylethanolamine and phophatidylserine and to subsequently transduce an inhibitory signal that suppresses NK cell-mediated cytotoxicity (101,102).

1.1.4. NCR ligands

Until now, only some NCR ligands have been identified: NCRs are able to recognise a wide spectrum of ligands of different origin, ranging from viral, parasite, and bacterial ligands to cellular ones (Table 1), thus playing a key role in the recognition and killing of infected and tumour cells. The very different nature of these molecules, together with the possible low affinity of ligand-receptor interactions, may be one reason hindering the identification of novel ligands. Other factors could be related to the chemical nature of the ligands (they might be not only proteins, but also sugars, lipids, or complex structures), or to the possibility that the formation of receptor complexes is necessary for a more stable receptor-ligand interaction (56,103–105).

NKp46 ligands

NKp46 recognises different viral ligands, such as hemagglutinin (HA) of influenza and Sendai virus (106,107), and hemagglutinin-neuraminidase (HN) of Newcastle Disease virus and Orthopox virus family (108,109). Among other microbial ligands, unknown ligands on *Plasmodium falciparum* (110) and *Fusobacterium nucleatum* (111), as well as the glycan-binding lectins Epa1, Epa6, and Epa7 of *Candida glabrata* (112), were identified.

Vimentin, an intracellular filamentous protein that is part of the cytoskeleton, was the first identified NKp46 cellular ligand: in particular, a peculiar form of vimentin can be expressed on the cell surface of *Mycobacterium tuberculosis*-infected monocytes, where it is recognised by NK cells and stimulates their cytotoxic activity (113). More recently, NKp46 has been shown to recognise unknown ligands expressed on healthy tissues, such as salivary glands, hepatic stellate cells, and pancreatic β-cells; importantly, NK cell- mediated recognition of pancreatic β-cells has been correlated to the development of type I diabetes (114–116). NKp46 ligands are also expressed on tumour cells (42,56), but the identity of these molecules is still unknown.

The most recently identified NKp46 ligand is the Complement Factor P (CFP or properdin), a plasma glycoprotein produced by neutrophils, monocytes, and T cells, able to positively regulate the

alternative complement pathway. Narni-Mancinelli et al. reported that CFP-NKp46 interaction does not affect neither NK cell degranulation nor IFN-γ secretion, while it has been suggested that, through

NCR	Ligand	Expression	Localisation	Ref.
NKp46	Viral HA and/or HN	Influenza virus, Sendai virus, Poxvirus, Newcastle disease virus infected cells	Plasma membrane	(106–109)
	Unknown ligand(s)	*P. falciparum*, *F. nucleatum*	Bacterial wall	(110,111)
	Epa1, Epa6, Epa7	*C. glabrata*	Fungal wall	(112)
	Vimentin	*M. tuberculosis* infected monocytes	Cytoplasm of healthy cells, plasma membrane of infected cells	(113)
	CFP	Neutrophils, monocytes, T cells	Soluble	(117)
	HSPG	All cells, up-regulated/ modified on tumour cells	Plasma membrane	(118)
	Unknown ligand(s)	Pancreatic β-cells, liver stellate cells, salivary glands, tumour cells	Plasma membrane	(115,116)
NKp44	Viral HA and/or HN	Influenza virus, Sendai virus, West Nile virus, Dengue virus, Newcastle disease virus infected cells	Plasma membrane	(106,119, 120)
	Unknown ligand(s)	*M. tuberculosis*, *M. bovis*, *N. farcinica*, *P. aeruginosa*	Bacterial wall	(121–123)
	PCNA	Up-regulated in tumour cells	Nucleus of healthy cells, plasma membrane of tumour cells	(124)
	MLL5 isoform	HIV-infected T cells, tumour cells	Plasma membrane	(104,125)
	Syndecan-4	Tumour cells	Plasma membrane	(126)
	PDGF-DD	Up-regulated in tumour cells	Soluble	(127)
	HSPG	All cells, up-regulated/ modified on tumour cells	Plasma membrane	(118)
	Unknown ligand(s)	Chondrocytes, astrocytes, tumour cells	Plasma membrane	(128,129)
NKp30	Viral HA	Poxvirus, vaccinia virus infected cells	Plasma membrane	(109)
	pp65	HCMV infected cells	Cytoplasm	(130)
	PfEMP-1	*P. falciparum* infected erythrocytes	Plasma membrane	(110)
	BAT3/BAG6	Up-regulated in tumour cells	Cytoplasm of healthy cells, plasma membrane and exosomes of tumour cells, soluble	(131,132)
	B7-H6	Tumour cells	Plasma membrane, shed in a soluble form	(133,134)
	Galectin-3	Intestinal epithelium, tumour cells	Soluble	(135)
	HSPG	All cells, up-regulated/ modified on tumour cells	Plasma membrane	(118)

Table 1. Summary table of NCR ligands

the binding of different bacterial components, CFP might facilitate the recognition of NCR bacterial ligands and subsequent NK cell activation essential to control bacterial infections (117).

NKp30 ligands

NKp30 has been shown to bind HA of Poxviruses, such as human vaccinia virus and murine ectromelia virus: NKp30-HA interaction impairs NKp30-mediated NK cell activation, as opposed to the activating role of NKp46 interaction with HA of the same viruses (109). NKp30 displays an inhibitory function also upon interaction with the tegument protein pp65 of HCMV, due to the dissociation of NKp30 from CD3ζ chain. Since pp65 is localised in infected cell cytoplasm, it has been proposed that NKp30 could interact with a pp65 soluble form released from apoptotic infected cells: this explanation is supported by the presence of anti-pp65 antibodies in the serum of HCMV infected patients (130). On the other hand, NKp30 interaction with PfEMP1 of *Plasmodium falciparum* expressed on parasitised erythrocytes results in the induction of an activating signal (110).

The first identified NKp30 cellular ligand was HLA-B-associated transcript 3 (BAT3), also known as Bcl-associated anthanogene 6 (BAG6), a nuclear protein involved in the p53-mediated cellular response to stress and DNA damage (131). Another NKp30 cellular ligand is represented by B7-H6, a transmembrane protein belonging to B7 family that is selectively expressed on several tumour cell types (such as lymphomas, leukaemia, melanoma, and carcinoma), and on monocytes and neutrophils upon stimulation with TLR ligands or with proinflammatory cytokines (133,136). B7-H6 expression has been shown to be down-regulated upon treatment of tumour cells with histone deacetylase (HDAC) inhibitors: this modulation results in a reduced NK cell-mediated cytotoxicity and could influence the outcome of anti-tumour therapies based on HDAC inhibitors (137). However, other types of cancer therapies, such as cysplatin and 5-fluorouracil chemotherapy, radiation therapy, and cytokine therapy (i.e. localised administration of TNF-α), are able to induce in tumour cells a stress response that results in the up-regulation of B7-H6 expression and increased susceptibility to NK cell cytolysis (138). Finally, NKp30 has been demonstrated to bind to Galectin-3 (Gal-3), expressed by tumour cells (135).

NKp44 ligands

NKp44 has been demonstrated to recognise ligands of viral origin, such as HA of influenza (119), HA and hemagglutinin-neuraminidase (HN) of Newcastle Disease virus, and envelope glycoproteins of West Nile and Dengue viruses (120). In particular, NKp44 recognition of Newcastle Disease virus stimulates both IFN-γ and TNF-α production and NKp44-mediated cytolytic activity. Microbial ligands for NKp44 are expressed on the surface of *Mycobacterium* family members, such as *Mycobacterium bovis* bacillus Calmette-Guérin (BCG) (121), *Mycobacterium tuberculosis* (122), *Nocardia farcinica*, and *Pseudomonas aeruginosa* (123). NKp44 interaction with BCG can induce proliferation, IFN-γ

production, and NK cell cytotoxic activity (121), whereas the outcome of NKp44 interaction with the other *Mycobacterium* family members is still unclear.

The first identified cellular ligand for NKp44 was PCNA (Proliferating Cell Nuclear Antigen), a nuclear protein expressed by actively replicating cells and involved in DNA repair and replication (124). PCNA expression increases during tumour progression and decidua development; in these conditions, it can be expressed on the cell membrane in association with HLA-I molecules (139). When exposed at the cell surface, PCNA can interact with NKp44 receptor, inducing the transduction of an inhibitory signal through its ITIM sequence, probably representing a mechanism of tumour escape from NK cell-mediated killing (124). PCNA is also overexpressed in the decidua during the first trimester of pregnancy, as well as in a subset of decidual DCs reported to interact with dNK cells. Since dNK cells express higher levels of NKp44-1 than pNK cells, it was suggested that PCNA-induced NK cell inhibition through NKp44 could be one of the mechanisms enabling the regulatory and immunotolerant phenotype of dNK cells (77,124).

More recently, another cellular ligand for NKp44 was described. Vieillard et al. observed that Human Immunodeficiency Virus (HIV) infected $CD4^+$ T cells express a ligand (NKp44L) for NKp44 receptor: its expression is induced by the interaction of gp41 HIV protein with gC1qR (receptor for the complement component C1q) and is able to stimulate NK cell-mediated killing of infected T cells (125,140). Subsequently, this NKp44L was identified as an isoform of Mixed-Lineage Leukaemia Protein 5 (MLL5) nuclear protein: MLL5 splicing variant (21spe-MLL5) lacks exon 5 and contains at the C-terminal the 21spe exon allowing the expression of this molecule at the cell surface (104).

The expression of NKp44 ligand(s) was also observed on the surface of articular chondrocytes, but the nature of these ligands is still unknown. NKp44 ligand recognition may induce chondrocyte killing by IL-2 activated NK cells, thus contributing to cartilage destruction occurring in rheumatoid arthritis (128). Recently, astrocytes have been shown to express a NKp44 ligand, whose expression can be down-regulated by HIV infection, suggesting a viral escape mechanism (129).

A peculiar interaction between NKp44 receptor and the HSPG syndecan-4 was described: these two molecules can interact in *cis* on the NK cell surface, regulating NKp44 surface distribution and function, since syndecan-4 can mask NKp44 binding site necessary for the interaction in *trans* with other ligands (126).

Finally, PDGF-DD was recently identified as a novel NKp44 soluble ligand able to trigger NK cell-mediated cytokine release and correlating with reduced tumour dissemination in NCR2-transgenic mice (127).

Heparan sulphates proteoglycans

Heparan sulphate proteoglycans (HSPGs) can be found attached to the cell surface and in the Extracellular Matrix (ECM): HSPGs, such as syndecans and glypicans, are long anionic polysaccharides

composed of repeated disaccharide units of iduronic or glucuronic acid and glucosamine that are differentially sulphated at N, 2-O, 3-O and 6-O positions and are conjugated to protein structures (141,142). All three NCRs have been demonstrated to recognise different epitopes on HSPGs, but appear to preferentially bind to highly sulphated structures (two or three sulphate groups for each disaccharide unit) through basic amino acids on the receptor surface (118). Since tumour cells often display an altered heparan sulphate (HS) expression, NCRs might be able to recognise peculiar epitopes expressed by transformed cells. HS structures on proteoglycans could act as a bridge between NK and tumour cells, as supported by the observation that cells lacking HS, but not chondroitin sulphate, are recognised to a lesser extent, and for this reason NK cells are less efficient in killing such cellular targets (143).

Recent studies focused on NCR interactions with their ligands suggest that in many cases recognition can be influenced by the presence of co-ligands. HLA-I and HSPGs were suggested to be co-ligands that could act as docking proteins able to connect NCRs to their respective ligands or to bind to other molecules generating complexes that are recognised by NCRs in their wholeness (105). In addition, it has been demonstrated that HSPGs act as co-ligands involved in the recognition of tumour cells by NCRs and can induce IFN-γ release but not NK cell-mediated cytotoxicity (118,143). HLA-I might represent another co-ligand, since it localizes with NCR ligands, such as PCNA and BAT3 on tumour cell surface (105,132,139). The involvement of these co-ligands in the interactions between NCRs and their ligands could also play a role in the outcome of NK cell response to a stimulus: since in some conditions this interaction can result in NK cell inhibition, the presence or the absence of co-ligands might favour an activating or an inhibitory effect on NK cells (105).

1.1.5. Soluble ligands for NK cell receptors

In the last years, an increasing number of soluble ligands for NK cell activating receptors have been described: these soluble molecules are often represented by peculiar isoforms of ligands usually expressed at the cell surface or cleaved forms of cell surface ligands. Many of the soluble ligands described until now act as decoy molecules, preventing the interaction of activating receptors with their ligands expressed on target cells; in other cases, soluble ligands induce down-regulation of their specific receptors on NK cell surface. Both mechanisms result in the inhibition of NK cell cytotoxicity, thus representing a strategy of tumour escape.

Soluble ligands for NKG2D receptor have been extensively characterised. ADAM (A Disintegrin And Metalloprotease) and ERp5 proteases can cleave MICA/B releasing soluble forms able to induce NKG2D internalisation upon receptor engagement (144–146); similarly, ULBPs can be released in soluble forms due to the activity of ADAM10 and ADAM17 proteases and could trigger NKG2D down-regulation (147,148).

Also DNAM-1 ligands can be found in soluble form. PVR splice variants may lack the transmembrane region: PVRβ and PVRγ, in contrast to PVRα, are soluble forms whose levels can be increased in the serum of cancer patients. However, the biological significance of these soluble molecules, as compared to membrane-bound PVRα, is still unclear (149–151).

Regarding NCRs, soluble ligands for all three receptors have been identified: in the case of CFP, no activating effect through the interaction with NKp46 receptor has been observed (117). NKp30 interaction with its membrane-bound ligands and subsequent transduction of activating signals are impaired in the presence of soluble ligands such as BAT3, B7-H6, and Gal-3. BAT3 and Gal-3 are released from tumour cells, whereas B7-H6 is shed in a soluble fragment through ADAM10 and ADAM17 proteases, which can be released in the tumour microenvironment (134). The inhibitory role of soluble BAT3 has been described in the case of Chronic Lymphocytic Leukaemia (CLL) (152), whereas soluble B7-H6 has been found to mediate NKp30 down-regulation in NK cells derived from ovarian cancer patients (153). It is of note that BAT3 and B7-H6 can be released not only in soluble form but also associated with exosomes: BAT3-containing exosomes secreted from DCs and tumour cells are able to induce both cytotoxicity and cytokine secretion through the interaction with NKp30 receptor. Due to their ability to stimulate NK cell cytotoxicity, a role for BAT3-positive exosomes derived from DCs in the induction of DC editing process has been suggested (131,132). NKp30 also recognises Gal-3, a soluble protein expressed by tumour cells: Gal-3 expression has been shown to correlate with an increased apoptosis of tumour-associated lymphocytes and with a reduced NK cell cytotoxic activity, since Gal-3 is able to interfere with NKp30-mediated recognition of tumour cells (135). PDGF-DD is the most recently identified NCR ligand and the first documented soluble molecule recognised by NKp44 receptor. Barrow and colleagues demonstrated that PDGF-DD recognition by NKp44 triggers IFN-γ and TNF-α release by NK cells, as well as other proinflammatory cytokines involved in tumour growth arrest. Moreover, they observed that the spread of PDGF-DD-expressing tumour cells is limited in NCR2-transgenic mice as compared to non transgenic mice. Based on these data, Barrow et al. suggested that on one hand PDGF-DD induces tumour growth, while on the other hand it stimulates NK-, ILC1- and ILC3-mediated immune responses through its interaction with NKp44 (127).

1.1.6. NK cell function in tumour immunosurveillance

Tumour immunosurveillance is one of the most important NK cell functions, as supported by different observations (for example, individuals with low NK cell cytotoxic activity have a higher incidence of cancer). Several reports show that NK cells are able to efficiently kill tumour cells *in vitro* through their natural cytotoxic activity or through the induction of apoptosis via TNF-α, FasL, and TRAIL; nevertheless, it has been demonstrated that such activity can be often impaired *in vivo* (154,155).

In the last years an important role for NK cells in the therapy of high-risk leukaemia has been demonstrated (156). Haematopoietic Stem Cell Transplantation (HSCT) represents a primary therapy for these haematological malignancies: allogeneic HSCT is the major therapeutic option, but about 40% of patients does not find an HLA-matched donor; thus, an alternative source of HSCs can be obtained from haploidentical family members or from umbilical cord blood of unrelated subjects. In the case of haploidentical HSCT, patients are transplanted with HSCs from a donor that shares with the recipient one HLA haplotype and is mismatched for the other one: in this setting, donor HSCs can give rise to NK alloreactive populations, i.e. NK cells expressing KIRs specific for HLA alleles that are not expressed on recipient cells. In this kind of transplantation, alloreactive NK cells are essential to mediate Graft versus Leukaemia (GvL) effect, thus preventing leukaemia relapse. Moreover, alloreactive NK cells kill residual recipient DCs and T cells, preventing GvHD and graft rejection too. Several studies conducted on acute myeloid leukaemia (AML) and acute lymphoblastic leukaemia (ALL) patients confirmed that patients receiving grafts with alloreactive NK cells showed a significantly longer survival as compared to recipients of non-alloreactive grafts (156–159). These observations suggest the importance to overcome KIR-mediated inhibition in order to achieve full NK cell activation: based on this idea, fully humanised antibodies against inhibitory KIRs, such as lirilumab, have been developed and used in phase I and II clinical trials on AML and multiple myeloma patients (160,161).

In the case of solid malignancies, several studies have provided evidences that a high number of infiltrating NK cells correlates with improved prognosis and survival probability, by preventing metastasis. Nevertheless, it has also been shown that during tumour progression NK cell anti-tumour activity can be often limited either by their inefficient migration to tumour lesions or by the inhibition of their functions induced by the TME (162–164).

NK cell migration towards tumour site

NK cell recruitment into neoplastic tissues is highly influenced by the tumour type, as well as by the chemokine profile in the TME: for example, in the case of CCL19, CCL21, and CXCL9-expressing tumours, $CD56^{bright}$ NK cells are likely to preferentially migrate towards the tumour site due their higher expression levels of CXCR3 as compared to $CD56^{dim}$ NK cells (162,164); notably, $CD56^{bright}$ NK cell subset can survive more easily under oxidative stress conditions often characterising tumour tissues (162). NK cell function and migration can be indirectly influenced by MMP and ADAM proteases, since they are involved in ECM remodelling, cytokine and growth factor cleavage, and ectodomain shedding of transmembrane proteins, including cell adhesion molecules and NK cell receptor ligands, thus modifying the expression of such molecules (162).

The tumour microenvironment (TME)

Tumour cells are characterised by deep genetic alterations that can lead to the overexpression of transcription factors, such as nuclear factor-κB (NF-κB), Signal Transducer and Activator of

Transcription 3 (STAT3), and Hypoxia-Inducible Factor (HIF)-1α, involved in promoting a favourable TME, characterised by an aberrant inflammation, promoting tumour cell survival, proliferation, and angiogenesis. Cell populations within the TME are represented by both tumour cells and tumour-associated cells: the latter ones include TAFs, MSCs, and several immune cells with immunosuppressive functions, such as TAMs, Tumour-Associated Neutrophils (TANs), Myeloid-Derived Suppressor Cells (MDSCs), iDCs and Treg. Altogether these cells inhibit NK cell anti-tumour activity, mainly through modulating the cell surface expression of ligands in tumour cells and of receptors in NK cells (Fig. 4) (162–165). In the first case, both tumour cell genetic alterations and a process of immune selection through NK cell-mediated killing, especially during the initial phases of tumour development, can favour the selection of resistant tumour cells. Selected tumour cells often display a poor expression of ligands recognised by activating NK cell receptors or sometimes overexpress PCNA, whose interaction with NKp44 results in reduced NK cell-mediated cytotoxicity. Moreover, IFN-γ, GM-CSF, IL-10, and Leukaemia Inhibitor Factor (LIF) can induce HLA-G expression on tumour cells: HLA-G binding to the inhibitory receptor ILT2 on NK cells can raise the threshold for NK cell activation or induce NK cell apoptosis. Furthermore, HLA-G can be transferred by intercellular membrane exchange (trogocytosis) from APCs and tumour cells to NK cells, leading to HLA-G$^+$ NK cells with regulatory functions (166). Surface expression of NK cell receptor ligands can also be modulated by tumour-derived proteases, which can shed surface ligands, (including B7-H6, BAT3, sMICA/B, and ULBPs), in a soluble form: these soluble molecules can compete with the membrane-bound ones, leading to the inhibition of NK cell cytotoxicity (131,134,145–148,152,153).

The second mechanism leading to the suppression of NK cell anti-tumour activity is NK cell receptor down-regulation that can be induced both by soluble factors and by cell-to-cell contact. Soluble factors can be represented by shed NK cell receptor ligands, such as MICA/B (144), as well as by cytokines and metabolites (i.e. PGE2, lactate, adenosine, and galectins) produced by tumour cells and/or tumour-associated cells (163). The main immunosuppressive cytokines within the TME are TGF-β, IL-4, and IL-10: TGF-β inhibits the expression of NKp30 and NKG2D receptors, while IL-4 reduces the ability of NK cells to kill susceptible cellular targets, to produce cytokines, and to functionally interact with DCs (82,162–164,167). Several cell populations in the TME express IDO, whose metabolic activity results in the depletion of tryptophan (Trp), essential for immune cell functions, and promotes the production of the immunosuppressive Trp catabolite L-kynurenine, able to inhibit NKp46 and NKG2D expression (162–164). Furthermore, TAFs can inhibit NK cell functions by preventing the IL-2-induced up-regulation of NKp44, DNAM-1, and NKp30 receptors through both cell-to-cell contact and PGE2; also tumour cells have been shown to inhibit NKp30, NKp44, and NKG2D expression through IDO- and PGE2-dependent mechanisms (73,163,164). In addition, different studies have reported that NK cells infiltrating the tumour display high levels of NCR inhibitory isoforms, while the expression of activating

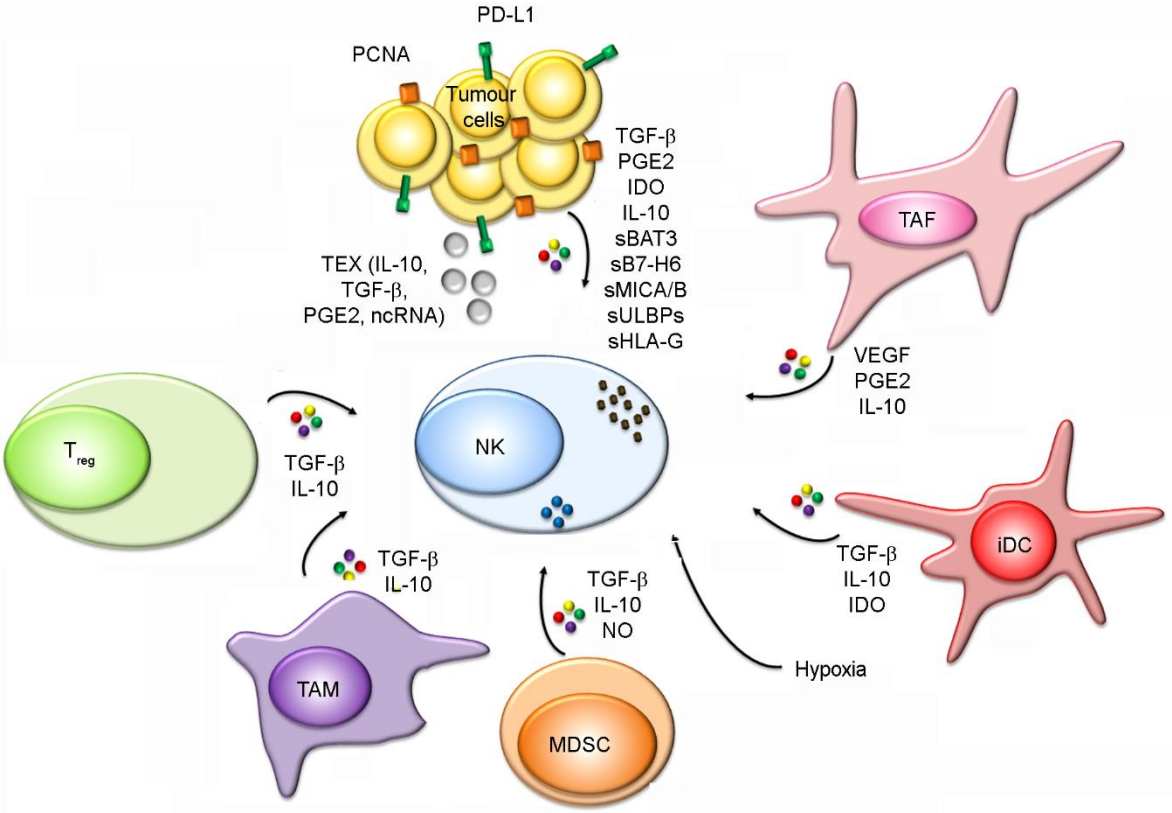

Figure 4. Inhibition of NK cell functions by tumour microenvironment (TME)
Schematic representation of soluble factors and surface molecules inhibiting NK cell functions within the TME.

isoforms has been correlated with a better prognosis. The expression of NKp30 a, b, and c isoforms has been studied in several tumours: in long-term surviving melanoma patients, higher levels of activating NKp30a isoform have been observed (78), whereas gastrointestinal stromal tumour (GIST) and metastatic neuroblastoma patients with predominant expression of NKp30c have a reduced survival, since they are less responsive to B7-H6^{+} tumour cells (75,168). Some studies showed a differential expression of NKp44 isoforms in NK cells infiltrating solid tumour tissues as compared to the ones in surrounding normal tissues: NK cells in the TME appear to express higher levels of potentially inhibitory NKp44-1 isoform (77). Moreover, in a recent study, Shemesh et al, observed that AML patients with high expression levels of NKp44-1 isoform have a poorer survival than those mainly expressing NKp44-2 and -3 isoforms (169).

Within the TME, extracellular vesicles derived from tumour and tumour-associated cells have also been found: these vesicles, released by normal and tumour cells, are able to transfer functionally active proteins, lipids, and nucleic acids, and play an important role in intercellular communication in both physiological and pathological conditions. Extracellular vesicles can be primarily divided in exosomes, that are endosomal-derived nanovesicles, and microvesicles (MVs) generated by the outward budding from the plasma membrane (170,171). Tumour-related exosomes (TEXs) released from cancer cells are involved in tumour angiogenesis, ECM remodelling, tumour migration, and metastasis formation.

Analysis of TEX derived from tumour patients, revealed that TEXs can contain immunosuppressive molecules, ranging from immune checkpoint receptor ligands (such as PD-L1), inhibitory cytokines (IL-10, TGF-β, and PGE2) to noncoding RNAs (172). One of the well-known mechanisms is TEX-mediated down-regulation of NKG2D activating receptor, but TEXs are also able to reduce expression of perforin and signalling pathway components, resulting in the inhibition of NK cell-mediated cytotoxicity (172). Hypoxia is frequently observed in TME; the hypoxic condition can be involved in the induction of tumour resistance and in the regulation of immunosuppressive cells (173,174). In particular, hypoxia has been shown to directly affect NK cell function by reducing granzyme and perforin expression levels and by inducing the up-regulation of HIF-1α: this results in the impairment of NCR and NKG2D up-regulation in the presence of activating cytokines including IL-2, IL-15, and IL-12 (173). Importantly, HIF-1α expression affects NK cell natural cytotoxicity, while it does not alter ADCC function, since CD16 expression is not altered. HIF-1α expression impairs NK cell functions also indirectly, by down-regulating NKG2D ligands, inducing TGF-β secretion by tumour cells, increasing the number of infiltrating Treg and MDSCs, and favouring M2 polarisation (163,174).

1.2. NIDOGEN-1 (NID1)

Nodogen-1 (NID1), also called Entactin, is a sulphated glycoprotein, member of Nidogen family together with the closely related Nidogen-2 (NID2): Nidogens are two monomeric glycoproteins involved in the stabilisation of Basal Membrane (BM) and in the maintenance of ECM structure (175,176). NID1 and NID2 share the same basic structure composed of three globular domains (G1-3): the first two domains (G1 and G2) are connected by a link region, while G2 and G3 domains are separated by a longer rod-like region. Protein sequence analysis shows that Nidogens contain structural motifs that are typical of ECM proteins, such as Epidermal Growth Factor-like (EGF), thyroglobulin type-1 (TY), low density lipoprotein receptor (LY), NIDO, and G2 Nidogen and fibulin module (G2F) domains. For both proteins, a splice variant exists, lacking at least one EGF domain in the rod-like region. NID1 and NID2 display an overall sequence homology of about 46%, but comparison of the single protein motifs indicates that the sequence homology ranges from 39,5% to 71,8% (Table 2). NID1 and NID2 main structural differences are located in the G3 domain and in the rod-like region, which is longer in NID2 than in NID1 (Fig. 5) (176,177). These proteins also partially differ for their expression in human tissues, since NID1 is ubiquitously and more abundantly expressed than NID2 (176). A third important difference is the presence of an RGD (Arg-Gly-Asp) sequence in the first EGF motif in the rod-like region of both NID1 isoforms, but not in NID2. The RGD sequence has been shown to be involved in the interaction of NID1 with integrins expressed on the cell surface, thus suggesting that NID1 may display peculiar functions (178–182).

	NIDO	EGF	G2F	EGF	EGF-Ca	EGF	EGF-Ca	TY	LY	LY	LY	LY	NID1 protein
% of homology	46,7	57,9	49,7	56,4	41,9	46,3	71,8	58-63,3	39,5	55,8	73,3	60,5	46

Table 2. Percentage of homology between NID1 and NID2
NID1 protein motifs are listed from the N-terminal to the C-terminal. For each motif and for the entire protein, the percentage of homology with the corresponding motif of NID2 is indicated. In the case of TY motif, the percentage of homology was calculated comparing the NID1 motif with each of the two TY NID2 motifs of.

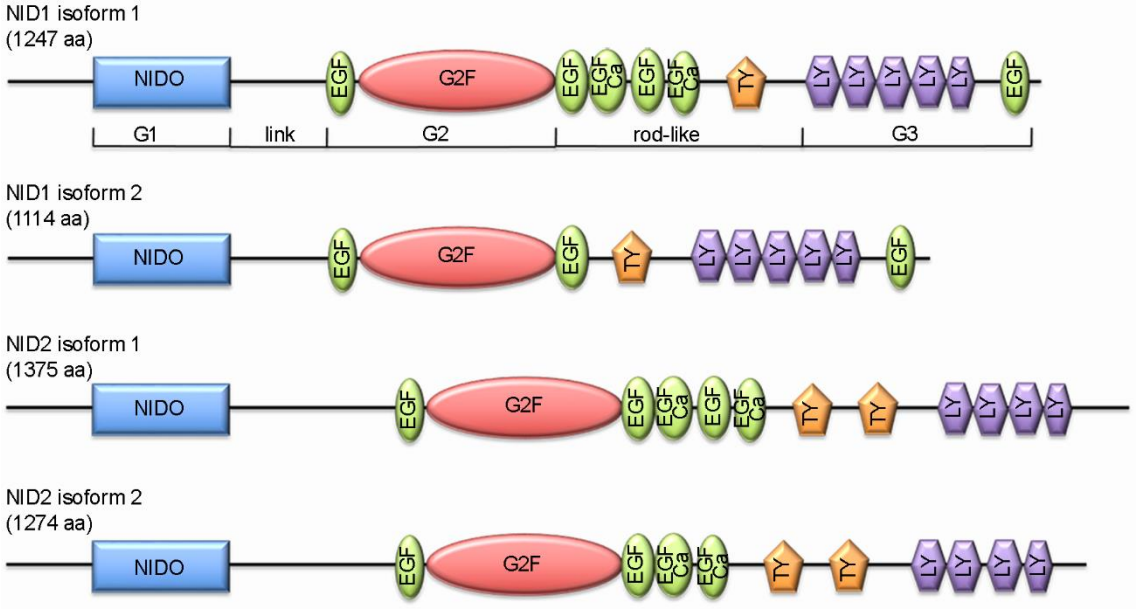

Figure 5. The Nidogen family
The modular structure characterising NID1, NID2, and their isoforms is shown. Both proteins display NIDO (Nidogen like domain), G2F (G2 Nidogen and Fibulin module), TY (Thyroglobulin type-1 module), EGF (Epidermal Growth Factor like module), and LY (Low density lipoprotein receptor) domains. For each protein the protein length is indicated. This representation is based on sequence analysis performd with SMART database (http://smart.embl-heidelberg.de).

1.2.1. NID1 functions and protein interactions

NID1 is involved in the formation and maintenance of ECM structure, especially in BM, and has been shown to play an important role in cellular adhesion, neutrophil chemotaxis, nerve development, and tumour angiogenesis (176,179,180,182–185).

Being involved in the assembly of BM, Nidogens are able to interact with different ECM and BM components, such as laminin, fibrinogen, collagen IV, fibulin, and the HSPG perlecan. Several studies have elucidated the domains involved in such interactions: G3 domain is important for the connection with laminin, while G2 domain is mainly involved in the interaction with perlecan and collagen IV, whose binding surfaces are probably partially overlapped (176,186,187). NID1 is also able to bind fibulin-1 or -2, in contrast with NID2 that is, however, able to bind collagen XVIII, endostatin, and tropoelastin, components of elastic lamellae in the larger arteries. Interactions between MSC-released NID1 and epithelial cell-derived laminin are essential for maintaining ECM structure, and, thus, for organ development. Nevertheless, NID1 absence has no evident effect on development in NID1-

knockout mice, probably because NID2 can compensate NID1 loss; moreover, only some slight neurological effects in worms and mice models arise in the absence of both NID1 and NID2 (176).

For both NID1 isoforms, interactions with cell surface proteins are possible through the RGD sequence that allows NID1 to bind $\alpha3\beta1$ (CD49c/CD29) (178). NID1 can also interact with $\alpha V\beta3$ integrin (CD51/CD61), but in this case a cysteine-rich EGF repeat in the G2 domain seems to be involved in the binding (181). Until now, studies conducted in order to elucidate the functions of these interplays suggest that NID1-integrin interaction is not responsible for the structural role of NID1 in the ECM; however, the RGD sequence in NID1 has been shown to be essential for blastocyst outgrowth and migration in an *in vitro* murine model (180). The observation that NID1 can be found in decidual tissue during early post-implantation development, and displays a chemotactic activity on different cell types (such as neutrophils), suggests that NID1 plays an important role in trophoblast adhesion and migration. Both trophoblast and neutrophil migration and adhesion appear to be mediated by $\alpha V\beta3$ and $\alpha3\beta1$ integrins (179,182,183).

It has been demonstrated that the membrane protein Tumour Endothelial Marker 7 (TEM7) is a ligand for NID1. TEM7 is mainly expressed on endothelial cells during tumour angiogenesis, but also in healthy tissues, such as embryonic vasculature, and in some neurons (188). NID1 has been shown to play a role in nerve development in a *C. elegans* experimental model (184); based on these findings, NID1 involvement in Schwann cell regulation was investigated and found to exert on these cells a prosurvival and promigratory effect mediated by $\beta1$ integrins; this function can be blocked using a soluble TEM7 ectodomain, probably due to competition with integrins for NID1 binding. However, a direct involvement of TEM7-NID1 interaction in this process has not been demonstrated (185).

1.2.2. Role of NID1 in tumours and other diseases

The wide NID1 binding potential, together with its high protease sensitivity might play an important role in the modulation of BM functions under both normal and pathological conditions. Several studies report an involvement of NID1 in different types of cancer and in the metastatic process. Moreover, some recent reports propose NID1 as a candidate biomarker for some types of neoplasia. It is well known that ECM structures, such as BM, play a key role in cancer metastatic processes, and that the up-regulation of proteases often associates with metastasis spreading. NID1 link region between G1 and G2 domains, as well as G3 domain can be hydrolysed by serine proteases, i.e. thrombin, trypsin, kallikrein, and MMPs, while NID1 can acquire more resistance when forming a complex with laminin molecules (189). Sage et al. showed that the cysteine protease cathepsin S (CatS) can degrade NID1 as well as NID2: the cleavage sites are located in G2 and G3 domains, essential for NID1 interaction with other ECM components such as laminin; therefore, this cleavage results in an impaired NID1 binding to other ECM proteins (190). A more recent study showed that the previously identified CatS cleavage

site at the level of TY domain in the rod-like region produces a specific peptide, called NIC, whose serum levels could be used as a biomarker in patients with Non-Small Cell Lung Cancer (NSCLC) (191). For both MPP-19 and ADAMTS1 (a disintegrin and metalloprotease with thrombospondin repeats 1), distinct studies report conflicting results, probably because of the different experimental models: it has been shown that these proteases can prevent neoangiogenesis, important for tumour development, but also that they can degrade the ECM, thus promoting tumour cell migration and metastatic processes (192,193).

In the last years, several studies have described the presence of NID1 in exosomes and, in particular, in exosomes derived from cancer patients (194–199). NID1-positive exosomes were detected in urinary samples from healthy patients but also in the serum of patients with melanoma, nasopharyngeal carcinoma, breast cancer, and ovarian cancer; in some of these cases, NID1 has been proposed as a biomarker able to reflect tumour burden (199,200). Studying NID1 involvement in ovarian cancer, Zhou et al. observed that NID1 can promote Endothelial-Mesenchymal Transition (EMT), thereby potentially supporting metastasis formation in a $\alpha 3$ integrin-dependent manner; in addition, in this report, NID1-induced chemoresistance to cisplatin treatment was also observed (201). Aberrant expression of NID1 was detected in gastrointestinal and endometrial cancers too, but with opposite effects: in the first case, reduced NID1 expression resulted in the loss of BM integrity, favouring tumour invasion, metastasis, and angiogenesis (202), whereas in endometrial cancer, NID1 overexpression positively correlated with tumour invasiveness (203).

Dysregulation of Nidogen expression has been reported in various pathologies, such as Hirschsprung's disease and osteoarthritis; a NID1 nonsense mutation has been associated with an autosomal dominant pathology, the Dandy-Walker malformation and occipital cephaloceles, characterised by cerebellar hypoplasia, meningeal anomalies, and occipital skull defects (204). Kruegel et al. demonstrated a differential expression of NID1 and NID2 in human cartilage; increased amounts of both proteins were observed in late-stage osteoarthritis, where they could play a role in restoring cartilage integrity. In this study, it has also been proposed that NID1 could be involved in inflammation processes of osteoarthritis due to its chemotactic activity (205). NID1 was also found to be involved in Hirschsprung's disease: NID1 expression could be regulated by miR-192 and miR-215, which are down-regulated in colon tissues of Hirschsprung patients; as a consequence, NID1 expression is up-regulated in these subjects. Since Hirschsprung's disease is caused by an incorrect migration of enteric neural crest cells, it has been suggested that NID1 altered expression could be the cause of such incorrect migration (206).

2. AIM OF THE STUDY

Based on the observation that NK cell receptor ligands can be released in a soluble form by tumour cells concurring to tumour escape mechanisms, for the aim of the study was the search for novel NKp44 soluble ligands. To this end, we used chimeric molecules consisting of the extracellular portion of different NK cell receptors fused with a mutated Fc portion of human IgG1 (Fc molecules) that cannot be recognised by Fc receptors. The finding of novel soluble ligands for NKp44 could be useful in order to better understand the interactions between NK and tumour cells, and how tumour cells either directly or through the modification of TME, could modulate NK cell responses. Moreover, since soluble ligands often represent a mechanism of tumour escape, the finding of novel released molecules affecting NK cell functions could have an impact also on the development of prognostic systems and, possibly, on the improvement of NK cell-based cancer immunotherapy.

3. MATERIALS AND METHODS

3.1. CELL CULTURE

In this study the following cell lines were used: HEK293T (human embryonic kidney); K562 (human erythroleukemia); Bw1547 (murine thymoma); P815 (murine mastocytoma); C-32 and Mewo (melanoma); A172 and U87-MG (glioblastoma); LOVO and SW480 (colon cancer); GI-LI-N, GI-ME-N, and SH-SY5Y (neuroblastoma); LCL721.221 (B-EBV); HeLa (cervical adenocarcinoma); LNCap and PC3 (prostate cancer); A2780 (ovarian adenocarcinoma); JEG-3 (placental choriocarcinoma). Cell lines were cultured either in DMEM (HEK293T) or in RPMI1640 medium supplemented with 10% Foetal Calf Serum (FCS), 2mM L-glutamine, 100 U/ml penicillin, and 100 μg/ml streptomycin (Euroclone). K562 stable transfectants were selected and cultured in the presence of G418 sulphate (Calbiochem) at the final concentration of 1.2 mg/ml.

3.2. ANTIBODIES

The following monoclonal antibodies (mAbs), produced in our laboratory, were used in this study: 7A6 and AZ20 (IgG1, anti-NKp30), BAB281 (IgG1, anti-NKp46), Z231 (IgG1, anti-NKp44), GN18 (IgG1, anti-DNAM-1), L95 (IgG1, anti-PVR), KS38 (IgM, anti-NKp44), and 3C8 (IgM, anti-CD63).

The following commercial antibodies were also used: anti-CD335 (IgG1, clone 19A1.4.9), hamster anti-mouse CD29-PE (IgGλ, clone HMβ1-1), hamster anti-mouse CD61-PE (IgGκ, clone 2C.9.G2), and human anti-mouse CD49a-PE (IgG1, clone REA493) (Miltenyi Biotec); mouse anti-laminin γ-1 mAb (IgG1; clone D-3), mouse anti-vimentin mAb and mouse anti-Na^+/K^+-ATPase α1 (0.T.1) mAb (Santa Cruz Biotechnology); mouse anti-laminin mAb (IgG1; clone LAM-89) (Leica Biosystems); mouse anti-NID1

mAb (IgG1; clone 302117) and goat anti-NID1 polyclonal Ab (R&D); goat anti-human IgG Horseradish Peroxidase (HRP)-conjugated mAb, goat anti-mouse Ig HRP-conjugated mAb, goat anti-IgM HRP-conjugated mAb, mouse anti-goat IgG HRP-conjugated mAb, goat anti-rabbit HRP-conjugated mAb, and goat anti-mouse IgG1 PE-conjugated mAb (Southern Biotech); goat anti-human IgG PE-conjugated mAb (Jackson ImmunoResearch); goat anti-mouse IgM-AlexaFluor 647, rabbit polyclonal anti-glyceraldehyde-3-phosphate dehydrogenase (GAPDH) Ab (ThermoFisher); sheep anti-mouse IgG (GAM, MP Cappel); mouse anti-His mAb (Roche).

3.3. PREPARATION OF CELL CULTURE SUPERNATANTS AND METABOLIC LABELLING

Wild type or transfected HEK293T, K562, and Bw5147 cell lines were maintained either in medium supplemented with 1% FCS or in protein-free CD Hybridoma medium (ThermoFisher) for 48-72 h before the collection of culture supernatant (SN). When indicated, SN obtained from cell cultures in protein-free medium was concentrated with Amicon Ultracel-10K (Millipore) before the subsequent use: HEK293T-SN was concentrated up to 30-fold, while SN from wild type and transfected K562 cells were concentrated about 10-fold. Assessment of protein concentration of SN derived from culture in protein-free medium was determined using Bradford Protein Assay (Bio-Rad).

In order to perform metabolic labelling of glycoproteins, HEK293T cells were cultured in protein-free medium with 40 μM N-azidoacetylmannosamine-tetraacylated (ManAz) (ThermoFisher); after 72 h, the collected SN was concentrated about 24-fold with Amicon Ultracel-10K, then secreted glycoproteins containing azido-sugars were labelled with 200 μM Biotin-PEG_3-Phosphine (ThermoFisher) O/N at room temperature (r.t.). After labelling, HEK293T-SN-biot was dialysed in PBS (Phosphate Buffer Saline; 137 mM NaCl, 2.7 mM KCl, 10 mM Na_2HPO_4, 2 mM KH_2PO_4), using D-Tube Dialyzer Maxi, MWCO 6-8 kDa (Novagen).

3.4. PREPARATION OF SOLUBLE CHIMERIC RECEPTORS

Chimeric Fc receptors were prepared as described in (28). The sequences encoding for the extracellular portion of the different receptors (NKp30, NKp44, NKp46, and DNAM-1) were subcloned in the pRB1-2B4Fcmut vector (kindly provided by Dr. M. Falco, Ist. G. Gaslini, Genoa, Italy) in frame with the sequence coding for the human IgG1 Fc portion. In order to obtain a mutated Fc portion that does not bind to Fc receptors, three residues of the amino acid sequence were mutated as followed: L234A, L235E, and G237A. These constructs were stably transfected into HEK293 cell line using JetPEI (Polyplus) following manufacturer's instructions, and after 48-72 h cells were selected with 0.5 mg/ml G418 sulphate (Calbiochem) and subcloned by limiting dilution. Cell clones were cultured either in DMEM/10% Ultra-low IgG FCS (ThermoFisher) or in Ex-CELL ACF CHO medium (Sigma) and the soluble Fc molecules released in the collected SN were purified by affinity chromatography on Protein A

Sepharose 4 Fast Flow (Amersham Biosciences) normalised with PBS at r.t. The column was extensively washed with PBS and Fc molecules were eluted using 0.1 M glycine pH 3; next, Tris pH 8 at a final concentration of 0.1 M was used to restore the neutral pH. Fc molecules were concentrated and dialysed in PBS using Amicon Ultracel-30K (Millipore). The purified recombinant proteins were quantified using Bradford Protein Assay and checked by SDS-PAGE followed by gel staining with $AgNO_3$, and by ELISA with mAbs specific for the different receptors.

3.5. ENZYME-LINKED IMMUNOSORBENT ASSAY (ELISA)

Control of purified Fc molecules was performed coating 5 μg/ml Fc molecules diluted in PBS O/N at 4°C and saturated using PBS/3% Bovine Serum Albumin (BSA) for 3 h at r.t.. Saturated wells were washed and incubated with anti-NKp30, anti-NKp44, anti-NKp46, or anti-DNAM-1 mAbs for 1 h at r.t. followed by HRP-conjugated mAb.

In direct ELISA experiments, 100 μl of concentrated SN derived from HEK293T cells cultured in protein-free medium, 5 μg/ml recombinant human proteins (rNID1 or rNID2 (R&D), or HMGB1), exosomes, or MVs were diluted in PBS and coated on ELISA plates O/N at 4 °C. Recombinant HMGB1, obtained in the baculovirus system, was kindly provided by Dr. Marco Pedrazzi (Dept. Experimental Medicine, University of Genoa, Italy). After saturation, samples were incubated with 1 μg/ml mouse anti-NID1 or anti-CD63 mAbs, or with Fc molecules at the final concentration of 10 μg/ml (except when otherwise indicated), followed by HRP-conjugated secondary reagents.

Indirect ELISA were performed using ELISA plates coated with Fc molecules or mouse anti-NID1 mAb (5 μg/ml diluted in PBS), saturated, and incubated with 100 μl HEK293T-SN-biot or with SN of NID1-transfected or wild type HEK293T, K562, and Bw5147 cells cultured in medium with 1% FCS or in protein-free medium. HEK293T-SN-biot was then incubated with HRP-conjugated Streptavidin (Southern Biotech); alternatively, incubation with HEK293T, K562, and Bw5147 transfectant-derived SN was followed by incubation with 0.5 μg/ml polyclonal goat anti-NID1 Ab and HRP-conjugated anti-goat IgG mAb.

Competition experiments were performed on ELISA plates coated with 5 μg/ml rNID1, saturated, and incubated with 1 μg/ml Fc molecules, followed by 0.5 μg/ml goat anti-NID1 Ab and mouse anti-goat HRP-conjugated mAb.

For all ELISA experiments, the HRP substrate ABTS (2,2'-azino-di-(3-ethylbenzthiazoline sulfonic acid) (Roche) was used and the colorimetric reaction was measured with a microplate reader (TECAN Sunrise) at an optical density (O.D.) of 405 nm.

3.6. CELL LYSIS AND MEMBRANE PREPARATION

Cells were lysed in 1% Nonidet P-40 (NP-40, Sigma) in a buffer containing 150 mM NaCl, 10 mM Tris-HCl (pH 7.5), 1 mM $MgCl_2$, and protease inhibitor cocktail cOmplete (Roche).

For cell membrane preparations, cells were pelleted and lysed with 3 volumes of 0.25 M sucrose, 10 mM Tris-HCl pH 7.4, 5 mM EDTA, and protease inhibitor cocktail cOmplete and subsequently sonicated (100% amplitude 1 cycle) for 30'' for 4 times using VialTweeter (Hielscher). Next, samples were centrifuged at 500 g x 10' and the pellet containing nuclei was discarded, while the supernatant was centrifuged again at 7,500 g x 20' in order to remove the pellet containing cellular organelles contained in the pellet. Supernatant was then ultracentrifuged at 100,000 g x 1 h (Beckman Optima^{TM} Max-E) and the pellet containing cell membranes was washed twice and resuspended in PBS. Protein concentration of cell lysates and membrane preparations was determined using Bradford Protein Assay.

3.7. SDS-PAGE AND WESTERN BLOT ANALYSIS

For the control of Fc molecules, 2 μg of each sample and control mouse IgG (Sigma) were diluted in sample buffer (10% glycerol, 2% SDS, 62.5 mM Tris-HCl pH 6.8, 0.01% bromophenol blue) with the addition of 5% β-mercaptoethanol (Sigma) for 5' at 100 °C. Samples were separated by SDS-PAGE on 10% polyacrylamide gel using Tris-Glycine running buffer (4.25 M Tris-HCl pH 7.5, 2 M glycine, 1% SDS); gel was then subjected to silver staining.

For western blot experiments the following amounts of samples were used: 100 μg of cell lysates and membrane preparations, 28 μg or 30 μl of protein-free or RPMI/1% FCS SN, respectively, 160 ng of rND1, 20 μg of ECM (Sigma), Matrigel (BD Biosciences), exosomes, or MVs, or 0.2 μg of purified human laminin (Millipore). Samples were run on 7.5% or 10% polyacrylamide gel under non-reducing conditions and transferred to Immobilon-P PVDF membranes (Millipore). Immunoprecipitated samples, exosomes, and MVs were run on gel prepared with 7.5% TGX Stain-Free Acrylamide Solutions (Bio-Rad). Membranes were blocked with 5% BSA in Tris-buffered-saline containing 0.05% Tween-20 (TBS-T) and probed with 0.7 μg/ml anti-NID1 mAb, mouse anti-CD63 mAb, mouse anti-laminin γ-1 mAb (1:200, Santa Cruz Biotechnology), rabbit anti-GAPDH Ab (1:5,000), or Fc molecules (7 μg/ml) followed by the appropriate HRP-conjugated secondary reagent. The SuperSignal West Pico Chemiluminescent Substrate (ThermoFisher) was used for detection. Images were acquired with ChemiDoc Touch Imaging System (Bio-Rad) and analysed with Image Lab software (Bio-Rad).

3.8. SILVER STAINING

Silver staining of Fc molecules separated by SDS-PAGE was performed through subsequent incubation of the gel in the following solutions: A solution (50% methanol, 12% CH_3COOH) for 30'; B solution (20% ethanol, 10% CH_3COOH) for 20'; B solution/0.4 mM $KMnO_4$ for 15'; 0.7 mM K_2CO_3 for 15'; H_2O for 5'; 15 mM $AgNO_3$ for 15'; H_2O for 5'; developing solution (0.1 M K_2CO_3, 0,01% formaldehyde); fixing solution (1% CH_3COOH) for 10'.

3.9. TWO-DIMENSIONAL ELECTROPHORESIS (2-DE) AND WESTERN BLOT

Concentrated HEK293T-SN and HEK293T-SN-biot (300 μg for Western blot and 600 μg for preparative gels) were solubilised in the reduction/alkylation solution containing 8 M urea, 4% CHAPS, 5 mM tributylphosphine, 20 mM iodoacetamide (IAA), 40 mM Tris, and 0.1 mM EDTA for 3 h. To prevent over-alkylation during the isoelectro focusing (IEF) step, excess of IAA was neutralised by adding an equimolar amount of DTT. Finally, samples were dissolved in the focusing/re-hydratation solution, i.e. 7 M urea, 2 M thiourea, 4% CHAPS, and 15 mM dithioerythritol and a 0.6% carrier ampholyte cocktail, containing 40% of the pH 3.5–10 and 60% of the pH 4–8 intervals (BDH Biochemicals) and loaded onto home-made non-linear pH 3-10 strips (207). After IEF runs, the strips were equilibrated in 6 M Urea, 50 mM Tris-HCl pH 8.8, 2% SDS, 30% glycerol, and trace of bromophenol blue and the proteins were separated using a SDS-PAGE (T% 8–16) and transferred onto nitrocellulose membranes (Protean BA85, Whatman) with a semidry system. The membranes were saturated with 3% polyvinyl-pyrrolidone in TBS and incubated overnight separately with NKp44Fc, NKp30Fc, NKp30Fc, NKp46Fc in 3% BSA in TBS-T 0.15%. Then, membranes were rinsed in TBS-T and incubated with anti-human IgG HRP-conjugated antibody or Neutravidin-HRP (ThermoFisher). For preparative experiments, SDS-gels were stained with "blue silver" colloidal Coomassie (208). Images were digitalised using GS-800 scanner (Bio-Rad) and analysed with PDQuest advance 8 software (Bio-Rad).

3.10. MASS SPECTROMETRY

Spots excised from 2D-PAGE were fully discoloured and digested with trypsin. All mass spectrometric measurements were performed using a LTQ linear ion trap mass spectrometer (Thermo Electron) coupled to a HPLC Surveyor (Thermo Electron) equipped with a Jupiter C18 column 250 mm × 1 mm (Phenomenex). Protein identification was performed using SEQUEST software and searched against a Human protein database. Peptide MS/MS assignments were filtered following very high stringent criteria: Xcorr ≥1.9 for the singly charged ions, Xcorr ≥2.2 for doubly charged ions, Xcorr ≥3.7 for triply charged ions, peptide probability ≤0.01, delta Cn ≥0.1 and Rsp ≤4.26.

Polyclonal IL-2-activated NK cells derived from four different healthy donors were incubated for 21 h at 37 °C in FCS- and IL-2-deprived medium in the presence or absence of the following stimuli: directly coated rNID1 (20 μg/ml) or anti-NKp44 mAb coated via GAM. Next, cells were collected and lysed for subsequent proteomic analysis. Samples were processed by in-StageTip processing method, containing 2 SDB-RPS disks (209). 25 μL of 2% SDC, 10 mM TCEP, 40 mM CAA and 100 mM Tris pH 8.5 were added to the pellets and the cells were lysed, reduced, and alkylated in a single step and then loaded into StageTip. The lysates were diluted with 25 mM Tris pH 8.5 containing 1 μg of trypsin. Samples were acidified with 100 μl of 1% TFA and washed three times with 0.2 % TFA. Elutions were performed with

60 µl of 5% ammonium hydroxide, 80% ACN. Samples were loaded from the sample loop directly into a 75-µm ID × 50 cm 2 µm, 100 Å C18 column mounted in the thermostatated column compartment and the peptides were separated with increasing organic solvent at a flow rate of 250 nl/min using a non-linear gradient of 5-45 % solution B (80% CAN and 20% H_2O, 5% DMSO, 0.1% FA) in 180'. Eluted peptides were analysed using an Orbitrap Fusion Tribrid mass spectrometer (Thermo Scientific Instruments). Orbitrap detection was used for both MS1 and MS2 measurements at resolving powers of 120 K and 30 K (at m/z 200), respectively. Data dependent MS/MS analysis was performed in top speed mode with a 2 sec. cycle time, during which precursors detected within the range of m/z 375−1500 were selected for activation in order of abundance. Quadrupole isolation with a 1.8 m/z isolation window was used, and dynamic exclusion was enabled for 30s. Automatic gain control targets were 2.5 × 10E5 for MS1 and 5 × 10E4 for MS2, with 50 and 54 ms maximum injection times, respectively. The signal intensity threshold for MS2 was 1×10^4. HCD was performed using 28% normalised collision energy. One microscan was used for both MS1 and MS2 events.

MaxQuant software (210) (version 1.6.0.1), was used to process the raw data, setting a false discovery rate (FDR) of 0.01 for the identification of proteins, peptides and PSM (peptide-spectrum match), a minimum length of 6 amino acids for peptide identification was required. Andromeda engine, incorporated into MaxQuant software, was used to search MS/MS spectra against Uniprot human database (release UP000005640_9606 February 2017). In the processing the variable modifications are Acetyl (Protein N-Term) Oxidation (M), Deamidation (NQ), on the contrary the Carbamidomethyl (C) was selected as fixed modification. The intensity values were extracted and statistically evaluated using the ProteinGroup Table and Perseus software. Algorithm MaxLFQ was chosen for the protein quantification with the activated option 'match between runs' to reduce the number of the missing proteins.

The mass spectrometry proteomics data have been deposited to the ProteomeXchange Consortium via the PRIDE76 partner repository with the dataset identifier PXD008252. Project Name: Nidogen-1 is a novel extracellular ligand for the NKp44 activating receptor. Project accession: PXD008252. Reviewer account details: Username: reviewer37086@ebi.ac.uk Password: P4JxwhXj.

3.11. IMMUNOPRECIPITATION

Immunoprecipitation experiments were performed with 12 µg NKp44Fc, NKp30Fc, or DNAM-1Fc molecules linked to Dynabeads Protein G (ThermoFisher) and incubated O/N at 4 °C with 500 µg concentrated HEK293T-SN. Elution was carried out for 5' at 60 °C using non-reducing sample buffer.

3.12. TRANSIENT AND STABLE CELL TRANSFECTANTS

HEK293T cells were transiently transfected with pcDNA3.1-NID1 (Geneart) or with the empty vector (mock) using JetPEI following manufacturer's instructions. After 24 h the culture medium was replaced

by DMEM/1% FCS or by protein-free medium and SN were collected after 72 and 120 h.
Similarly, K562 cell line was transfected with pcDNA3.1 vector encoding for NID1 using JetPEI; after 72 h 1.2 mg/ml G418 sulphate was added to the culture medium in order to select stably transfected cells. At the end of the selection period, surviving cells were subcloned by limiting dilution.
NID1 was cloned from pcDNA3.1-NID1 into pMXs-IG (IRES-GFP) retroviral vector (kindly provided by Dr. Kitamura, Tokyo, Japan). Alternatively, NKp44 ORF and DAP12 ORF cDNAs were cloned in the two available cloning sites of pMXs-IG vector (GFP-encoding sequence was replaced by DAP12 ORF cDNA). The pMXs-IG-NID1 and pMXs-IG-NKp44/DAP12 constructs were transiently transfected into Plat-E packaging cell line in order to generate viral particles that were used to infect Bw5147 cells. NID1-positive cells were sorted according to GFP expression, while Bw-NKp44 cells were sorted based on NKp44 expression. Both cell lines were subcloned by limiting dilution. Bw-NKp30 cells, expressing a chimeric molecule composed of the extracellular region of NKp30 fused to murine CD3ζ, were kindly provided by Eric Vivier (Marseille, France).

3.13. RT-PCR ANALYSIS

Total RNA was extracted from different cell lines using RNAeasy Mini Kit (Qiagen). Oligo(dT)-primed cDNA was prepared starting from 1 μg of RNA using Transcriptor First Strand cDNA Synthesis Kit (Roche) following manufacturer's instructions. RT reaction was conducted for 10' at 42 °C followed by 50' at 55 °C. PCR reactions were carried out for 30 cycles utilising Platinum TAQ DNA Polymerase (ThermoFisher) at an annealing temperature of 58 °C (β-actin) or 62 °C (NID1). Primers used were: β-actin for 5' ACTCCATCATGAAGTGTGACG and β-actin rev 5' CATACTCCTGCTTGCTGATCC; NID1 for 5' CTCCATTGGGCCTGTGAGG and NID1 rev 5' AGACACGGGGGCGTCATC. PCR products were separated by electrophoresis on a 1.5% agarose gel and visualised by ethidium bromide staining (PCR product length: 249 bp β-actin, 795 bp NID1 isoform 1, 396 bp NID1 isoform 2).

3.14. FUNCTIONAL ASSAYS ON BW5147 CELL TRANSFECTANTS

Bw-NKp44 and Bw-NKp30 cells were pre-treated for 1 h at 37 °C with 20 or 7.5 μg/ml rNID1 or rNID2, or with 100 μl SN obtained from K562 or Bw5147 transfectants cultured in RPMI/1% FCS. Pre-treated cells were plated on 96-well cell culture plates ($1x10^5$ cells/well) coated with 5 μg/ml GAM alone or GAM plus 5 μg/ml anti-NKp44 or -NKp30 mAbs (except when indicated); alternatively, Bw5147 call transfectants were stimulated with 25 or 250 ng/ml rPDGF-DD (R&D) upon pre-treatment. For co-culture experiments, Bw cells were incubated for 1 h at 37 °C with wild type or NID1-transfected K562 or Bw cells at an effector-target (E:T) ratio of 1:1 and then transferred on mAb-coated plates. For stimulation experiments, $1x10^5$ Bw-NKp44 cells were plated on cell culture plates directly coated with 5 μg/ml of rNID1 or indirectly coated using 5 μg/ml mouse anti-NID1 or mouse anti-His mAbs followed

by rNID1. After 21 h stimulation at 37 °C, SN were collected and analysed for their IL-2 content by ELISA using the Mouse IL-2 ELISA Ready-SET-Go kit (eBioscience) following manufacturer's instructions. The range of quantification for the assay was 2-200 pg/ml. Each sample was run in duplicate.

3.15. GENERATION OF POLYCLONAL NK CELLS

NK cells were purified from peripheral blood of healthy donors using the RosetteSep™ NK Cell Enrichment Cocktail (StemCell Technologies). Cell populations displaying more than 95% of $CD56^+CD3^-CD14^-$ NK cells were selected. Purified NK cells were cultured on irradiated feeder cells in the presence of 100 U/mL rhIL-2 (Proleukin, Novartis) and 1.5 ng/mL phytohemagglutinin (Gibco Ltd) in round-bottomed 96-well microtiter plates. After 3/4 weeks of culture the expanded NK cells were used for functional experiments.

3.16. FUNCTIONAL ASSAYS ON POLYCLONAL NK CELLS

NK cell-mediated cytotoxicity against Bw and Bw-NID1 transfected cells or against the P815 $Fc\gamma R^+$ cells was evaluated in a 4 h ^{51}Cr-release test. In the redirected killing assay against P815 cells, mAbs were used as hybridoma supernatants (appropriately titrated to induce specific functional response in NK cells). 100 μl of K562-SN or K562-NID1-SN were added on NK cells 1 h before the onset of the test.

For the IFN-γ secretion assay, $1x10^5$/well NK cells were pre-treated with 100 μl K562-SN or K562-NID1-SN and cultured O/N on GAM-coated wells either in the absence or in the presence of the indicated mAbs; alternatively, pre-treated NK cells were stimulated with 50 or 250 ng/ml rPDGF-DD. Culture supernatants were then collected and analysed for the presence of IFN-γ using the IFN gamma Human ELISA kit (ThermoFisher).

3.17. FLOW CYTOMETRY

Cells were incubated with primary mAbs (50 μl of hybridoma SN or 1 μg/ml anti-NID1 mAb) or Fc molecules (20 μg/ml) in PBS/2% FCS for 30' at 4 °C, washed with 0.9% NaCl/2% FCS, and stained with the appropriate phycoerithrin (PE)- or AlexaFluor 647-conjugated isotype-matched secondary mAbs for 30' at 4 °C. For intracellular staining, cells were fixed with PBS/4% formaldehyde and permeabilised with PBS/0.01% NP-40 prior incubation with primary mAbs. Bw-NKp44 and Bw-NKp30 cell transfectants were incubated with PE-conjugated anti-integrin antibodies for 30' at 4 °C. For double immunofluorescence staining, NK cells were incubated for 1h at 4 °C with 100 μl of wild type or transfected HEK293T-derived SN obtained from cell culture in protein-free medium; next mAbs were added in the following order: anti-NID1, goat anti-mouse IgG1 PE-conjugated, anti-NKp44 IgM, and goat anti-mouse IgM-AlexaFluor 647 mAbs. All samples were analysed using a FACSCalibur flow cytometer and Kaluza software (Beckman Coulter).

3.18. IMAGING FLOW CYTOMETRY

HEK293T cells were incubated with anti-NID1 mAb followed by PE-conjugated anti-mouse IgG1 mAb. Prior to analysis, cells were stained with the nuclear dye Hoechst 33342 (ThermoFisher). Cells were acquired with a 12 channel MultiMag system ImageStream^X Mark II imaging flow cytometer (IFC) (Merck) using INSPIRE acquisition software (Amnis Corporation). Three ImageStream channels were used: channel 1 for the brightfield, channel 3 for NID1-PE (excited by a 488 nm laser), channel 7 for Hoechst44432 (excited by a 405 nm laser). In order to collect only focus-single-cells, we first restricted our analysis on the brightfield (BF) parameters analysis. Single cells were selected using a biparametric dot plot representing *BF aspect ratio* (*i.e.* width/height) versus *BF cell area* then, by mean of the *BF gradient RMS* (root mean square), which measures the sharpness quality of an image, we gated only on focus cells. For each staining condition, 4,000 raw images were collected using a 40x objective. To avoid spectral overlaps, single-colour compensation controls (500 cells each) were gathered and a compensation matrix was generated.

The raw image files were then analysed using IDEAS 6.0.3 software (Amnis Corporation) setting compensation on the basis of the calculated matrix. To verify the correspondence between data derived from traditional cytometry and IFC, we compared NID1 expression with its negative control (i.e. cells labelled only with secondary PE-conjugated antibodies) by mean of their MFI (mean fluorescence intensity). To grant a better visualization of these data, we merged the two files.

3.19. SILENCING EXPERIMENTS

NID1 expression was transiently silenced in HEK293T cells by siRNA transfection using iBONi siRNA 4-duplexes Plus sense 5'-UAAACCAUCUUGUCCACGCCCCC-3' and antisense 5'-GGGGGCGUGGACAAGAUGGUUUA-3' siRNA-NID1 (ID4811_4) and sense 5'-ACAACAUUCAUAUAGCUGCCCCC-3' and antisense 5'-GGGGGCAGCUAUAUGAAUGUUGU-3' siRNA-CTR (iBONi Negative Control-N3) (Riboxx Life Sciences). Cells were transfected with 300 nM siRNA using Amaxa Cell Line Nucleofector Kit V (Lonza) and analysed by flow cytometry after 48 and 72 h for NID1 expression. Alternatively, 50 nM siRNA were transfected in HEK293T cells with Interferin (Polyplus) following manufacturer's instructions and after 72 h SN obtained from cells cultured in protein-free medium were collected, concentrated, and analysed by Western blot with anti-NID1 mAb and NKp44Fc followed by appropriate HRP-conjugated secondary reagents.

3.20. ISOLATION OF EXTRACELLULAR VESICLES

Extracellular vesicles were isolated from SN of HEK293T cells cultured in DMEM with exosome-depleted FCS. FCS was depleted from exosomes by ultracentrifugation at 140,000 g for 2 h at 16 °C. For the isolation of extracellular vesicles, SN was first centrifuged at 16,000 g to remove cell debris and mitochondrial fraction; the microvesicles (MVs) were then isolated from the 16,000 g supernatant by

centrifugation at 22,000 g in a JA-20 rotor (Beckman Avanti™ J-25) O/N at 16 °C. The 22,000 g pellet was washed 3 times with 1 ml of PBS each time and centrifuged at 16,000 g for 10 min at 4 °C to remove any proteins. The 22,000 g supernatant was ultracentrifuged at 100,000 g in a Ti 90 rotor (Beckman Optima™ l-90K) O/N at 18 °C to pellet the exosomes. The pellet was treated as described above. The amount of proteins in exosomes and microvesicles was measured using Quant-iT Protein Assay Kit for Qubit fluorometer (ThermoFisher); prior to quantification, exosomes and microvesicles were incubated for 10' at 60 °C in 2% SDS in order to lyse the vesicles.

3.21. DOT BLOT

0.2 μg of purified human laminin or 20 μg of concentrated HEK293T-SN were spotted on nitrocellulose membrane (Whatman), saturated with TBS/5% BSA and subsequently stained with mouse anti-laminin mAb (1:200, Leica Biosystems) or with 7 μg/ml Fc molecules followed by the appropriate HRP-conjugated secondary mAbs. The SuperSignal West Pico Chemiluminescent Substrate (ThermoFisher) was used for detection. Images were acquired with ChemiDoc Touch Imaging System (Bio-Rad) and analysed with Image Lab software (Bio-Rad).

3.22. STATISTICAL ANALYSES

Data were analysed using GraphPad Prism 6 by non-parametric two-tailed Mann-Whitney test or by non-parametric one tailed Wilcoxon test. A *p* value of less than 0.05 (*), 0.01 (**), or 0.001 (***) was considered statistically significant. Data obtained from mass spectrometry experiments were analysed with R or Perseus software.

4. RESULTS

4.1. CHARACTERISATION OF SOLUBLE LIGAND(S) FOR NKp44 RECEPTOR

In order to identify novel NKp44 soluble ligand(s), we selected HEK293T cell line as experimental model, since flow cytometry analysis, performed with NKp44Fc on a panel of different cell lines, revealed that HEK293T cells could express NKp44 ligand(s). Moreover, these cells can be easily cultured in protein-free medium, essential in order to obtain cell culture SN containing only proteins released from cultured cells. To this end, HEK293T-SN was collected after 72 h cell culture in protein-free medium; subsequently, it was concentrated and used in direct ELISA experiments to test NKp44Fc reactivity against coated HEK293T-SN. Our results indicated within HEK293T-SN the presence of soluble ligand(s) for NKp44Fc and NKp46Fc chimeric receptors, while no reactivity was observed with neither NKp30Fc nor DNAM-1Fc (Fig. 6A). With the aim of further characterising NKp44 soluble

ligand(s), we analysed HEK293T-SN by SDS-PAGE and immunoblotting using different Fc molecules: NKp44Fc and NKp46Fc were the only chimeric molecules interacting with HEK293T-SN, as already observed in ELISA experiments (Fig. 6B). Notably, NKp44Fc clearly identified a band of approximately 180 kDa, in contrast with NKp46Fc that weakly recognised multiple bands at different molecular weights. Finally, as secreted proteins are frequently glycosylated, we investigated whether NKp44 ligand(s) could be represented by glycoproteins. To this end, we collected SN of HEK293T cell line cultured in the presence of protein-free medium supplemented with modified sugars (i.e. azido-sugars). Cultured cells can uptake the azido-sugars from the medium and employ them to glycosylate proteins; moreover, the presence of an azido group allows the conjugation of labelled glycoproteins with biotin.

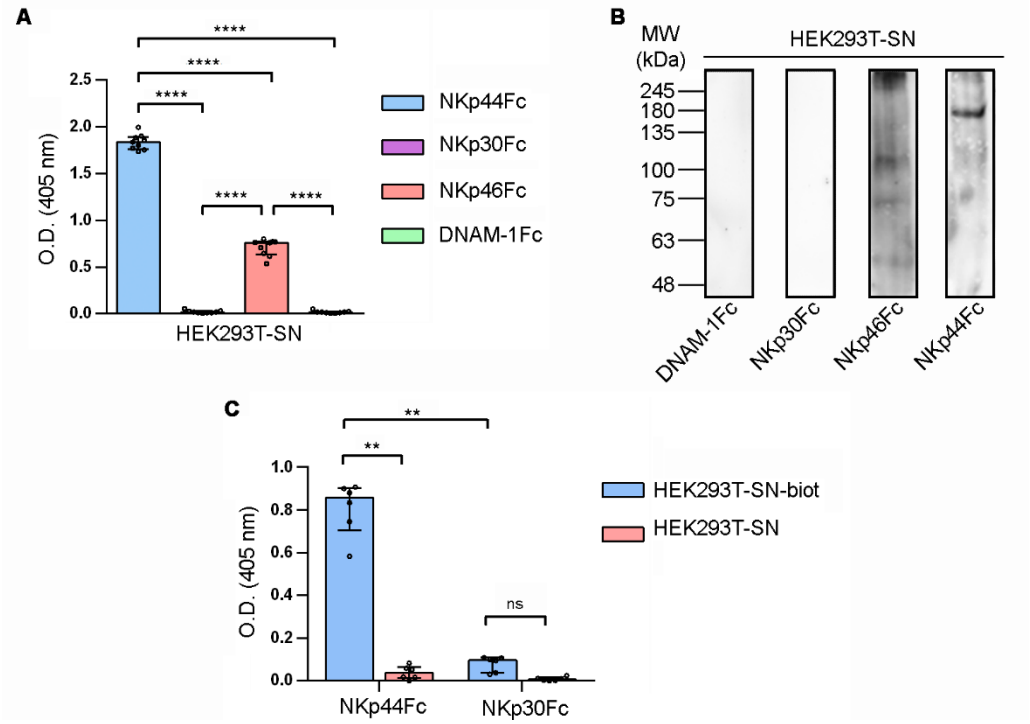

Figure 6. Reactivity of different Fc molecules with HEK293T-SN
A) HEK293T-SN-coated ELISA plates were incubated with the indicated Fc molecules followed by HRP-conjugated anti-human IgG mAb. Graph represents the absorbance at 405 nm after normalization to background (nonspecific binding of the HRP-conjugated mAb). Data are medians ± interquartile range of three independent experiments performed in triplicate, dots represent single values; ****p<0.0001 by two-tailed Mann-Whitney test. (B) Concentrated HEK293T-SN was loaded in each lane and analysed by SDS-PAGE on a 7.5% polyacrylamide gel. Samples were immunoblotted with the indicated Fc molecules followed by HRP-conjugated anti-human IgG mAb. One representative experiment of three is shown. (C) HEK293T-SN-biot or HEK293T-SN, as negative control, was incubated on NKp44- or NKp30-coated ELISA plates followed by HRP-conjugated Streptavidin. Graph represents the absorbance at 405 nm after normalization to background (nonspecific binding of the HRP-conjugated Streptavidin). Data are medians ± interquartile range of three independent experiments performed as duplicates, dots represent single values; **p=0.0022, ns (not significant)=0.0606 by two-tailed Mann-Whitney test.

Next, biotin-tagged soluble glycoproteins contained in HEK293T-SN (HEK293T-SN-biot) were concentrated and incubated on NKp44Fc- or NKp30Fc-coated ELISA plates, followed by HRP-

conjugated Streptavidin. Results indicated that NKp44Fc could recognise soluble glycoprotein(s), while no reactivity was detected in NKp30-coated wells (Fig. 6C).

4.2. IDENTIFICATION OF A NKp44 CANDIDATE LIGAND

Once established that NKp44 could recognise soluble glycosylated protein(s) at high MW, we combined two-dimensional electrophoresis (2-DE) and mass spectrometry analyses in order to identify such ligand(s). Proteins contained in HEK293T-SN and HEK293T-SN-biot were resolved by 2-DE and subsequently immunoblotted with different Fc molecules or HRP-conjugated Neutravidin, respectively (Fig. 7A-D). Notably, 2-DE analysis of HEK293T-SN with distinct Fc molecules revealed a stronger reactivity of all Fc molecules than that observed in the previously shown mono-dimensional SDS-PAGE: we hypothesise that this different reactivity might reflect differences in experimental procedures. Fig. 7E shows a preparative gel in which HEK293T-SN proteins were stained with Blue Coomassie: from this

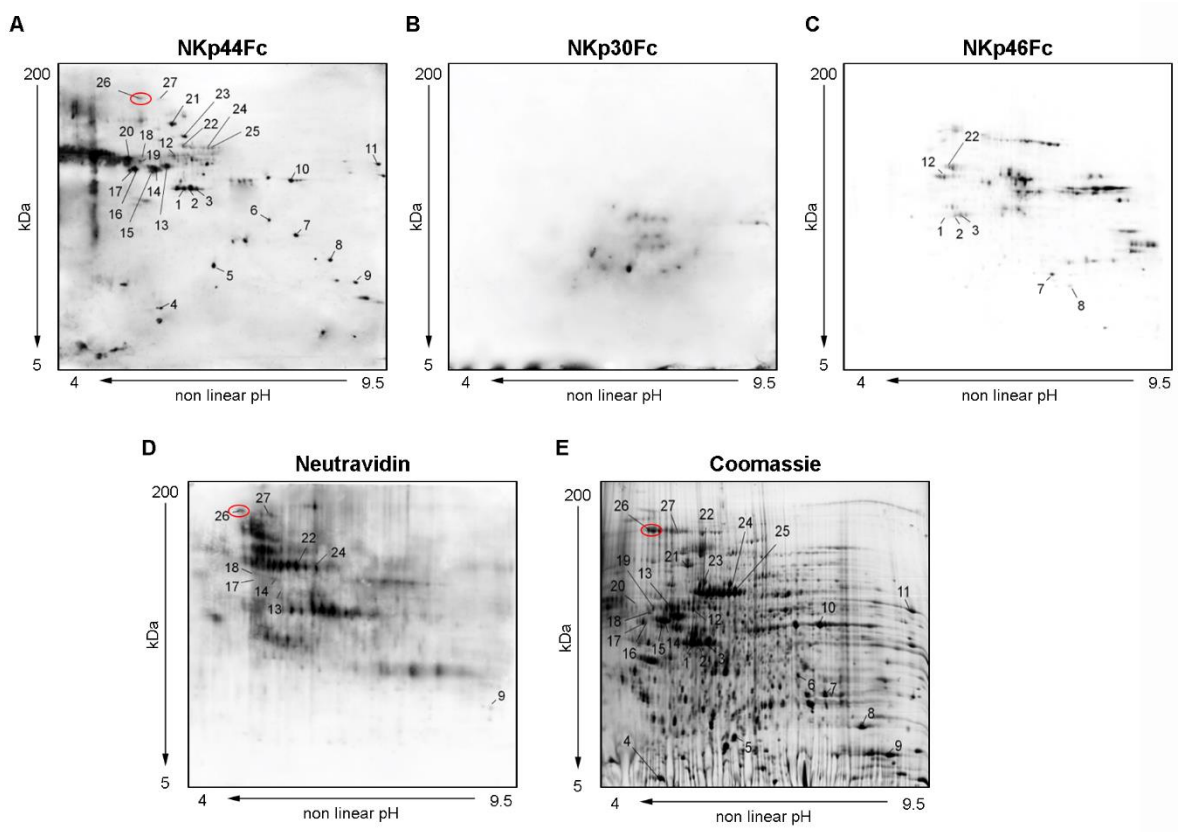

Figure 7. Analysis of HEK293T-SN and HEK293T-SN-biot by two-dimensional electrophoresis (2-DE)
(A, B, C) Concentrated HEK293T-SN was analysed by 2-DE and, after blotting, membranes were stained with NKp44Fc (A), NKp30Fc (B), or NKp46Fc (C) followed by HRP-conjugated anti-human IgG mAb. (D) 2-DE separation was applied to concentrated HEK293T-SN-biot and the membrane was probed with HRP-conjugated Neutravidin. (E) HEK293T-SN proteins, separated by 2-DE, were stained with "blue silver" colloidal Coomassie. Spots excised for the subsequent mass spectrometry analysis are numbered from 1 to 27; spot 26 is highlighted with a red circle in panels (A), (D), and (E).

Spot number	Protein name	Accession number	Gene name	MW [kDa]	Calculated pI	Glycosylation	Coverage	Score	Unique Peptides	Peptides
1	Actin, alpha cardiac muscle 1	P68032	ACTC1	42	5,39		47,75	2205,43	10	36
	Actin, cytoplasmic 1, N-terminally processed	B4DW52		38,6	5,35		72,33	6267,78	23	55
2	Creatine kinase B-type	P12277	CKB	42,6	5,59		68,24	6481,06	31	37
	DDB1- and CUL4-associated factor 7	P61962	DCAF7	38,9	5,52		11,99	140,7	3	3
3	Beta-actin-like protein 2	Q562R1	ACTBL2	42	5,59		32,71	1061,2	7	23
	Mannose-6-phosphate isomerase	P34949	MPI	46,6	5,95		19,86	300,36	7	7
4	**Phosphoglycerate mutase 1**	E7EMA8		16,1	6,19		22,22	61,59	2	2
5	**Heat shock protein beta-1**	P04792	HSPB1	22,8	6,4		13,17	5,36	2	2
	Hypoxanthine-guanine phosphoribosyltransferase	P00492	HPRT1	24,6	6,68		48,62	354,32	8	8
	Isoform 2 of Triosephosphate isomerase	P60174-1	TPI1	26,7	6,9		34,94	306,14	6	6
	Peroxiredoxin-6	P30041	PRDX6	25	6,38		78,57	2435,06	33	33
	Protein-L-isoaspartate O-methyltransferase	B7Z972		20,7	6,87		19,27	57,93	3	3
6	**Isoform 2 of Syntenin-1**	O00560-2	SDCBP	32,3	7,53		12,12	6,34	2	2
	S-formylglutathione hydrolase	P10768	ESD	31,4	7,02		58,16	1197,5	15	15
	Ubiquitin-like modifier activating enzyme 1 (Fragment)	Q5JRR9	UBA1	29,2	4,98		9,23	59,57	2	2
7	Carbonic anhydrase 2	P00918	CA2	29,2	7,4		48,08	1445,49	15	15
8	Phosphatidylethanolamine-binding protein 1	P30086	PEBP1	21	7,53		45,45	1289,65	7	7
9	**Peptidyl-prolyl cis-trans isomerase A**	P62937	PPIA	18	7,81	+	74,55	5039,91	25	25
10	Alpha-enolase	P06733	ENO1	47,1	7,39		74,42	9589,04	36	41
11	**Pyruvate kinase isozymes M1/M2**	P14618	PKM	57,9	7,84		59,51	4605,29	32	32
12	Protein disulfide-isomerase A3	P30101	PDIA3	56,7	6,35		56,44	1807,68	26	26
	Xaa-Pro dipeptidase	P12955	PEPD	54,5	6		32,66	876,84	14	14
13	**ATP synthase subunit beta (Fragment)**	H0YH81	ATP5B	38,2	5,55		26,8	248,48	7	7
	Drebrin-like protein	B4DDP6	DBNL	43	5,03		6,54	39,66	2	2

Table 3. Proteins identified in 27 selected spots analysed by mass spectrometry

Proteins are grouped according to the spots in which they were identified. For each protein, name, accession number, gene name, MW, calculated pI, glycosylation, coverage, score, unique peptides, and total peptides are indicated. The symbol '+' indicates the presence of glycosylation according to protein databases. Underlined proteins derive from glycosylated spots; bolded proteins have been identified in spots specifically stained by NKp44Fc; Nidogen-1 is highlighted in red.

	Hydroxymethylglutaryl-CoA synthase, cytoplasmic	Q8N995		56,2	5,41		9,23	89,13	4	4
	Isoform 2 of 26S protease regulatory subunit 6B	P43686-2	PSMC4	43,5	5,26		5,94	4,95	2	2
	Probable serine carboxypeptidase CPVL	Q9H3G5	CPVL	54,1	5,62	+	9,66	61,54	4	4
	Tubulin alpha-1A chain	G3V1U9	TUBA1A	46,3	5,08		75	5334,93	2	49
	Tubulin alpha-1C chain	Q9BQE3	TUBA1C	49,9	5,1		69,04	5186,38	4	49
	Tubulin alpha-4A chain	A8MUB1	TUBA4A	48,3	5,01		57,74	2883,1	6	39
	Vimentin	B0YJC4	VIM	49,6	5,25		22,51	237,27	9	9
14	**Tubulin beta chain**	F8VW92		48,5	5,2		74,25	8104,68	9	54
	Tubulin beta-2B chain	Q9BVA1	TUBB2B	49,9	4,89		67,42	6186,49	2	48
	Tubulin beta-4B chain	P68371	TUBB4B	49,8	4,89		71,69	6533,26	3	50
	Tubulin beta-6 chain	B4DP54	TUBB6B	46,7	4,89		42,58	2363,26	4	30
15	**Cathepsin D**	F8WD96	CTSD	30	7,42		15,22	114,52	3	3
	Elongation factor 1-alpha 1	P68104	EEF1A1	50,1	9,01		4,98	69,65	2	2
	Fructose-bisphosphate aldolase A (Fragment)	H3BPS8	ALDOA	30,4	7,52		12,23	82,41	2	2
	Glyceraldehyde-3-phosphate dehydrogenase	E7EUT5	GAPDH	27,9	6,95		11,15	88,76	2	2
	Involucrin	P07476	IVL	68,4	4,61		3,93	41,89	2	2
	L-lactate dehydrogenase	F5H308		33,6	8,79		9,87	52,12	3	3
	Prelamin-A/C	Q3BDU5	LMNA	55,6	6,65		6,78	131,81	3	3
	Tubulin beta chain	F5H894		23,5	6,9		9,18	44,31	2	2
16	**Actin, cytoplasmic 2, N-terminally processed**	F5H0N0		37,4	5,58		14,11	144,91	3	3
17	**Alpha-galactosidase A**	P06280	GLA	48,7	5,6	+	9,56	134,69	3	3
	Isoform 3 of Histone-binding protein RBBP4	Q09028-3	RBBP4	46,1	5,07		32,2	790,49	11	11
18	**Isoform 2 of Carboxypeptidase E**	P16870-2	CPE	49,9	5,17	+	5,23	61,74	2	2
	Tubulin alpha-1C chain	E9PGK3		36,7	8,44		13,19	81,01	3	3
	UV excision repair protein RAD23 homolog B	P54727	RAD23B	43,1	4,84		44,01	960,84	17	17
19	**Protein disulfide-isomerase**	P07237	P4HB	57,1	4,87		20,67	279,19	9	9

20	**Telomeric repeat-binding factor 2-interacting protein 1**	Q9NYB0	TERF2IP	44,2	4,73		23,56	193,59	7	7
	Tubulin alpha-1A chain	F8VXZ4		33,5	4,93		7,05	43,17	2	2
	Tubulin beta chain	E7EWR1		39,7	4,93		9,07	140,13	3	3
	Zinc finger protein ZPR1	O75312	ZPR1	50,9	4,73		37,25	1840,08	15	15
21	**SUMO-activating enzyme subunit 2**	Q9UBT2	UBA2	71,2	5,29		17,5	247,75	9	9
	Transitional endoplasmic reticulum ATPase	P55072	VCP	89,3	5,26		53,85	2745,79	40	40
	Ubiquitin-like modifier-activating enzyme 1	P22314	UBA1	117,8	5,76		2,84	59,52	2	2
22	Dystroglycan	Q14118	DAG1	97,4	8,56	+	4,13	49,49	2	2
	Keratin, type I cytoskeletal 14	P02533	KRT14	51,5	5,16		9,11	106,95	3	4
	Keratin, type II cytoskeletal 5	P13647	KRT5	62,3	7,74		7,97	91,26	2	4
	POTE ankyrin domain family member I	P0CG38	POTEI	121,2	6,21		9,3	1326,49	4	15
23	**Heat shock 70 kDa protein 1A/1B**	P08107	HSPA1A	70	5,66		31,98	2037,29	15	17
	Heat shock cognate 71 kDa protein	P11142	HSPA8	70,9	5,52		44,43	2929,92	2	26
	Keratin, type I cytoskeletal 9	P35527	KRT9	62	5,24		7,22	33,47	4	4
	Stress-70 protein, mitochondrial	B7Z4V2		72,4	5,94		13,83	273,61	7	7
	V-type proton ATPase catalytic subunit A	B7Z1R5	ATP6V1A	64,7	5,66		12,84	169,13	6	6
24	**Isoform 2 of Tripeptidyl-peptidase 1**	O14773-2	TPP1	34,4	6,09	+	8,75	37,75	2	2
25	**Ras GTPase-activating protein-binding protein 1**	F8W7N6		34,7	5,66		9,42	41,47	2	2
26	**Nidogen-1**	P14543	NID1	121,9	5,47	+	7,18	149,94	6	6
	Isoform 2 of Ras GTPase-activating protein SynGAP	Q96PV0-2	SYNGAP1	141,2	9,03		3,04	28,85	3	3
	Laminin subunit beta-1	P07942	LAMB1	197,9	4,94	+	2,35	7,76	3	3
	Laminin subunit gamma-1	P11047	LAMC1	177,5	5,12	+	11,31	212,31	14	14
27	**Collagen alpha-1(VI) chain**	P12109	COL6A1	108,5	5,43	+	18,09	760,34	15	15
	Desmoplakin	P15924	DSP	331,6	6,81		3,03	130,84	8	8
	Nidogen-1	P14543	NID1	121,9	5,47	+	0,99	93,94	1	1
	Junction plakoglobin	P14923	JUP	81,7	6,14	+	4,43	154,74	3	3

gel, 27 spots corresponding to those visualised also in NKp44Fc blot were excised and analysed by mass spectrometry (Table 3). Next, by comparison with blot stained with NKp30Fc, NKp46Fc, and Neutravidin, we selected nine spots specifically recognised by NKp44Fc and containing glycosylated

proteins. Among these spots, we focused our attention on spots 26 and 27, corresponding to high MW proteins: within spot 26 we selected NID1 as a candidate ligand for NKp44 receptor.

4.3. NKp44 CAN INTERACT WITH NID1

In order to investigate whether NID1 could be specifically recognised by NKp44Fc in different conditions, we initially performed immunoprecipitation experiments from HEK293T-SN using NKp44Fc, NKp30Fc, and DNAM-1Fc molecules; immunoprecipitated samples were separated by SDS-PAGE under non-reducing conditions. Subsequent immunoblotting with anti-NID1 monoclonal antibody (mAb) revealed that NID1 was immunoprecipitated by NKp44Fc, but not by NKp30Fc nor by DNAM-1Fc (Fig. 8A). In addition, we performed mass spectrometry analysis, confirming the presence of NID1 in NKp44-immunoprecipitated samples and its absence in NKp30Fc and DNAM-1Fc immunoprecipitates (Table 4). Since NID1 is a BM component, we next analysed two commercial solubilised BM preparations, ECM (Sigma-Aldrich) and Matrigel (BD Bioscience): as expected, and in accordance with previously published data (211), Western Blot analysis confirmed the presence of NID1 in both preparations. In particular, anti-NID1 mAb identified two different bands, probably representing NID1 cleaved forms, due to the presence of proteases within ECM and Matrigel. Interestingly, in both samples NKp44Fc recognised a band of about 80 kDa, possibly corresponding to a proteolytic product of NID1 (Fig. 8B). Immunoprecipitation experiments performed on ECM with different Fc molecules and analysed by mass spectrometry confirmed that NKp44Fc, but not other Fc molecules, could bind NID1. Interestingly, we also detected ADAMTS1 protease within NKp44Fc immunoprecipitates from both ECM and HEK293T-SN (Table 4), supporting the idea that NID1 degradation products could derive from NID1 cleavage by proteases, such as ADAMTS1, MMP-2, MMP-9, and urokinase, which are components of basement membrane-like matrix (211).

In order to specifically assess the interaction between NKp44Fc and NID1, we used a recombinant form of NID1 (rNID1). Fig. 8C shows that NKp44Fc, but not NKp30Fc nor DNAM-1Fc, recognised rNID1 in Western Blot experiments carried out under non-reducing conditions. rNID1 was also utilised in ELISA experiments: the recombinant protein was coated to ELISA plates and subsequently incubated with scalar concentrations of different Fc molecules, ranging from 2,5 to 80 μg/ml: also in this conditions, NKp44Fc was the only Fc molecule able to bind rNID1 (Fig. 8D). Finally, we performed competition experiments incubating NKp44Fc or NKp30Fc on rNID1-coated ELISA plates, followed by anti-NID1 Ab and its specific HRP-conjugated secondary antibody. We observed a reduction of anti-NID1 Ab binding in the presence of NKp44Fc as compared to control conditions (Fig. 8E), suggesting that NKp44Fc could compete with anti-NID1 Ab for NID1 binding.

Taken together, these results indicate that NKp44 could interact with denatured NID1, and more importantly, recognise NID1 also in its native conformation. In addition, these observations suggest

that NKp44 binds a linear epitope of NID1 and, thus, that also NID1 fragments cleaved by proteases could be recognised by NKp44 receptor.

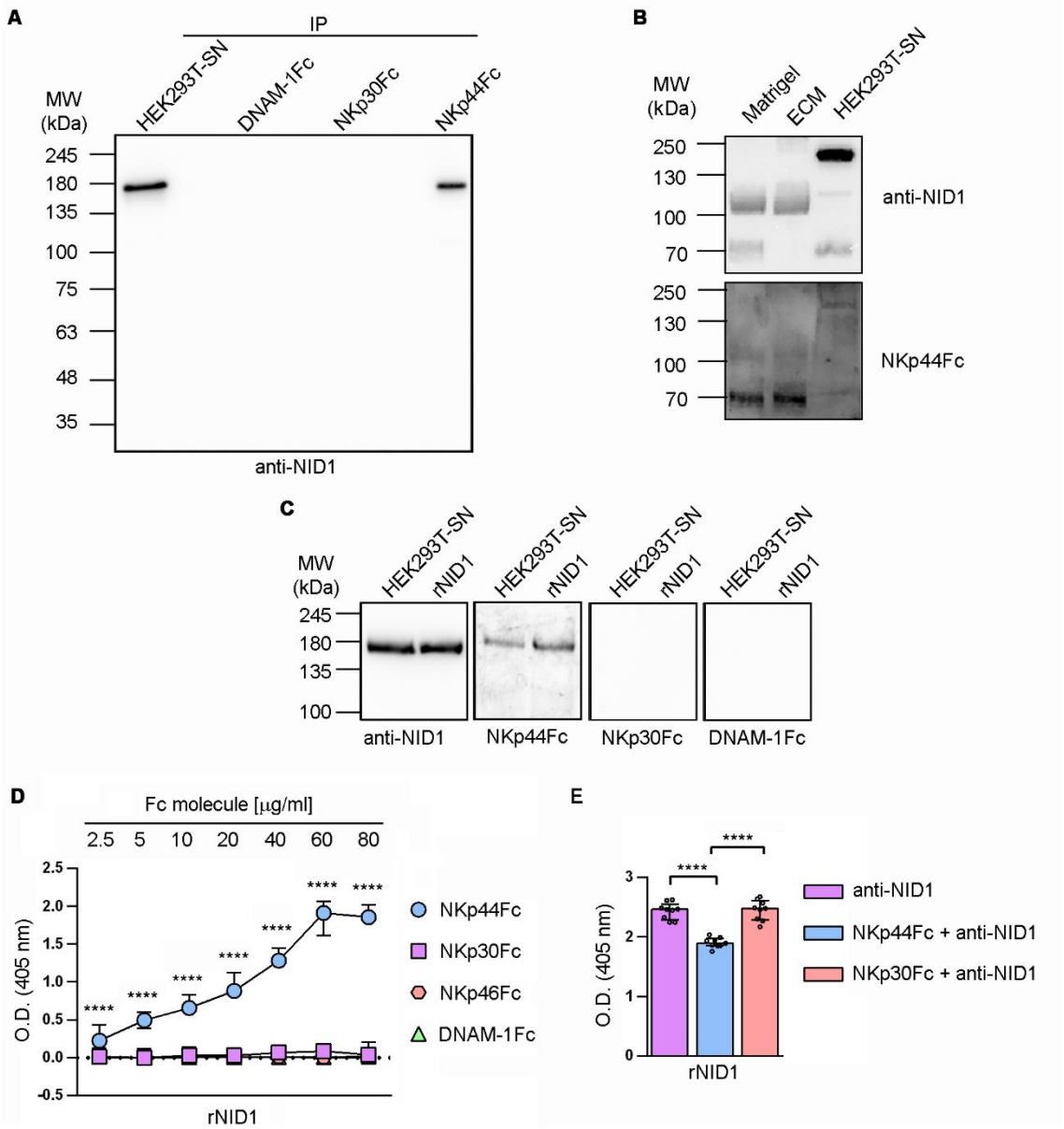

Figure 8. Specific recognition of NID1 by NKp44Fc soluble receptor

(A) HEK293T-SN immunoprecipitated with the indicated Fc molecules was analysed by 7.5% SDS-PAGE under non-reducing conditions together with concentrated HEK293T-SN, as positive control. After blotting, the membrane was probed with mouse anti-NID1 mAb followed by HRP-conjugated anti-mouse IgG mAb. (B) Matrigel, ECM, and HEK293T-SN samples were separated by 10% SDS-PAGE and, after blotting, the membrane was stained with anti-NID1 or NKp44Fc followed by HRP-conjugated anti-mouse IgG or anti-human IgG mAb, respectively. (C) HEK293T-SN and rNID1 were analysed by SDS-PAGE on a 7.5% polyacrylamide gel under non-reducing conditions and, after blotting, stained with the indicated Fc molecules or with anti-NID1 mAb, followed by HRP-conjugated anti-human or anti-mouse IgG, respectively. One representative experiment of three (A and B) or five (C) is shown. (D) rNID1-coated ELISA plates were incubated with scalar doses of the indicated Fc molecules followed by HRP-conjugated anti-human IgG mAb. (E) NKp44Fc or NKp30Fc, as negative control, were incubated on rNID1-coated ELISA plates, subsequently goat anti-NID1 Ab was added followed by HRP-conjugated anti-goat IgG mAb. Graphs represent the absorbance at 405 nm after normalization to background (nonspecific binding of the secondary reagent). Data are medians of triplicates ± interquartile range and are the pooled results of three independent experiments, in (D) dots represent single values; ****p<0.0001 by two-tailed Mann-Whitney test.

Experiment	NID1	ADAMTS1	Protein	Score	Peptides	Coverage
IP NKp44Fc from SN	+	+	NID1	25.03	8	10.50
			ADAMTS1	54.03	8	15.10
Total ECM	+	-	NID1	508	33	40.40
			ADAMTS1	-	-	-
IP NKp44Fc from ECM	+	+	NID1	68.82	17	19.84
			ADAMTS1	10.10	1	1.91
IP NKp30Fc from ECM	-	-	-	-	-	-
IP DNAM-1Fc from ECM	-	-	-	-	-	-

Table 4. Summary table of samples analysed by mass spectrometry
The symbols '+' and '-' indicate the presence or the absence of the protein, respectively. Score, number of identified peptides, and the sequence coverage are indicated for each identified protein.

4.4. PRODUCTION AND ANALYSIS OF NID1 TRANSFECTANTS

In order to further support our observations, we decided to investigate whether a correlation exists between NKp44Fc binding and NID1 expression, utilising cell transfectants as a model. In particular, we analysed NID1 expression both in total cell lysates and in SN obtained from different NID1 transfectants (Figs. 9-11). Since FCS contains NID1, the experiments were performed by culturing cells in medium supplemented with 1% FCS, in order to reduce the possible interference of NID1 contaminants, or, alternatively, in protein-free medium. At first, we transiently transfected HEK293T cells (already expressing NID1) with an expression vector containing NID1 cDNA or with an empty vector (mock) as control. Western blot analysis performed with anti-NID1 mAb both in cell lysates and in non concentrated SN obtained from transfectants cultured in protein-free medium revealed an increase of NID1 levels in HEK293T-NID1 samples; moreover, NKp44Fc staining indicated the presence of a band of approximately 180 kDa in NID1-trasfected cell lysates and in the corresponding SN (Fig. 9A-B). In contrast with the results displayed in Fig. 8C, only a weak signal was detected in HEK293T-SN using anti-NID1 mAb (Fig. 9A): this discrepancy is due to the fact that in the former experiment concentrated HEK293T-SN was used, whereas in the latter one SN was not concentrated. For the same reason, NKp44Fc did not reveal any band in non concentrated HEK293T-SN (Fig. 9B). SN derived from HEK293T-transfected cells was also analysed by ELISA: when ELISA plates were coated with anti-NID1 mAb and subsequently incubated with SN followed by an anti-NID1 polyclonal Ab, a positive signal was detected only in the wells incubated with HEK293T-NID1-SN (Fig. 9C), confirming an increased secretion of NID1 by NID1-transfected cells. More importantly, we performed sandwich ELISA in which NKp44Fc- or NKp30Fc-coated ELISA plates were incubated with SN derived from transfected and wild type cells, followed by anti-NID1 Ab. In this experimental setting, we obtained a positive result only when HEK293T-NID1-SN was incubated on NKp44Fc-coated wells (Fig. 9D). Similar results were obtained when SN from HEK293T transfectants cultured in DMEM/1% FCS was utilised (data not shown).

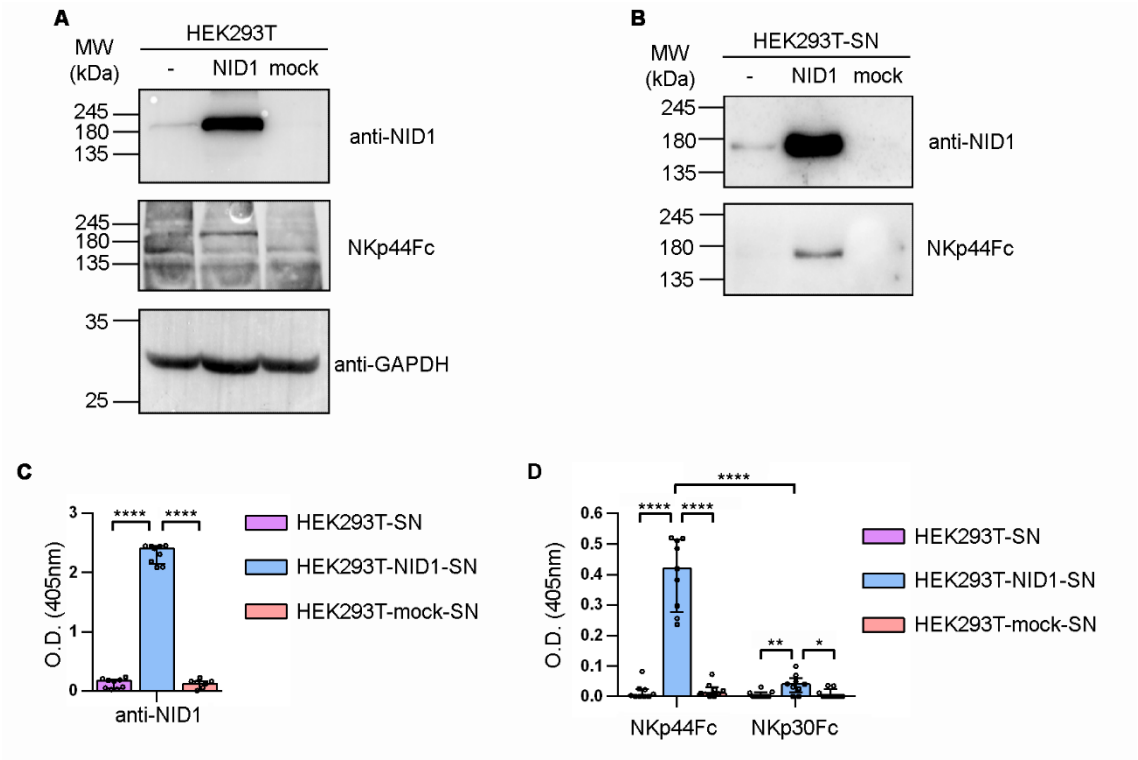

Figure 9. NID1 protein expression in HEK293T NID1- transfected cells and in the corresponding SN
(A, B) Total cell lysates (A) and SN (B) derived from HEK293T and the corresponding NID1 and mock transfectants cultured in protein-free medium were analysed in SDS-PAGE on a 10% and 7.5% polyacrylamide gel, respectively; membranes were probed with NKp44Fc molecule, mouse anti-NID1, or rabbit anti-GAPDH Abs followed by the appropriate HRP-conjugated secondary mAb. One representative experiment of three is shown. (C, D) SN obtained from HEK293T transfectants cultured in protein-free medium were incubated on ELISA plates coated with mouse anti-NID1 mAb (C) or the indicated Fc molecules (D), followed by goat anti-NID1 Ab and HRP-conjugated anti-goat IgG Ab. Graphs represent absorbance at 405 nm after normalization to background (nonspecific binding of goat anti-NID1 plus secondary reagent). Data are medians of triplicates ± interquartile range and are the pooled results of three independent experiments, dots represent single values. ****p<0.0001, *p=0.0239 and **p=0.0093 by two-tailed Mann-Whitney test.

Next, we produced NID1 stable transfectants; to this end, we chose two different recipient cells that did not express NID1 mRNA: human K562 and murine Bw5147 cell lines (Figs. 10-11). NID1 expression in K562 transfectants was confirmed both at the mRNA and protein levels. Fig. 10A shows NID1 mRNA expression in wild type and NID1-transfected K562 cells. By Western blot and ELISA, NID1 protein expression was demonstrated in both total cell lysates and concentrated SN derived from K562-NID1 cells but not from wild type cells. It is of note, however, that K562 transfectants expressed lower NID1 levels as compared to HEK293T-NID1 cells: this could explain why we were not able to detect NID1 in total cell lysates using NKp44Fc (Fig. 10B). K562-NID1 transfectants were cultured in protein-free medium and because of the relatively low NID1 protein levels, the collected SN were concentrated before analysis: Western blot on concentrated K562-NID1-SN revealed NID1 expression both with anti-NID1 mAb and with NKp44Fc (Fig. 10C). In addition, in line with results obtained with HEK293T-NID1-SN, sandwich ELISA revealed NID1 in K562-NID1-SN but not in K562-SN (Fig. 10D-E).

Similar experiments were performed with Bw-NID1 transfected cells cultured in RPMI/1% FCS, demonstrating that NID1 could be *de novo* expressed and released in stably transfected cells (Fig. 11A-D).

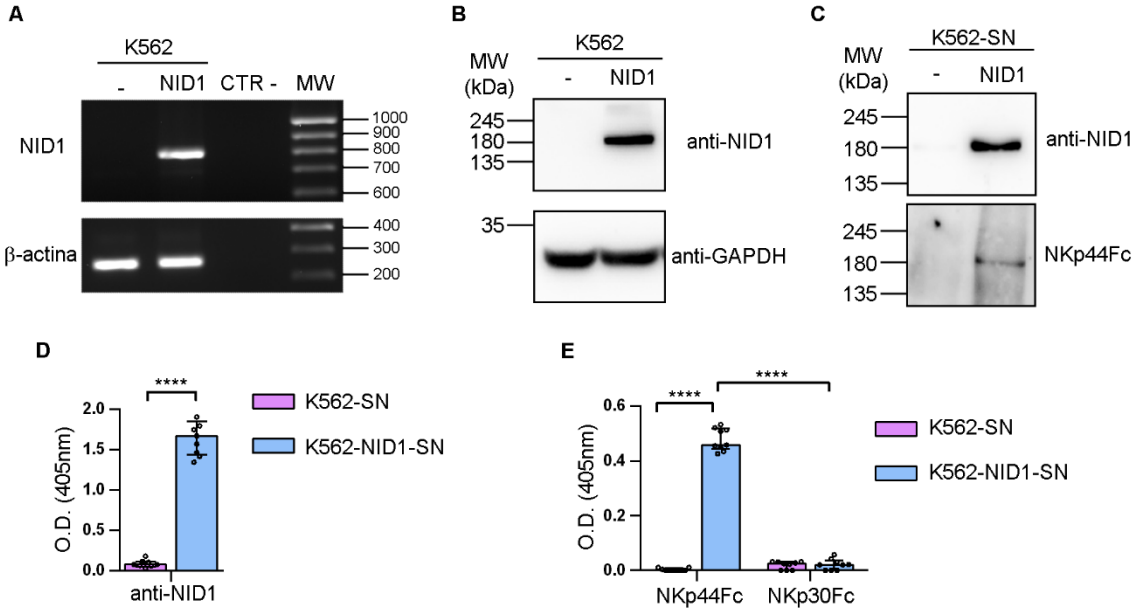

Figure 10. NID1 mRNA and protein expression in K562 cell line and transfectants
(A) NID1 mRNA expression was assessed by RT-PCR in wild type and NID1-transfected K562 cells. Primers specific for β-actin were utilised as positive control. PCR products were run on 1.5% agarose gel and visualised by ethidium bromide staining. One representative experiment of three is shown. (B, C) Total cell lysates (B) and concentrated SN (C) derived from K562 and the corresponding NID1 transfectants cultured in protein-free medium were analysed in SDS-PAGE on 10% and 7.5% polyacrylamide gel, respectively; membranes were probed with NKp44Fc molecule, mouse anti-NID1, or rabbit anti-GAPDH Abs followed by the appropriate HRP-conjugated secondary mAb. One representative experiment of three is shown. (D, E) Concentrated SN obtained from K562 cell transfectants cultured in protein-free medium was incubated on ELISA plates coated with mouse anti-NID1 mAb (D) or the indicated Fc molecules (E), followed by goat anti-NID1 Ab and a HRP-conjugated anti-goat IgG Ab. Graphs represent absorbance at 405 nm after normalization to background (nonspecific binding of goat anti-NID1 plus secondary reagent). Data are medians of triplicates ± interquartile range and are the pooled results of three independent experiments; dots represent single values. ****p<0.001 by two-tailed Mann-Whitney test.

4.5. SOLUBLE NID1 INHIBITS NK CELL FUNCTIONS

Having demonstrated NID1 recognition by NKp44, we evaluated the functional effects induced by soluble NID1 (sNID1) through NID1-NKp44 interaction. To this end, we utilised an experimental model consisting of Bw5147 transfectants expressing either NKp44/DAP12 receptor complex (Bw-NKp44) or chimeric NKp30-CD3ζ receptor (Bw-NKp30): receptor cross-linking with specific mAbs induces IL-2 release, which can be assessed by ELISA. Since different soluble ligands for activating NK cell receptors have been described to interfere with the transduction of activating signals, we investigated a possible inhibitory effect exerted by rNID1 on IL-2 release by Bw-NKp44 and Bw-NKp30 cells. The experiment was carried out by pre-treating cells with 20 μg/ml rNID1 and stimulating them by mAb-mediated receptor crosslinking. Pre-treatment with rNID1 could inhibit IL-2 release by Bw-NKp44 cells stimulated with two different anti-NKp44 mAb concentrations; in this experimental setting, however, rNID1 could

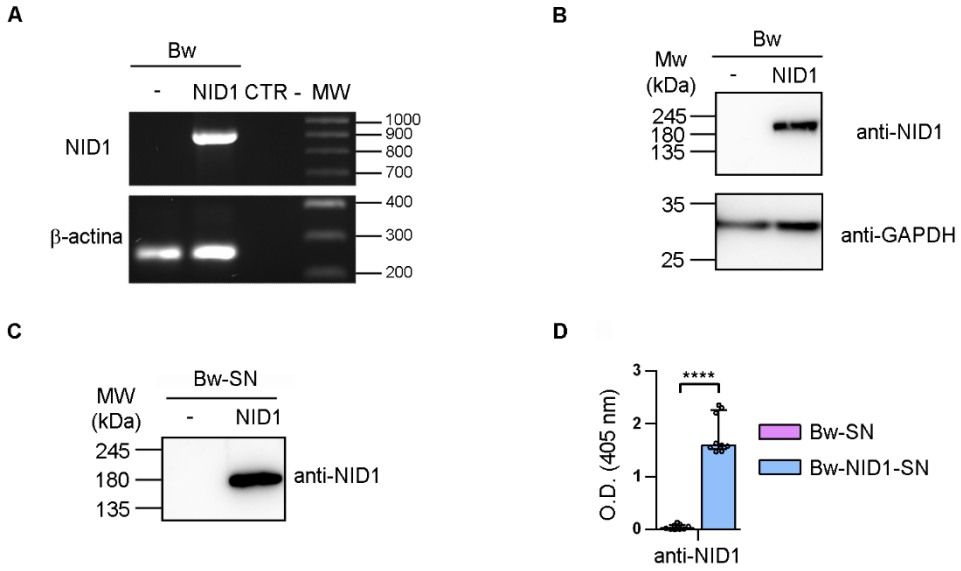

Figure 11. NID1 mRNA and protein expression in Bw5147 cell line and transfectants
(A) NID1 mRNA expression was assessed by RT-PCR in Bw5147 cells and in the corresponding NID1 transfectants. Primers specific for β-actin were utilised as positive control. PCR products were run on 1.5% agarose gel and visualised by ethidium bromide staining. One representative experiment of three is shown. (B, C) Total cell lysates (B) and SN (C) derived from Bw5147 cells and the corresponding NID1 transfectants were analysed by SDS-PAGE on a 10% and 7.5% polyacrylamide gel, respectively; membranes were probed with mouse anti-NID1 or rabbit anti-GAPDH Abs followed by the appropriate HRP-conjugated secondary mAbs. One representative experiment of two is shown. (C) SN obtained from Bw5147 cell transfectants cultured in RPMI/1% FCS was incubated on ELISA plates coated with mouse anti-NID1 mAb, followed by goat anti-NID1 Ab and HRP-conjugated anti-goat IgG Ab. Graph represents absorbance at 405 nm after normalization to background (nonspecific binding of goat anti-NID1 plus secondary reagent). Data are medians of triplicates ± interquartile range and are the pooled results of three independent experiments; dots represent single values. ****p<0.0001 by two-tailed Mann-Whitney test.

also inhibit cytokine release induced in Bw-NKp30 cells by NKp30 triggering, even if at a lesser extent and only at the highest concentration of anti-NKp30 mAb tested (Fig. 12A). Next, the effect of two different rNID1 doses on IL-2 release induced by the highest mAb concentration was investigated. Fig. 12B shows that both rNID1 doses were able to inhibit NKp44-mediated IL-2 release, while only the highest concentration of rNID1 decreased IL-2 release in Bw-NKp30 cells.

As different studies reported the interaction between NID1 and αVβ3 and α3β1 integrins (178,181) we analysed the expression levels of some integrins on Bw5147 transfectants in order to rule out a possible side effect of NID1 through integrins differentially expressed between the two cell transfectants. Fig. 13 shows the expression of CD29 (β1 integrin), CD49a (α3 integrin), and CD61 (β3 integrin) on Bw5147 transfectants, indicating no statistically significant differences between the two cell lines (Fig. 13B) and suggesting that integrins were not influencing our functional experiments.

Next, we investigated whether also NID1-containing cell culture SN could exert an inhibitory effect on cytokine release. To this end, Bw-NKp44 and Bw-NKp30 cells were incubated with K562-NID1-SN obtained from cells cultured in RPMI/1% FCS, and subsequently stimulated with anti-NKp44 or anti-NKp30 mAbs. The evaluation of IL-2 levels revealed that pre-treatment with K562-NID1-SN specifically

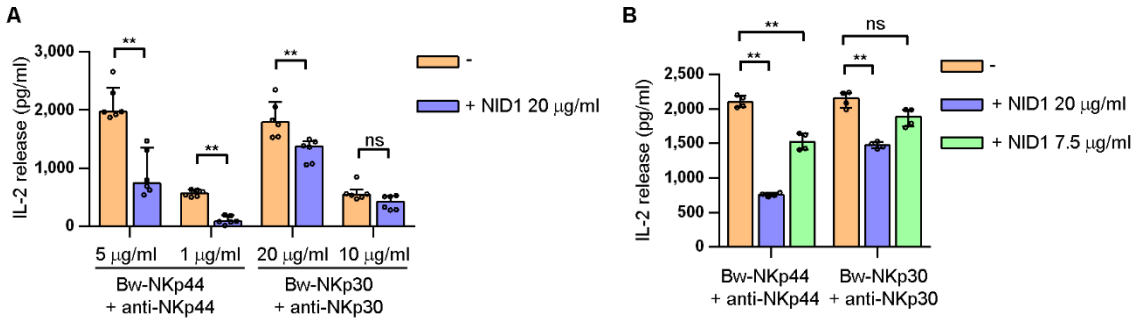

Figure 12. Effect of rNID1 pre-treatment on NKp44-induced IL-2 production in Bw-NKp44 cells
(A) Bw-NKp44 and Bw-NKp30 cells were left untreated or pre-treated with rNID1 (20 μg/ml) and subsequently incubated on plates coated with two different concentrations of anti-NKp44 or anti-NKp30 mAb. (B) Bw-NKp44 and Bw-NKp30 cells were left untreated or pre-treated with rNID1 (20 or 7.5 μg/ml) and subsequently incubated on anti-NKp44 or anti-NKp30 mAb-coated plates. Graphs represent IL-2 release (pg/ml) evaluated by ELISA. The background (from GAM-stimulated cells) was subtracted for each value. Data are medians of duplicates ± interquartile range and are the pooled results of three independent experiments. ***p*=0.0022, ns=0.0649 (A); ***p*=0.0022, ns=0.584 (B)) by two-tailed Mann-Whitney test.

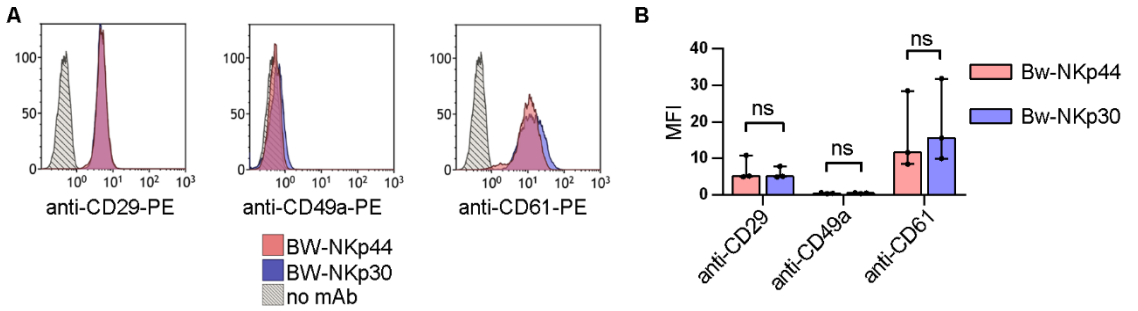

Figure 13. Integrin expression in Bw-NKp44 and Bw-NKp30 cell transfectants
(A) Bw-NKp44 and Bw-NKp30 cells were stained with PE-conjugated anti-CD29, anti-CD49a, and anti-CD61 mAbs and subsequently analysed by flow cytometry. One representative experiment of three is shown. (B) MFI data obtained from flow cytometry analysis are represented as medians ± interquartile range of three independent experiments; dots represent single values. ns=0.25 by two-tailed Wilcoxon test.

inhibited NKp44-induced, but not NKp30-induced cytokine release (Fig. 14A). Similar results were obtained pre-treating Bw-NKp44 and Bw-NKp30 cells with SN derived from Bw-NID1 cells (Fig. 14B).

Having evaluated NID1 effects in a simplified experimental system, we asked whether a similar effect could be exerted also on NK cells. Human NK cells, obtained from different healthy donors and cultured in IL-2 in order to induce NKp44 expression, were incubated with K562-NID1-SN or with K562-SN as control. As shown in Fig. 15A, NK cell-mediated IFN-γ release, induced by stimulation through NKp44 receptor, was inhibited by K562-NID1-SN, but not by control SN. It is of note that IFN-γ secretion induced by anti-NKp46 or anti-NKp30 mAb stimulation was not impaired by K562-NID1-SN. Subsequently, we assessed whether sNID1 could also affect NK cell cytotoxicity through the interaction with NKp44: to this end, NK cells pre-treated with K562-NID1-SN were utilised in a P815-redirected killing assay. Pre-treatment with NID1-containing SN inhibited NK cell cytotoxicity against P815 cells in the presence of anti-NKp44 mAb, while it was ineffective in the presence of anti-NKp30 or anti-NKp46 mAbs (Fig. 15B).

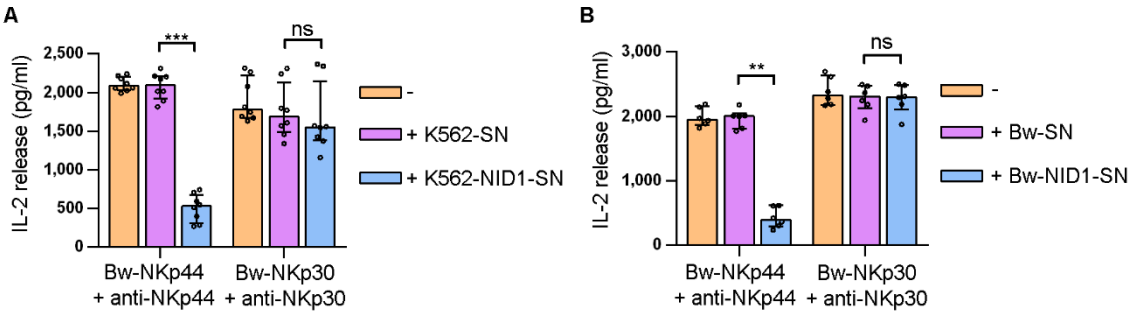

Figure 14. Effect of NID1-containing SN on NKp44-induced IL-2 production in Bw-NKp44 cells
(A, B) Bw-NKp44 and Bw-NKp30 cells were left untreated or pre-treated with SN derived from untransfected or NID1-transfected K562 (A) or Bw5147 (B) cells and subsequently incubated on anti-NKp44 or anti-NKp30 mAb-coated plates. Graphs represent IL-2 release (pg/ml) evaluated by ELISA. The background (from GAM-stimulated cells) was subtracted for each value. Data are medians of duplicates ± interquartile range and are the pooled results of four (A) or three (B) independent experiments; dots represent single values. ***p=0.0002, ns=0.1044 (A); **p=0.0022, ns=0.8983 (B) by two-tailed Mann-Whitney test.

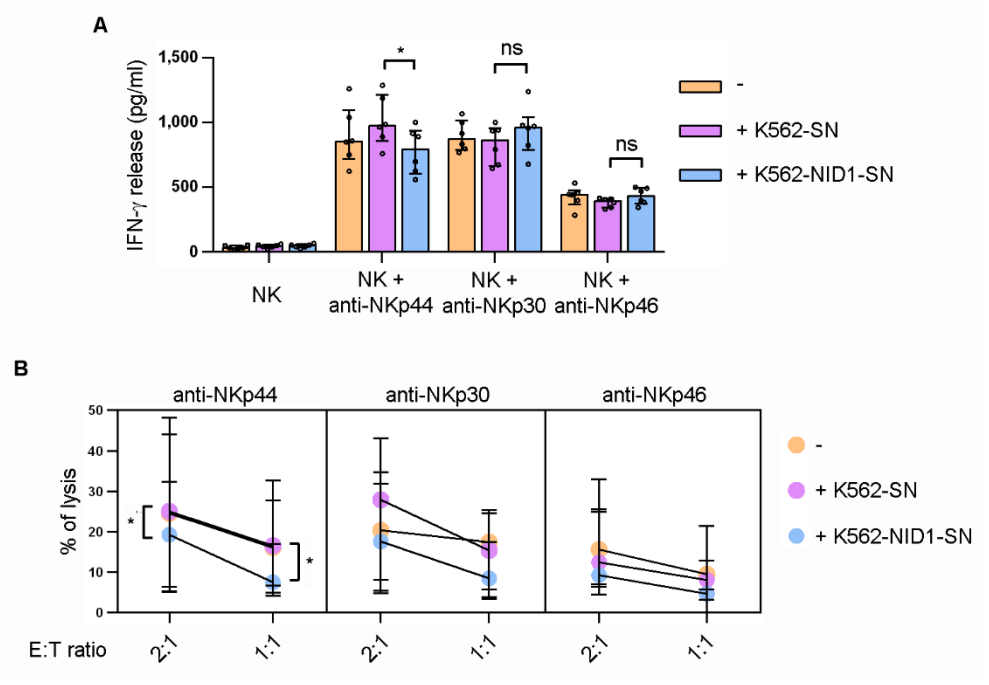

Figure 15. Effect of sNID1 on NK cells
(A) Polyclonal NK cells were pre-treated with SN derived from wild type or NID1-transfected K562 cells and subsequently cultured on plates coated with anti-NKp44, -NKp30, or -NKp46 mAbs. IFN-γ release was evaluated by ELISA. Data are medians ± interquartile range of six independent experiments performed on NK cells derived from three healthy donors. *p=0.0156, ns=0.1094 (NKp30) and ns=0.0983 (NKp46) by one-tailed Wilcoxon test. (B) Polyclonal NK cells were incubated with SN derived from wild type or NID1-transfected K562 cells, and their cytotoxic activity against P815 target cells in the presence of anti-NKp44, anti-NKp30, or anti-NKp46 mAbs was evaluated. Data are represented as percentage of lysis and are the medians ± interquartile range of six different experiments conducted on NK cells derived from three different healthy donors. *p=0.0313 (2:1 ratio) and *p=0.0156 (1:1 ratio).

In order to further evaluate whether NID1 could bind NKp44 receptor expressed at the NK cell surface, NK cells were incubated with SN derived from HEK293T-NID1 transfectants and stained with anti-NID1 and anti-NKp44 mAbs. This double staining revealed that NK cells did not express NID1 at the cell

surface and that HEK293T-NID1-SN could bind NK cells; data shown in Fig. 16 suggest that SN-derived NID1 could bind to NK cells displaying the highest NKp44 expression levels.

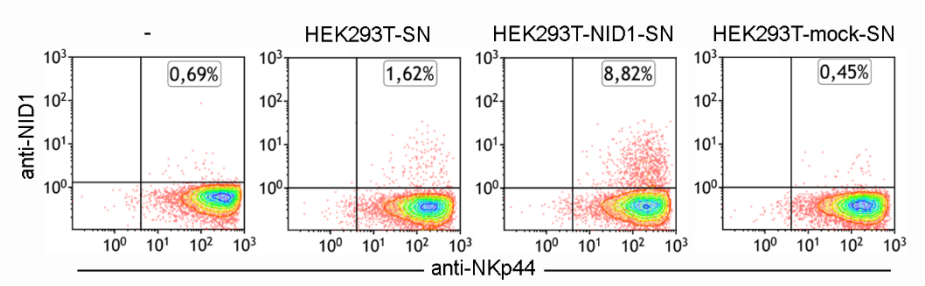

Figure 16. Binding of sNID1 on NK cells
Polyclonal NK cells were incubated with SN derived from wild type, mock-transfected, and NID1-transfected HEK293T cells and stained with both anti-NID1 and anti-NKp44 mAbs, followed by PE-conjugated anti-mouse IgG1 and Alexa Fluor 647-conjugated anti-mouse IgM mAb. Density plots represent the fluorescence intensity of anti-NKp44 (x-axis) and anti-NID1 (y-axis) mAb staining. One representative experiment of three, performed on NK cells from three different donors, is shown.

Recently, PDGF-DD was identified as a novel soluble ligand for NKp44 receptor. PDGF-DD has been shown to induce a robust cytokine production through NKp44 engagement, whereas no effect on NK cell-mediated cytotoxic activity has been observed (127). These novel findings prompted us to investigate whether NID1 could inhibit PDGF-DD-induced cytokine secretion. To this end, Bw-NKp44 were pre-treated with two different concentrations of rNID1 or with K562-NID1-SN and subsequently stimulated with 25 or 250 ng/ml PDGF-DD. Fig. 17A shows that sNID1 interfered with PDGF-DD by reducing PDGF-DD-induced IL-2 production; as expected, PDGF-DD did not induce IL-2 production in Bw-NKp30 cells. Similar experiments were performed also on polyclonal NK cells, demonstrating that also in this case sNID1 was able to inhibit PDGF-DD-mediated IFN-γ production (Fig. 17B). These observations sustained the idea that NID1 could act as a decoy ligand by interfering with the interaction between NKp44 and its specific ligands, such as PDGF-DD, thus reducing NKp44-mediated IFN-γ release.

4.6. CELLULAR LOCALISATION OF NID1

Several studies described NID1 interaction with integrins (178,181); nevertheless, none of them clearly demonstrated NID1 expression at the cell surface by immunofluorescence experiments; for this reason we decided to analyse more thoroughly NID1 localisation. At first, we analysed total cell lysates and membrane preparations from HEK293T cell line by Western blot, revealing the presence of NID1 in both samples; indeed, enhanced NID1 levels were detected in membrane-enriched preparations (Fig. 18A); in parallel, immunoblotting with anti-Na^+/K^+ ATPase and anti-GAPDH Abs confirmed the enrichment in membrane proteins. To directly assess NID1 expression on the plasma membrane, we performed cytofluorimetric assays with a NID1-specific mAb: analysis of HEK293T cell line revealed the expression of NID1 at the cell surface; in parallel, NID1-negative K562 cells were analysed. As expected,

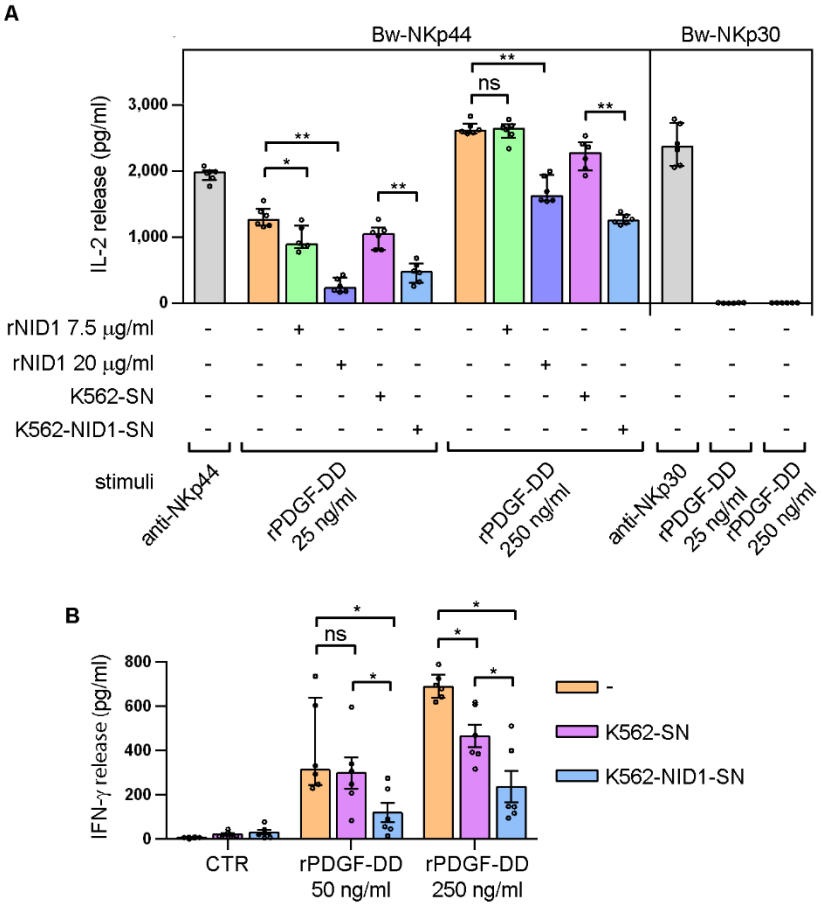

Figure 17. sNID1 inhibits PDGF-DD-mediated cytokine release

(A) Bw-NKp44 and Bw-NKp30 cells were pre-treated with rNID1 (7.5 or 20 μg/ml) or with SN derived from wild type or NID1-transfected K562 cells, and subsequently stimulated with rPDGF-DD at 25 or 250 ng/ml. (B) Polyclonal NK cells were pre-treated with SN derived from wild type or NID1-transfected K562 cells and subsequently stimulated with rPDGF-DD at 50 and 250 ng/ml. Graphs represent IL-2 (A) or IFN-γ (B) concentrations evaluated by ELISA; in (A) the background from GAM-stimulated or unstimulated cells was subtracted. Data are medians ± interquartile range and are the pooled results of three independent experiments performed as duplicates (A) or six independent experiments performed on NK cells derived from three healthy donors (B). **p*=0.0152, ***p*=0.0022, ns>0.9999, by two-tailed Mann-Whitney test (A); **p*=0.0156, **p*=0.0325 (K562-SN vs. K562-SN-NID1 PDGF-DD 50 ng/ml), ns=0.2188 by one-tailed Wilcoxon test (B).

NID1-specific mAb did not stain these cells, neither at the cell surface nor in the cytoplasm (Fig. 18B). Subsequently, NID1 surface expression on HEK293T cells was confirmed by imaging flow cytometry; data shown in Fig. 18C-D indicated a reproducible signal obtained through NID1-specfic mAb staining. We decided to further confirm our observations by investigating whether NKp44 could recognise membrane-bound NID1 (mNID1). To this end, we performed experiments with K562-NID1 and Bw-NID1 stable transfectants: both anti-NID1 mAb and NKp44Fc bound to K562-NID1 and Bw-NID1 but not to the corresponding wild type cells (Fig. 19A).

Next, we silenced NID1 expression in HEK293T cells and analysed NID1 expression after 24 and 72 h: Fig. 19B shows that staining with both NKp44Fc and anti-NID1 mAb was reduced in the presence of siRNA-NID1 but not of siRNA-CTR. NID1 silencing was also confirmed in HEK293T total cell lysates and

in the corresponding SN by Western blot experiments (Fig. 19C-D). These data confirm that NID1 is able to interact not only with sNID1 but also with mNID1.

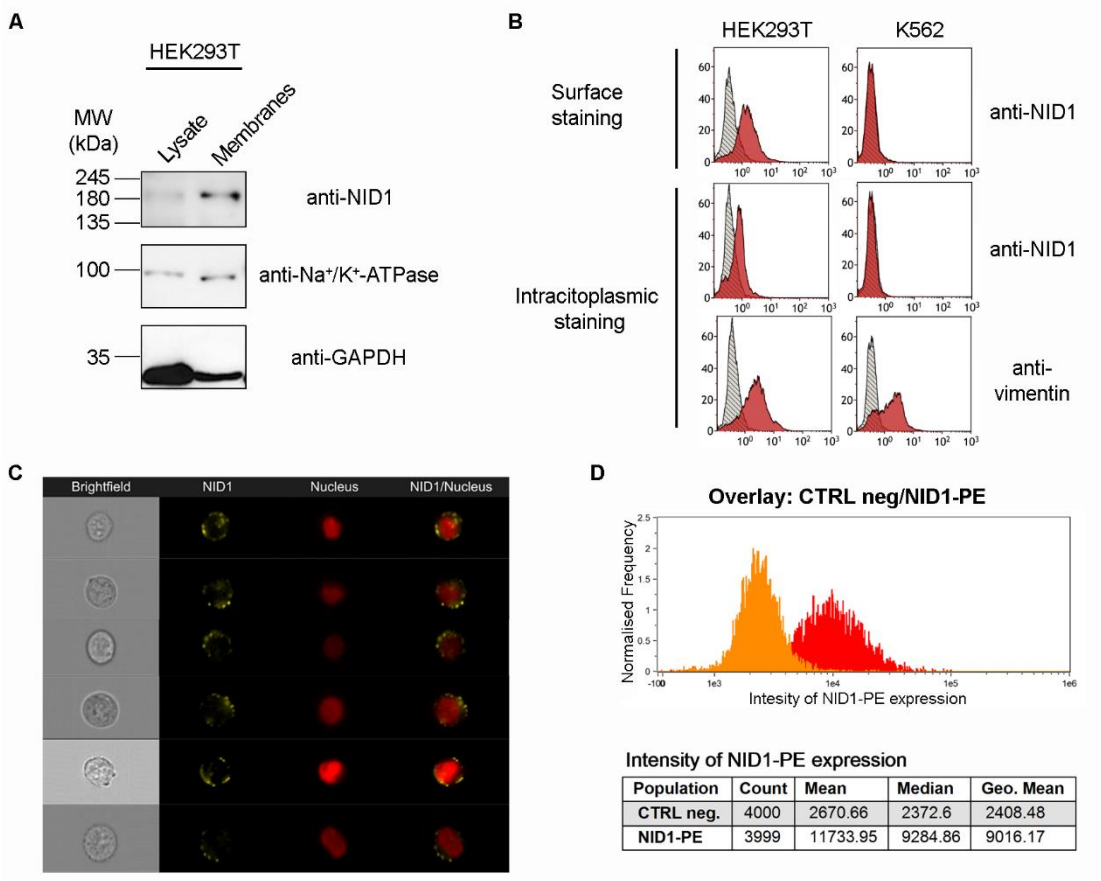

Intensity of NID1-PE expression

Population	Count	Mean	Median	Geo. Mean
CTRL neg.	4000	2670.66	2372.6	2408.48
NID1-PE	3999	11733.95	9284.86	9016.17

Figure 18. Analysis of NID1 surface expression in HEK293T cell line and in NID1 cell transfectants
(A) HEK293T total cell lysate and membranes were run on a 10% polyacrylamide gel and subsequently immunoblotted with mouse anti-NID1, mouse anti-Na^+/K^+-ATPase, and rabbit anti-GAPDH Abs followed by the appropriate HRP-conjugated secondary reagents. One experiment representative of three is shown. (B) Surface or intracytoplasmic staining of HEK293T cells was performed with mouse anti-NID1 or mouse anti-vimentin mAbs followed by PE-conjugated anti-mouse IgG1 mAb; grey profiles represent isotype control. (C, D) HEK293T cells were stained with a NID1-specific mAb followed by PE-conjugated anti-mouse IgG1 mAb. Next, cells were incubated with Hoechst 33342 nuclear dye and analysed by Amnis ImageStream. NID1 expression on individual single cells is shown in (C), while histograms in (D) represent the overall fluorescence intensity of NID1-stained HEK293T cells as compared to isotype control. Data show representative images from one experiment out of three performed

Finally, a panel of human tumour cell lines was analysed, not only for NID1 mRNA and protein levels in cell lysates, but also for NID1 cell surface expression (Table 5 and Fig. 20). These experiments showed that NID1 can be expressed by several tumour cell types, although its expression levels are highly heterogeneous, also among cell lines belonging to the same histotype.

Several reports demonstrated that NID1 can be released in exosomes: NID1-positive exosomes have been detected in urinary samples of healthy subjects, as well as in the blood of tumour patients (194–199). Several ligands for activating NK cell receptors can be released in exosomes, sometimes acting as decoy molecules and representing a possible mechanism of tumour escape (136,212), in other cases (i.e. BAT3-positive exosomes) stimulating NK cell response (131,132). Based on these finding, we

investigated whether NID1 could be released in HEK293T-derived microvesicles (MVs) and/or exosomes and whether, in this form, it could be recognised by NKp44Fc. To this end, HEK293T cells were cultured in medium supplemented with serum deprived of exosomes, and SN was collected after 72 h, in order to purify extracellular vesicles (i.e. MVs and exosomes). Western blot analysis of HEK293T-derived MVs and exosomes revealed that exosomes were particularly enriched in NID1 as compared to MVs and that NKp44Fc was able to recognise a band with a MW corresponding approximately to that of NID1 (Fig. 21A). Next, we performed ELISA experiments on intact HEK293T-derived exosomes and MVs, in order to verify whether NID1 could be expressed on the vesicle surface.

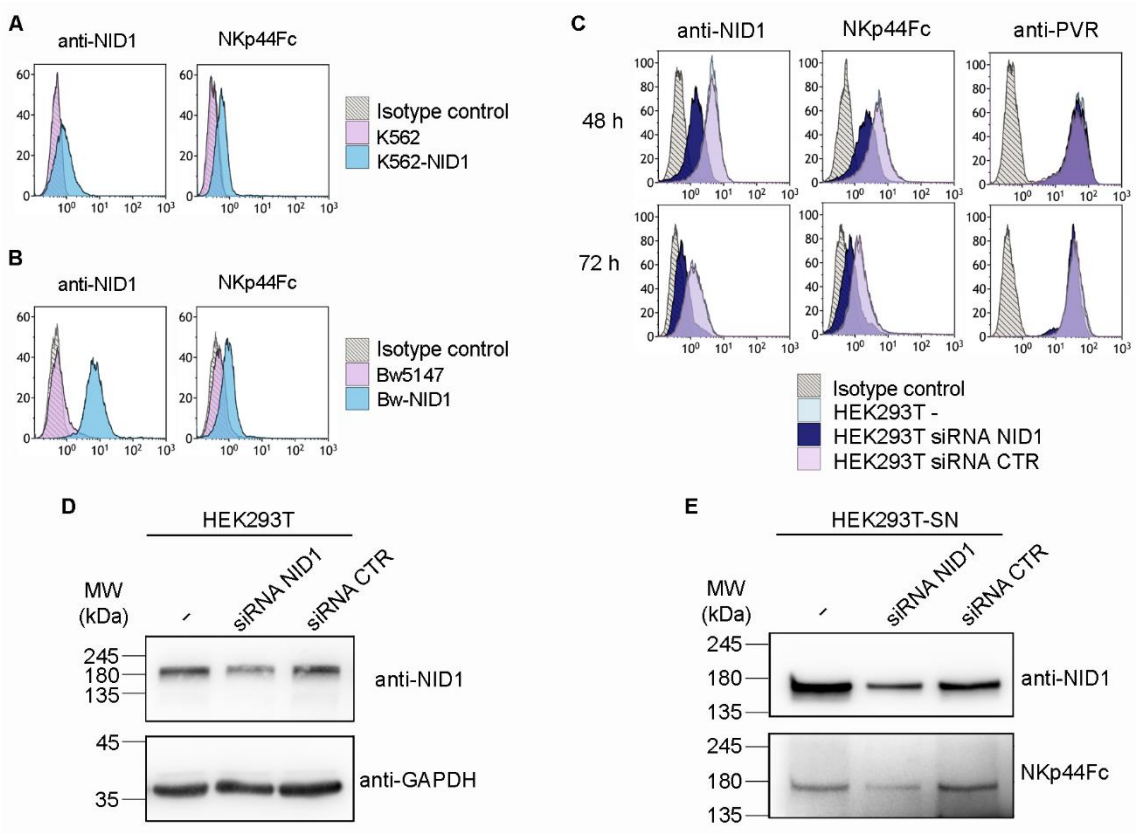

Figure 19. NKp44Fc recognises membrane-bound NID1
(A, B) K652, K562-NID1 (A), Bw, and Bw-NID1 (B) cells were stained with a mouse NID1-specific mAb or with NKp44Fc followed by the appropriate isotype-matched PE-conjugated secondary mAb. Samples were analysed by flow cytometry. One representative experiment of four is shown. (C) HEK293T cells were transfected with siRNA NID1 or siRNA CTR and after 48 and 72 h were analysed by flow cytometry with anti-NID1 or NKp44Fc followed by the appropriate PE-conjugated secondary mAb. (D, E) HEK293T cell lysates (D) and SN (E) obtained from cells transfected with siRNA NID1 or siRNA CTR were analysed by Western blot on 10% or 7.5% polyacrylamide gels. Samples were immunoblotted with mouse anti-NID1 mAb, rabbit anti-GAPDH Ab, or with NKP44Fc molecule followed by the appropriate HRP-conjugated secondary mAb. One experiment representative of three is shown.

To this end, intact exosomes and MVs purified from HEK293T cells were coated on ELISA plates and incubated with NKp44Fc, NKp30Fc, anti-NID1 mAb, or with anti-CD63 mAb as positive control. Fig. 21B shows that NID1 was exposed on the surface of both exosomes and MVs. This observation indicates that NID1-positive extracellular vesicles could mediate functional effects on NK cells through their

interaction with NKp44 receptor. Further studies are currently ongoing in order to elucidate the functional role of this interaction.

Cell line	mRNA	Cell lysate	Cell surface	
		anti-NID1	anti-NID1	NKp44Fc
Melanoma				
Mewo	+	+	+	+
C-32	+	+	+	+
Glioblastoma				
A172	+	+	-	+
U87-MG	+	+	-	+
Colon cancer				
LOVO	+	-	-	+
SW480	+	+	+	+
Neuroblastoma				
GI-LI-N	+	+	+	+
GI-ME-N	+	+	-	+
SH-SY5Y	+	+	+	+
B-EBV				
LCL721.221	+	+	+	+
Cervical adenocarcinoma				
HeLa	+	+	+	+
Prostate cancer				
LNCap	-	-	-	+
PC3	-	-	-	+
Ovarian adenocarcinoma				
A2780	+	+	-	+
Placental choriocarcinoma				
JEG-3	+	+	+	+

Table 5. Summary table of NID1 expression on the analysed tumour cell lines belonging to different histotypes
For each tumour cell line, NID1 expression at the mRNA level, in total cell lysates, and at the cell surface is indicated, together with NKp44Fc reactivity analysed by flow cytometry.

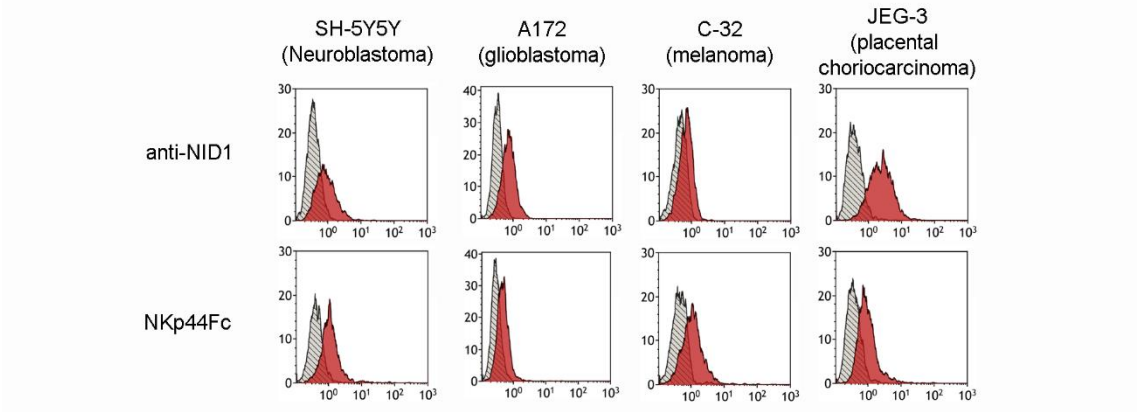

Figure 20. NID1 expression on human tumour cell lines
The indicated cell lines were stained with a NID1-specific mAb or with NKp44Fc followed by the appropriate isotype-matched PE-conjugated secondary mAb. Samples were analysed by flow cytometry. Grey profiles correspond to isotype control. One representative experiment of three is shown.

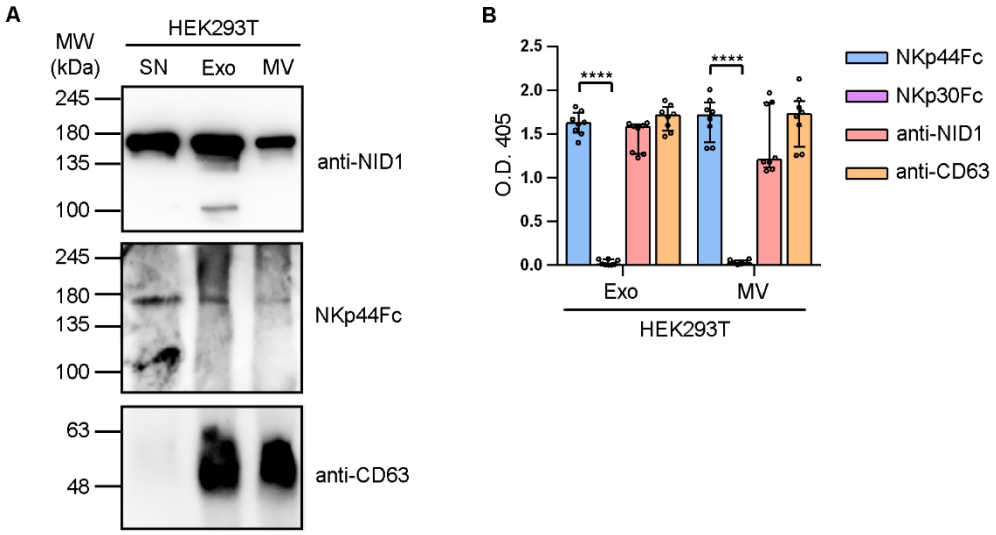

Figure 21. Analysis of NID1 expression in exosomes and microvesicles derived from HEK293T cells
(A) Exosomes (exo), microvesicles (MV) and concentrated SN derived from HEK293T cells cultured in DMEM supplemented with exosome-deprived FCS or in protein-free medium, respectively, were analysed by SDS-PAGE on a 7.5% polyacrylamide gel. Samples were immunoblotted with NKp44Fc, mouse anti-NID1 or anti-CD63 Abs followed by the appropriate HRP-conjugated secondary mAbs. One representative experiment of three is shown. (B) HEK293T-derived exosomes and MVs from cell cultured in DMEM supplemented with exosome-deprived FCS were coated on ELISA plates. Subsequently, coated wells were incubated with the indicated Fc molecules, goat anti-NID1 or mouse anti-CD63 Abs followed by the appropriate HRP-conjugated secondary mAbs. Graph represents absorbance at 405 nm after normalization to background (nonspecific binding of secondary reagent). Data are means of triplicates ± SD and are the pooled results of three independent experiments. ****p<0.0001 by two-tailed Mann-Whitney test.

4.7. EFFECT OF MEMBRANE-BOUND NID1 (mNID1)

Since NID1 can be exposed at the cell surface, we investigated whether mNID1 could exert any functional effect on Bw-NKp44 cell line and on polyclonal NK cells. Several studies have demonstrated that activating NK cell receptor ligands can be found both as surface-associated molecules and released as soluble proteins, inducing different effects on NK cell functions. For example, it has been shown that MICA/B, B7-H6, and BAT3 are able to induce NK cell activation when expressed on the surface of tumour cells, whereas they inhibit NK cell functions if released in soluble form (134,144,152). To evaluate the potential effect of mNID1, we performed co-culture experiments, in which Bw-NKp44 cells were incubated with NID1-transfected K562 or Bw5147 cells, and observed that NID1 expression did not modify basal IL-2 release (Fig. 22A-B). However, in this experimental setting an inhibitory effect of sNID1 released by NID1 cell transfectants, counteracting a possible activation by mNID1, cannot be excluded. In order to mimic mNID1, we performed experiments in which rNID1 was used as a stimulus: Fig. 22C shows that rNID1, coated on the plate either directly or through anti-NID1 or anti-His mAbs, did not affect IL-2 release by Bw-NKp44 cells.

In similar experiments, NK cells were stimulated on rNID1-coated wells: in keeping with what we observed in Bw-NKp44 cells, no induction of IFN-γ production was detected in rNID1-stimulated NK cells (Fig. 22D). Next, we tried to assess the effect of mNID1 on NK cell-mediated cytotoxicity; NID1-

transfected Bw cells were used as target cells, in order to avoid the interference of ligands for activating NK cell receptors expressed by K562 cell line. In this assay, NID1 released by Bw cell transfectants is less likely to interfere, since co-culture of NK cells with target cells lasts for only few hours. The analysis of NK cells derived from five healthy donors revealed that NK cell cytotoxic activity against Bw-NID1 cells was slightly increased, as compared to control cells, only at the effector-target (E:T) ratio of 5:1 (Fig. 22E). Nevertheless, the analysis of selected donors characterised by NK cells with a low cytotoxic activity against Bw cells, allowed to observe a statistically significant increase of NK cell cytotoxicity against Bw-NID1, as compared to wild type cells, at the different E:T ratios tested (Fig. 22F).

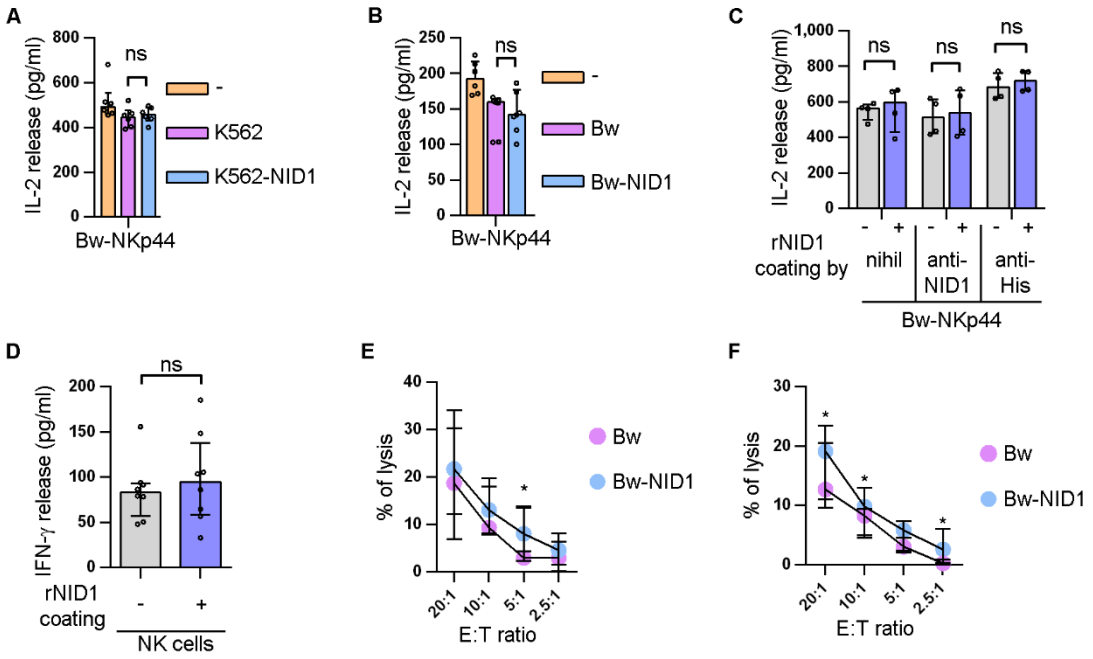

Figure 22. Functional effects of cell surface-associated NID1 or plastic-bound rNID1 in Bw-NKp44 and in NK cells

(A, B) Bw-NKp44 cells were cultured alone or in the presence of wild type or NID1-transfected K562 or Bw5147 cells. IL-2 release in the SN was evaluated by ELISA. Data are medians of duplicates ± interquartile range and are the pooled results of three independent experiments. ns=0.5714 by two-tailed Mann-Whitney test. (C) Bw-NKp44 cells were incubated on plates coated with rNID1, anti-NID1 + rNID1, or anti-His + rNID1. IL-2 release in the SN was evaluated by ELISA. Data are medians of duplicates ± interquartile range and are the pooled results of two independent experiments. ns=0.8286 (-) or ns=0.6571 (anti-NID1, anti-His) by two-tailed Mann-Whitney test. (D) Polyclonal NK cell lines were incubated on plates coated with rNID1. IFN-γ release in the SN was evaluated by ELISA. Data are medians ± interquartile range of 8 independent experiments with 3 different donors. ns=0.2305 by one-tailed Wilcoxon test. (E, F) NK cell cytotoxicity was evaluated against Bw and Bw-NID1 transfected cells. Data are represented as percentage of lysis and are the medians ± interquartile range of fifteen (D) or 9 (E) independent experiments conducted on 5 (E) or 2 (F) different healthy donors. *p=0.0277 (D), *p=0.0371 (20:1) and 0.0373 (10:1 and 2.5:1) (E) by one-tailed Wilcoxon test.

4.8. EFFECT OF NID1 STIMULATION ON NK CELL PROTEOMIC PROFILE

Our data showed that mNID1 induced only a slight increase of NK cell cytotoxicity and did not alter cytokine production. To gain further hints about the possible effect of NID1 on NK cell functions, we

stimulated NK cells from four healthy donors on NID1- or anti-NKp44 mAb-coated plates and subsequently performed a proteomic analysis of NK total cell lysates by high-resolution mass spectrometry. Data analysis through the MaxQuant software allowed the identification of 6903 total proteins, of which 5682 were quantified using a Label-Free Quantitation approach. Most of them (i.e. 5317 proteins) could be found in all samples, whereas only a small part was specific for each condition (Fig. 23A). Bioinformatic analysis showed that rNID1 as well as anti-NKp44 mAb stimuli modified NK cell proteomic profile, as compared to their corresponding control. Venn diagram of the identified proteins from stimulated and control samples revealed that 1663 and 1431 proteins were commonly down- or up-regulated, respectively, by both treatments (Fig. 23B), indicating that NID1 and NKp44 stimulations could result in the concordant modulation of a huge number of proteins. Instead, 69 and 84 proteins, were exclusively up- and down-regulated by NID1 treatment, respectively, while 91 and 123 proteins were selectively up- and down-regulated in NKp44-stimulated NK cells (Fig. 23B).

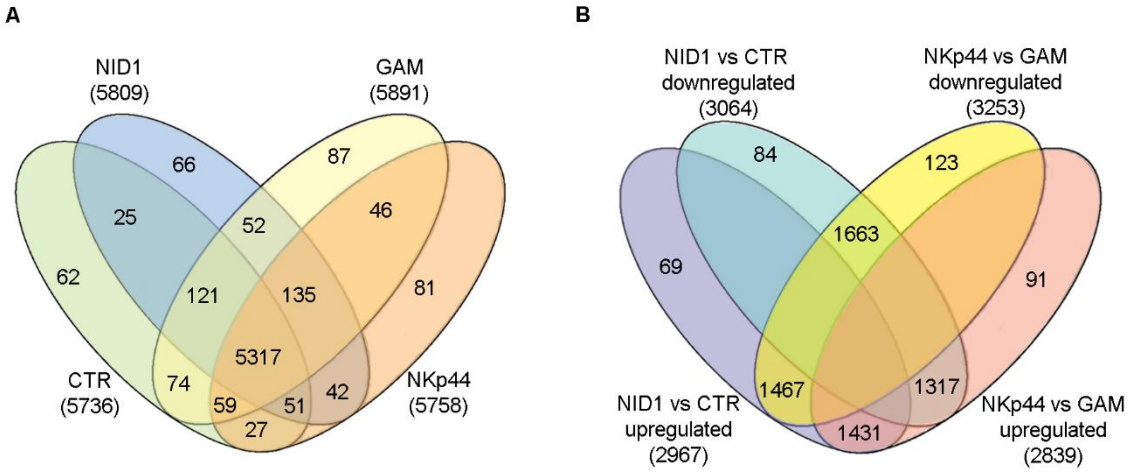

Figure 23. Venn diagram showing protein profile overlap between rNID1- and anti-NKp44 mAb-stimulated NK cells

(A) Venn diagram of total proteins identified in NK cells stimulated with rNID1 or anti-NKp44 mAb and their controls, CTR and GAM, respectively. The number of common and exclusive proteins is indicated in the respective overlapping and not-overlapping areas. (B) Venn diagram represents up- and down-regulated proteins by rNID1 or anti-NKp44 mAb stimulation in NK cells as compared to their controls. Numbers in not-overlapping areas indicate proteins exclusively identified in the rNID1vsCTR or NKp44vsGAM datasets.

Subsequently we focused our attention on statistically significant modulated proteins: two-sample t-test analysis, represented as volcano plots, indicated 112 proteins statistically regulated by NID1 treatment (Fig. 24A) and 129 by NKp44 stimulation (Fig. 24B); among them, only 15 proteins were common to both conditions.

In order to investigate the cellular processes modulated by NID1 stimulation, we performed a GO analysis of biological processes and cellular components: results indicated that NK cell stimulation with rNID1 induced the modulation of several biological processes, including cell proliferation, signal transduction, endo/exocytosis, immune response, and, in particular, cell metabolism (Fig. 25A-B).

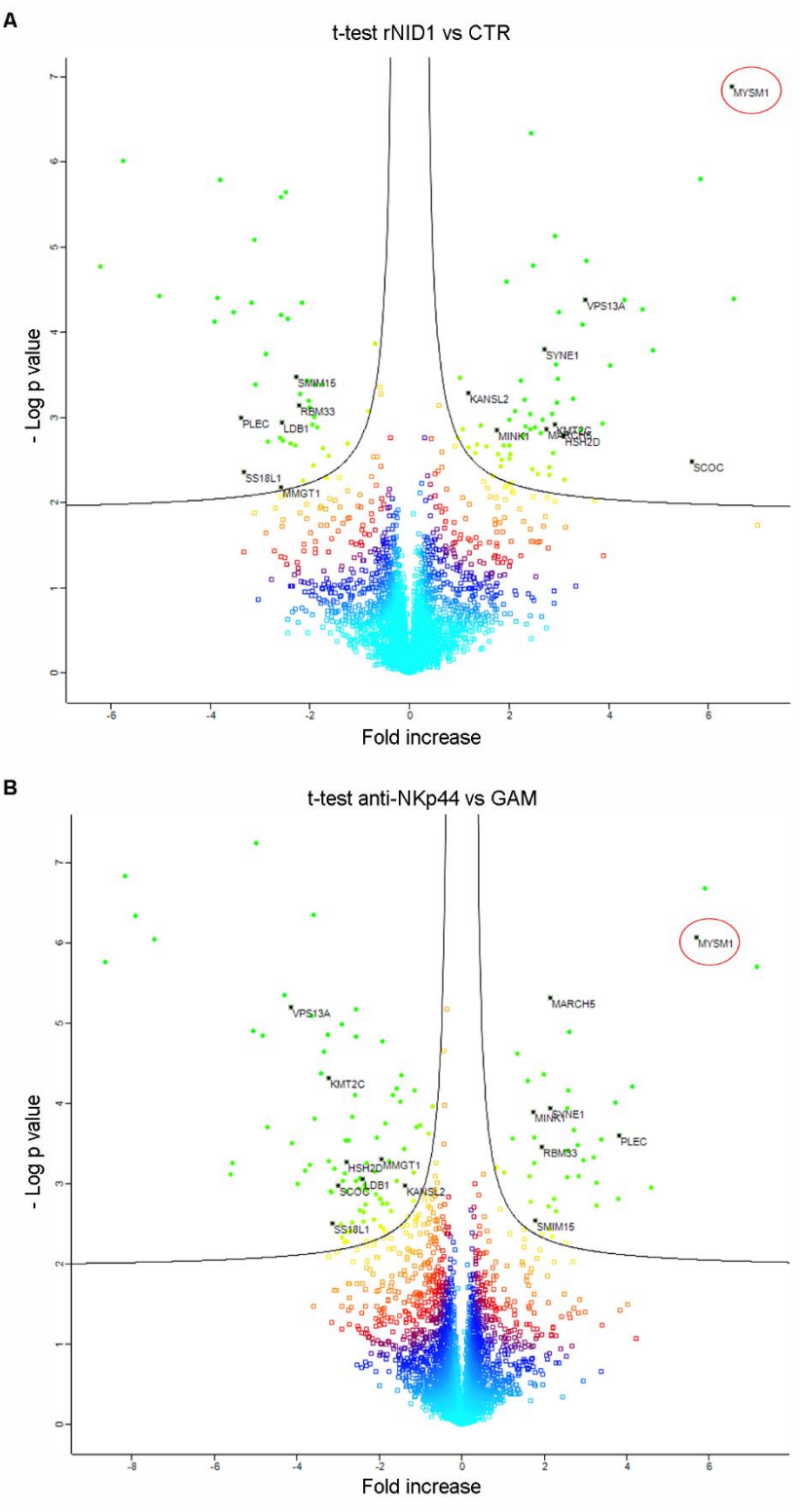

Figure 24. Proteomic analysis of NK cells stimulated with rNID1 or anti-NKp44 mAb
(A, B) Volcano plots represent differentially expressed proteins in rNID1-stimulated vs. not stimulated (CTR) NK cells (A) or anti-NKp44 mAb-stimulated vs. not stimulated (GAM) NK cells (B). Black line indicates FDR=0.05 and s0=0.1; coloured squares are not statistically significant proteins, dots represent proteins with a statistically significant modulation specific for anti-NKp44 or NID1 stimuli, black asterisks represent statistically significant proteins common to anti-NKp44 and NID1 stimuli. Magnitude of fold-change is represented on the x-axis (proteins up-regulated after treatment are shown on the right, the down-regulated ones on the left); y-axis represents statistical significance (-log10 of *p* value).

Since many of these biological processes were modulated also by NKp44 mAb-mediated NK cell stimulation, we analysed the biological processes and molecular functions modulated by the two stimuli as compared to their respective control. Fig. 25C shows a heatmap describing the modulation

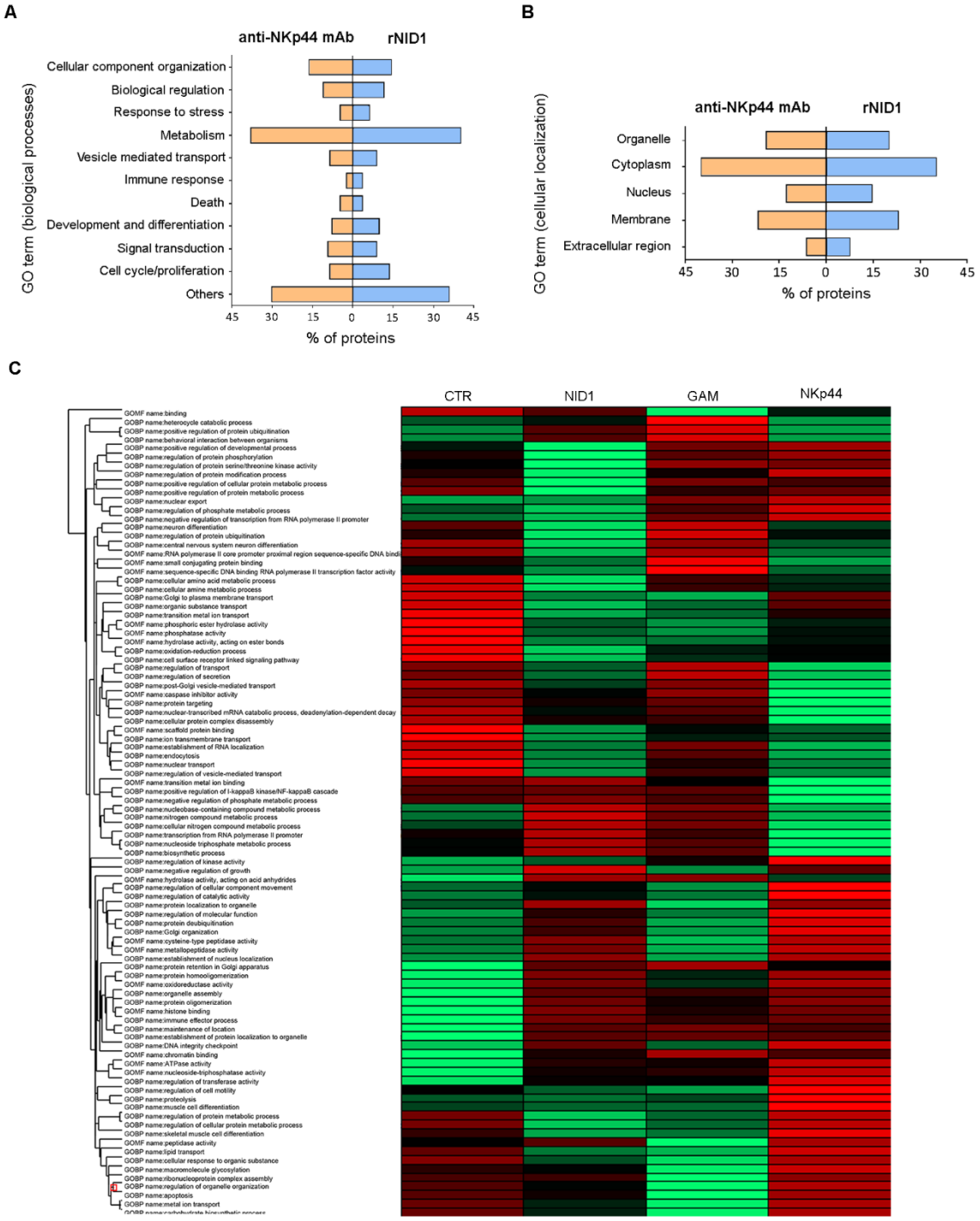

Figure 25. GO analysis of proteomic data obtained by NID1- and NKp44- stimulated NK cells
(A, B) GO classification based on biological processes (A) or cellular component (B) of proteins significantly modulated by rNID1 and anti-NKp44 mAb stimuli. (C) The output matrix contains a list of GO terms whose expression values have a statistically significant preference to be systematically larger or smaller than the overall distribution of expression values. GO terms were subsequently clustered based on such "enrichment profiles" using the simple Euclidian-distance–based average-linkage hierarchical clustering.

of NK cell proteotype in response to NID1 or anti-NKp44 stimuli: such analysis revealed that the two stimuli have partially overlapping effects on NK cell proteomic profile.

To summarise, these data suggest that NID1 could induce novel functional responses on NK cells. Analysis of SN obtained from NID1-stimulated NK cells is currently underway and might reveal whether NK cell secretome could be modified by NID1.

4.9. NID2 COULD REPRESENT ANOTHER SOLUBLE MOLECULE RECOGNISED BY NKp44

Since Nidogen family comprises NID1 and NID2 proteins that share similar functions and structure, we were interested in investigating whether NKp44 could also recognise NID2. To this end, the reactivity of different Fc molecules in the presence of NID2 was analysed by ELISA, utilising plates coated with rNID1, rNID2, or rHMGB1 as a negative control. Fig. 26A shows that NKp44Fc could interact with rNID2 more weakly than with rNID1. Given these results, we evaluated the effect of rNID2 pre-treatment on Bw-NKp44 cells: our preliminary results indicate that pre-treatment with two different rNID2 concentrations had no effect on Bw-NKp30 cells, while on Bw-NKp44 cells it produced a weaker inhibition as compared to that obtained with the same rNID1 concentration (Fig. 26B).

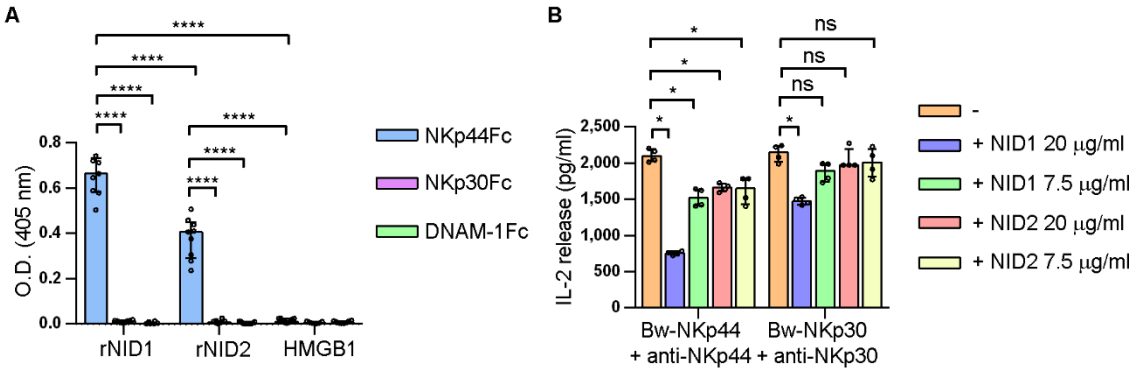

Figure 26. Recognition and functional effect of rNID2

(A) ELISA plates were coated with rNID1, rNID2 or HMGB1 followed by incubation with 20 μg/ml of different Fc molecules and HRP-conjugated anti-human IgG mAb. Graph represents absorbance at 405 nm after normalization to background (nonspecific binding of the secondary reagent). Data are medians of triplicates ± interquartile range and are the pooled results of three independent experiments; ****p<0.0001 by two-tailed Mann-Whitney test. (B) Bw-NKp44 and Bw-NKp30 cells were left untreated or pre-treated with rNID1 or rNID2 (20 or 7.5 μg/ml) and subsequently incubated on anti-NKp44 or anti-NKp30 mAb-coated plates, respectively. IL-2 release in the SN was evaluated by ELISA. The background (from GAM-stimulated cells) was subtracted for each value. Data are medians of duplicates ± interquartile range and are the pooled results of two independent experiments. *p=0.0286, ns=0.0571 (NID1 7.5 μg/ml), 0.3429 (NID2 20 μg/ml) or 0.4857 (NID2 7.5 μg/ml) by two-tailed Mann-Whitney test.

Further experiments will be conducted in order to elucidate the functional role of NID2-NKp44 interaction more precisely.

4.10 NKp44 DOES NOT RECOGNISE LAMININ

The initial analysis of spot 26 excised from 2-DE preparative gel also revealed the presence of laminin-γ1 as a second glycosylated protein identified by mass spectrometry with a high number of peptides.

In order to evaluate whether NKp44 could interact also with this protein, dot blot experiments were performed adsorbing human purified laminin and HEK293T-SN on a nitrocellulose membrane and probing it with different Fc molecules: Fig. 27A shows that no recognition of laminin by NKp44Fc under native conditions was observed. In order to rule out that NKp44Fc could recognize human laminin under denaturing conditions, we performed Western blot experiments, demonstrating that NKp44Fc was unable to recognize denatured laminin as well; moreover, the staining with an anti-laminin-γ1 mAb revealed in HEK293T-SN the presence of two bands with a different MW as compared to the band recognised by NKp44Fc (Fig. 27B). These experiments showed that NKp44 did not recognise laminin neither under denaturing conditions nor in its native conformation.

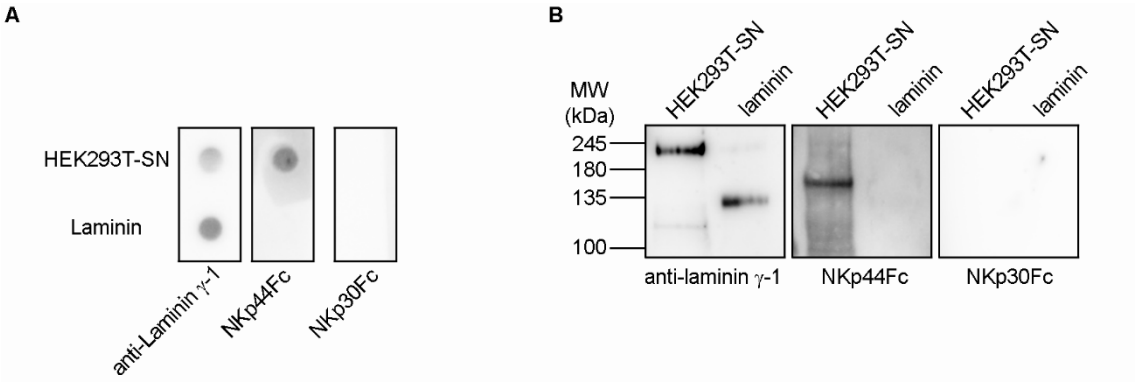

Figure 27. Analysis of NKp44Fc reactivity with purified human laminin
(A) Concentrated HEK293T-SN and purified human laminin were spotted on a nitrocellulose membrane and subsequently stained with anti-laminin γ-1 mAb, NKp44, or NKp30Fc followed by the appropriate secondary HRP-conjugated secondary mAb. One representative experiment of two is shown. (B) Concentrated HEK293T-SN and purified human laminin were analysed on a 7.5% polyacrylamide gel and subsequently immunoblotted with anti-laminin γ-1, NKp44Fc, or NKp30Fc followed by HRP-conjugated anti-mouse IgG or anti-human IgG mAbs. One representative experiment of two is shown.

5. DISCUSSION

Our data describe the identification and characterisation of Nidogen-1 (NID1 or Entactin), a component of the Extracellular Matrix (ECM) (176), as a novel NKp44 soluble ligand. A preliminary analysis of cell culture supernatant derived by HEK293T cell line, expressing NKp44 ligand(s), suggested the presence of soluble glycoproteins recognised by NKp44. The subsequent analysis of HEK293T-SN by 2-DE coupled with high resolution mass spectrometry led to the identification of NID1 as a candidate ligand for NKp44 NK cell receptor. NID1-NKp44 interaction was next confirmed by immunoprecipitation experiments performed on HEK293T-SN, and by Western blot and ELISA experiments conducted on rNID1. Importantly, these results suggested that NID1-NKp44 recognition could occur under native conditions. However, NKp44 was shown to interact also with denatured NID1, suggesting that it could bind a linear epitope.

Functional experiments, performed on the Bw-NKp44 cellular model showed that NID1 in soluble form (sNID1) could inhibit NKp44-induced IL-2 release: this inhibition was obtained using both rNID1 and sNID1 derived from cell transfectants. More importantly, we demonstrated that sNID1 derived from cell transfectants could inhibit NKp44-induced IFN-γ release in human polyclonal NK cells. We also evaluated the effect of sNID1 on NK cell cytotoxicity and observed a slight reduction of NK cell-mediated killing of P815 target cells in the presence of sNID1. sNID1-mediated inhibition of NK cell function was specific for NKp44 receptor, nevertheless we observed that high rNID1 concentrations slightly inhibited IL-2 release also in Bw-NKp30 cells. However, the inhibitory effect on NKp30 was not evident when both Bw-NKp30 and NK cells were treated with sNID1 derived from cell transfectants; indeed, the interaction between NKp30 and rNID1 was not observed neither by ELISA nor by Western blot. Notably, NID1-mediated inhibition of cytokine release through the interaction with NKp44 receptor was also demonstrated in both Bw-NKp44 and NK cells stimulated with PDGF-DD. These results indicate that NID1 could inhibit cytokine release not only induced by mAb-mediated NKp44 crosslinking but also stimulated by a specific NKp44 ligand, i.e. PDGF-DD (127). Altogether our data suggest that NID1 might be able to act as a decoy ligand, similarly to other NK cell receptor soluble ligands. High levels of soluble ligands for DNAM-1, NKG2D, and NKp30 receptors were associated to advanced stage of disease or poor prognosis in different types of cancer, such as melanoma, ovarian cancer, and CLL (89,131,135,136,144,151–153). Shedding of membrane-bound ligands, such as B7-H6 and MICA/B, is mediated by the activity of proteases that are usually highly expressed in the tumour site (134,145–148). In the last years, several studies described NID1 as a potential marker of tumour progression and prognosis: for example, elevated levels of sNID1 in the serum of ovarian cancer patients and in the secretome of lung metastasis, derived from breast cancer and melanoma, have been reported (194–200); moreover, a pro-tumoural and pro-metastatic role for NID1 has been demonstrated. Indeed, studies conducted on ovarian carcinomas showed that NID1 plays an important role in inducing EMT processes and chemoresistance in tumour cells, while NID1 involvement in tumour invasiveness and metastasis has been shown in the case of endometrial cancer and lung cancer (193,201,203). Therefore, sNID1-NKp44 interaction might represent a novel escape mechanism exploited by tumours to avoid NK cell-mediated killing. On the other hand, other studies demonstrated that NID1 loss may favour tumour invasiveness and spreading of tumour metastasis, due to the loss of BM integrity (192,202). Indeed, in the tumour microenvironment, NID1 could be exposed to the action of extracellular proteases, such as MMP-19, Cat-S, and ADAMTS1 (190,192,193): in particular, a specific fragment of NID1, derived from CatS-mediated degradation, found in the serum of NSCLC patients, was suggested to reflect the loss of BM integrity, typically associated to tumour progression (191). Western blot experiments performed with solubilised BM preparations indicated that NID1 could be present as a cleaved protein and that NKp44 could recognise a band of about 70 kDa, approximately

corresponding to the one detected with a NID1-specific mAb. This observation, together with the ability of NKp44Fc to recognise denatured NID1, might indicate that NKp44 interacts also with cleaved forms of NID1. Furthermore, NID1-NKp44 recognition and its functional outcome might be influenced not only by protease-mediated NID1 degradation but also by NID1 interaction with different ECM proteins, such as laminin, collagen type IV, and perlecan (176,186,187). Indeed, regarding NID1-NKp44 interaction, a possible functional role of perlecan should be considered. Since HSPGs, such as perlecan, have been described as co-ligands for NCRs (105,118), NKp44 recognition of NID1 in the presence of perlecan may induce a stronger modulation of NK cell-mediated cytokine release and cytotoxicity. Further studies should be undertaken to uncover the role of proteases and BM components in NID1-NKp44 interaction; additional insights in this direction and the identification of NID1 epitope recognised by NKp44 might provide new perspectives for NK cell-based cancer immunotherapy.

The presence of NID1 in exosomes derived from samples of healthy and cancer patients has been documented (194–199). Our preliminary data indicate that NID1 might be exposed at the surface of exosomes and MVs derived from HEK293T cells; therefore, it is possible that NK cell functions could also be influenced by $NID1^+$ extracellular vesicles. Different studies conducted on tumour-related exosomes revealed that they might carry immunosuppressive molecules (i.e. immune checkpoint receptor ligands, noncoding RNAs, and inhibitory cytokines) involved in the dampening of the immune response (172). Further studies are required to evaluate how $NID1^+$ exosomes might influence NK cell functions in the context of tumour microenvironment.

Importantly, we demonstrated that NID1 is not only a soluble protein but could also be detected at the cell surface. Several studies suggested that NID1 can be found associated to cell membrane through the interaction with $\alpha V\beta 3$ and $\alpha 3\beta 1$ integrins (178,181). Our data clearly demonstrated NID1 expression at the cell surface of different tumour cell lines by flow cytometry; this finding was also supported by single cell imaging analysis of HEK293T cells. In addition, these results were confirmed by flow cytometry analysis of K562- and Bw-NID1 transfectants, as well as by silencing experiments conducted on HEK293T cell line: staining with anti-NID1 mAb correlated with NID1 expression in both NID1 transfectants and NID1-silenced cells. Notably, also NKp44Fc staining was increased or reduced according to NID1 expression, indicating that NKp44 could recognise not only sNID1, but also mNID1. Functional experiments, performed in order to study the role of mNID1, revealed that neither plastic-bound NID1 nor NID1 cell transfectants could modulate the basal cytokine release in Bw-NKp44 and NK cells, whereas mNID1 could induce a slight increase of NK cell-mediated cytotoxicity. Interestingly, mass spectrometry analysis of NK cells stimulated with anti-NKp44 mAb or rNID1, revealed that plastic-bound NID1 induced changes in NK cell proteome, influencing pathways involved in NK cell immunologic functions, metabolism, proliferation, and development. GO analysis of modulated proteins showed that both rNID1 and anti-NKp44 mAb stimuli resulted in similar functional effects.

NID1 and NKp44 stimuli shared 15 proteins significantly modulated as compared to control samples: among them, 4 and 3 proteins were similarly up- and down-regulated, respectively, while 8 proteins were differentially modulated in rNID1- and NKp44-stimulated NK cells. One of the most significantly up-regulated proteins in both rNID1- and NKp44-stimulated NK cells was MYSM1. Interestingly, MYSM1 is a histone H2A deubiquitinase involved in mouse NK cell development (213), and mutations of *MYSM1* in humans have been associated to low NK and B cell counts, as well as to mild thrombocytopenia (214). Studies on human NK cell development demonstrated that immature NK cells at different maturation stages express NKp44 receptor (215). Therefore, the investigation of the functional role of NID1-NKp44 interaction on NK cell maturation and the effect of such interaction on MYSM1 expression, in both immature and cytokine-activated mature NK cells could be very relevant. Studies on mucosal ILC3 demonstrated that NKp44 engagement induces TNFα and IL-22 production (216), as well as a wide modification of ILC3 transcriptome (85). Similarly, proteomic data obtained from NID1-stimulated NK cells suggest that NID1 could be involved in modulating novel NKp44-mediated NK cell functions by inducing a broad alteration of NK cell proteomic profile. Since NID1 is highly expressed in different tissues, such as mucosae and decidua (182), where NKp44-expressing cells can be found (12,13), NID1 effect on ILC3 and other NKp44$^+$ cells should be explored. Within decidua tissue dNK cells play an important role in maintaining an immunosuppressive microenvironment (18–20): the role of sNID1-dNK cell interaction should be studied, keeping in mind that the outcome of this interaction could also be influenced by the expression of different NKp44 isoforms (76,77).

NID1 is a member of Nidogen family that comprises also NID2 protein (176): NID1 and NID2 share similar functions and structure. Our preliminary data suggest that rNID2 could interact with NKp44 and inhibit NKp44-mediated cytokine release, even if at a lesser extent than NID1. However, more data need to be collected regarding the relevance of NID2 in the context of NKp44 recognition.

In conclusion, NID1 characterization as an extracellular ligand for NKp44 provides new insights in the complexity of NK cell biology. Further investigations on the potential functional effects of NID1 degradation by ECM proteases and interaction with other ECM components are necessary to fully understand NKp44-mediated mechanisms regulating NK cell functions. Our proteomic analysis also suggests that NKp44 could be involved in regulating different biological processes, thus indicating novel NK cell functions. Collectively, our data and future studies might lead to new approaches for NK cell-based immunotherapy.

6. BIBLIOGRAPHY

1. Herberman RB, Nunn ME, Lavrin DH. Natural cytotoxic reactivity of mouse lymphoid cells against syngeneic acid allogeneic tumors. I. Distribution of reactivity and specificity. *Int J Cancer* (1975) **16**:216–229.
2. Kiessling R, Klein E, Wigzell H. „Natural" killer cells in the mouse. I. Cytotoxic cells with specificity for mouse Moloney leukemia cells. Specificity and distribution according to genotype. *Eur J Immunol* (1975) **5**:112–117. doi:10.1002/eji.1830050208
3. Pross HF, Jondal M. Cytotoxic lymphocytes from normal donors. A functional marker of human non-T lymphocytes. *Clin Exp Immunol* (1975) **21**:226–235.
4. Trinchieri G. Biology of natural killer cells. *Adv Immunol* (1989) **47**:187–376.
5. Vivier E. What is natural in natural killer cells? *Immunol Lett* (2006) **107**:1–7. doi:10.1016/j.imlet.2006.07.004
6. Moretta L, Montaldo E, Vacca P, Del Zotto G, Moretta F, Merli P, Locatelli F, Mingari MC. Human natural killer cells: origin, receptors, function, and clinical applications. *Int Arch Allergy Immunol* (2014) **164**:253–264. doi:10.1159/000365632
7. Spits H, Artis D, Colonna M, Diefenbach A, Di Santo JP, Eberl G, Koyasu S, Locksley RM, McKenzie ANJ, Mebius RE, et al. Innate lymphoid cells--a proposal for uniform nomenclature. *Nat Rev Immunol* (2013) **13**:145–149. doi:10.1038/nri3365
8. Montaldo E, Vacca P, Moretta L, Mingari MC. Development of human natural killer cells and other innate lymphoid cells. *Semin Immunol* (2014) **26**:107–113. doi:10.1016/j.smim.2014.01.006
9. Holder KA, Comeau EM, Grant MD. Origins of natural killer cell memory: special creation or adaptive evolution. *Immunology* **154**:38–49. doi:10.1111/imm.12898
10. Sun JC, Lanier LL. NK cell development, homeostasis and function: parallels with CD8+ T cells. *Nat Rev Immunol* (2011) **11**:645. doi:10.1038/nri3044
11. Ferlazzo G, Carrega P. Natural killer cell distribution and trafficking in human tissues. *Front Immunol* (2012) **3**: doi:10.3389/fimmu.2012.00347
12. Björkström NK, Ljunggren H-G, Michaëlsson J. Emerging insights into natural killer cells in human peripheral tissues. *Nat Rev Immunol* (2016) **16**:310–320. doi:10.1038/nri.2016.34
13. Melsen JE, Lugthart G, Lankester AC, Schilham MW. Human Circulating and Tissue-Resident CD56(bright) Natural Killer Cell Populations. *Front Immunol* (2016) **7**:262. doi:10.3389/fimmu.2016.00262
14. Freud AG, Mundy-Bosse BL, Yu J, Caligiuri MA. The Broad Spectrum of Human Natural Killer Cell Diversity. *Immunity* (2017) **47**:820–833. doi:10.1016/j.immuni.2017.10.008
15. Jouanguy E, Gineau L, Cottineau J, Beziat V, Vivier E, Casanova J-L. Inborn errors of the development of human Natural Killer cells. *Curr Opin Allergy Clin Immunol* (2013) **13**:589–595. doi:10.1097/ACI.0000000000000011
16. Voss M, Bryceson YT. Natural killer cell biology illuminated by primary immunodeficiency syndromes in humans. *Clin Immunol* (2015) doi:10.1016/j.clim.2015.11.004
17. Yoder JA, Litman GW. The phylogenetic origins of natural killer receptors and recognition:relationships, possibilities and realities. *Immunogenetics* (2011) **63**:123–141. doi:10.1007/s00251-010-0506-4
18. Moffett-King A. Natural killer cells and pregnancy. *Nat Rev Immunol* (2002) **2**:656–663. doi:10.1038/nri886
19. Vacca P, Mingari MC, Moretta L. Natural killer cells in human pregnancy. *J Reprod Immunol* (2013) **97**:14–19. doi:10.1016/j.jri.2012.10.008
20. Gaynor LM, Colucci F. Uterine Natural Killer Cells: Functional Distinctions and Influence on Pregnancy in Humans and Mice. *Front Immunol* (2017) **8**:467. doi:10.3389/fimmu.2017.00467
21. Caligiuri MA. Human natural killer cells. *Blood* (2008) **112**:461–469. doi:10.1182/blood-2007-09-077438

22. Vivier E, Tomasello E, Baratin M, Walzer T, Ugolini S. Functions of natural killer cells. *Nat Immunol* (2008) **9**:503. doi:10.1038/ni1582
23. Ziegler S, Weiss E, Schmitt A-L, Schlegel J, Burgert A, Terpitz U, Sauer M, Moretta L, Sivori S, Leonhardt I, et al. CD56 Is a Pathogen Recognition Receptor on Human Natural Killer Cells. *Sci Rep* (2017) **7**: doi:10.1038/s41598-017-06238-4
24. Moretta L. Dissecting CD56dim human NK cells. *Blood* (2010) **116**:3689–3691. doi:10.1182/blood-2010-09-303057
25. Long EO, Kim HS, Liu D, Peterson ME, Rajagopalan S. Controlling natural killer cell responses: integration of signals for activation and inhibition. *Annu Rev Immunol* (2013) **31**:227–258. doi:10.1146/annurev-immunol-020711-075005
26. De Maria A, Bozzano F, Cantoni C, Moretta L. Revisiting human natural killer cell subset function revealed cytolytic CD56(dim)CD16+ NK cells as rapid producers of abundant IFN-gamma on activation. *Proc Natl Acad Sci U S A* (2011) **108**:728–732. doi:10.1073/pnas.1012356108
27. Farag SS, Caligiuri MA. Human natural killer cell development and biology. *Blood Rev* (2006) **20**:123–137. doi:10.1016/j.blre.2005.10.001
28. Vacca P, Cantoni C, Prato C, Fulcheri E, Moretta A, Moretta L, Mingari MC. Regulatory role of NKp44, NKp46, DNAM-1 and NKG2D receptors in the interaction between NK cells and trophoblast cells. Evidence for divergent functional profiles of decidual versus peripheral NK cells. *Int Immunol* (2008) **20**:1395–1405. doi:10.1093/intimm/dxn105
29. Vacca P, Cantoni C, Vitale M, Prato C, Canegallo F, Fenoglio D, Ragni N, Moretta L, Mingari MC. Crosstalk between decidual NK and CD14+ myelomonocytic cells results in induction of Tregs and immunosuppression. *Proc Natl Acad Sci U S A* (2010) **107**:11918–11923. doi:10.1073/pnas.1001749107
30. Moretta A, Marcenaro E, Sivori S, Della Chiesa M, Vitale M, Moretta L. Early liaisons between cells of the innate immune system in inflamed peripheral tissues. *Trends Immunol* (2005) **26**:668–675. doi:10.1016/j.it.2005.09.008
31. Münz C, Steinman RM, Fujii S. Dendritic cell maturation by innate lymphocytes: coordinated stimulation of innate and adaptive immunity. *J Exp Med* (2005) **202**:203–207. doi:10.1084/jem.20050810
32. Wehner R, Dietze K, Bachmann M, Schmitz M. The bidirectional crosstalk between human dendritic cells and natural killer cells. *J Innate Immun* (2011) **3**:258–263. doi:10.1159/000323923
33. Thomas R, Yang X. NK-DC Crosstalk in Immunity to Microbial Infection. *J Immunol Res* (2016) doi:10.1155/2016/6374379
34. Mantovani A, Cassatella MA, Costantini C, Jaillon S. Neutrophils in the activation and regulation of innate and adaptive immunity. *Nat Rev Immunol* (2011) **11**:519–531. doi:10.1038/nri3024
35. Thorén FB, Riise RE, Ousbäck J, Della Chiesa M, Alsterholm M, Marcenaro E, Pesce S, Prato C, Cantoni C, Bylund J, et al. Human NK Cells induce neutrophil apoptosis via an NKp46- and Fas-dependent mechanism. *J Immunol Baltim Md 1950* (2012) **188**:1668–1674. doi:10.4049/jimmunol.1102002
36. Pesce S, Thoren FB, Cantoni C, Prato C, Moretta L, Moretta A, Marcenaro E. The Innate Immune Cross Talk between NK Cells and Eosinophils Is Regulated by the Interaction of Natural Cytotoxicity Receptors with Eosinophil Surface Ligands. *Front Immunol* (2017) **8**:510. doi:10.3389/fimmu.2017.00510
37. Bellora F, Castriconi R, Dondero A, Reggiardo G, Moretta L, Mantovani A, Moretta A, Bottino C. The interaction of human natural killer cells with either unpolarized or polarized macrophages results in different functional outcomes. *Proc Natl Acad Sci U S A* (2010) **107**:21659–21664. doi:10.1073/pnas.1007654108
38. Spaggiari GM, Moretta L. Cellular and molecular interactions of mesenchymal stem cells in innate immunity. *Immunol Cell Biol* (2013) **91**:27–31. doi:10.1038/icb.2012.62
39. Ljunggren HG, Kärre K. In search of the “missing self”: MHC molecules and NK cell recognition. *Immunol Today* (1990) **11**:237–244.

40. Cullen SP, Martin SJ. Mechanisms of granule-dependent killing. *Cell Death Differ* (2008) **15**:251–262. doi:10.1038/sj.cdd.4402244
41. Moretta A, Bottino C, Vitale M, Pende D, Biassoni R, Mingari MC, Moretta L. Receptors for HLA class-I molecules in human natural killer cells. *Annu Rev Immunol* (1996) **14**:619–648. doi:10.1146/annurev.immunol.14.1.619
42. Moretta A, Bottino C, Vitale M, Pende D, Cantoni C, Mingari MC, Biassoni R, Moretta L. Activating receptors and co-receptors involved in human natural killer cell-mediated cytolysis. *Annu Rev Immunol* (2001) **19**:197–223. doi:10.1146/annurev.immunol.19.1.197
43. Tomasello E, Bléry M, Vély F, Vivier E. Signaling pathways engaged by NK cell receptors: double concerto for activating receptors, inhibitory receptors and NK cells. *Semin Immunol* (2000) **12**:139–147. doi:10.1006/smim.2000.0216
44. Falco M, Moretta L, Moretta A, Bottino C. KIR and KIR ligand polymorphism: a new area for clinical applications? *Tissue Antigens* (2013) **82**:363–373. doi:10.1111/tan.12262
45. Sivori S, Carlomagno S, Pesce S, Moretta A, Vitale M, Marcenaro E. TLR/NCR/KIR: Which One to Use and When? *Front Immunol* (2014) **5**: doi:10.3389/fimmu.2014.00105
46. Guethlein LA, Norman PJ, Hilton HG, Parham P. Co-evolution of MHC class I and variable NK cell receptors in placental mammals. *Immunol Rev* (2015) **267**:259–282. doi:10.1111/imr.12326
47. Hilton HG, Parham P. Missing or altered self: human NK cell receptors that recognize HLA-C. *Immunogenetics* (2017) **69**:567–579. doi:10.1007/s00251-017-1001-y
48. Sivori S, Falco M, Carlomagno S, Romeo E, Soldani C, Bensussan A, Viola A, Moretta L, Moretta A. A novel KIR-associated function: evidence that CpG DNA uptake and shuttling to early endosomes is mediated by KIR3DL2. *Blood* (2010) **116**:1637–1647. doi:10.1182/blood-2009-12-256586
49. Orr MT, Lanier LL. Natural killer cell education and tolerance. *Cell* (2010) **142**:847–856. doi:10.1016/j.cell.2010.08.031
50. Shifrin N, Raulet DH, Ardolino M. NK cell self tolerance, responsiveness and missing self recognition. *Semin Immunol* (2014) **26**:138–144. doi:10.1016/j.smim.2014.02.007
51. Navarro F, Llano M, Bellón T, Colonna M, Geraghty DE, López-Botet M. The ILT2(LIR1) and CD94/NKG2A NK cell receptors respectively recognize HLA-G1 and HLA-E molecules co-expressed on target cells. *Eur J Immunol* (1999) **29**:277–283. doi:10.1002/(SICI)1521-4141(199901)29:01<277::AID-IMMU277>3.0.CO;2-4
52. Borrego F, Masilamani M, Marusina AI, Tang X, Coligan JE. The CD94/NKG2 family of receptors. *Immunol Res* (2006) **35**:263–277. doi:10.1385/IR:35:3:263
53. Della Chiesa M, Sivori S, Carlomagno S, Moretta L, Moretta A. Activating KIRs and NKG2C in Viral Infections: Toward NK Cell Memory? *Front Immunol* (2015) **6**:573. doi:10.3389/fimmu.2015.00573
54. Samaridis J, Colonna M. Cloning of novel immunoglobulin superfamily receptors expressed on human myeloid and lymphoid cells: structural evidence for new stimulatory and inhibitory pathways. *Eur J Immunol* (1997) **27**:660–665. doi:10.1002/eji.1830270313
55. Cantoni C, Bottino C, Augugliaro R, Morelli L, Marcenaro E, Castriconi R, Vitale M, Pende D, Sivori S, Millo R, et al. Molecular and functional characterization of IRp60, a member of the immunoglobulin superfamily that functions as an inhibitory receptor in human NK cells. *Eur J Immunol* (1999) **29**:3148–3159. doi:10.1002/(SICI)1521-4141(199910)29:10<3148::AID-IMMU3148>3.0.CO;2-L
56. Koch J, Steinle A, Watzl C, Mandelboim O. Activating natural cytotoxicity receptors of natural killer cells in cancer and infection. *Trends Immunol* (2013) **34**:182–191. doi:10.1016/j.it.2013.01.003
57. Joyce MG, Sun PD. The Structural Basis of Ligand Recognition by Natural Killer Cell Receptors. *BioMed Res Int* (2011) **2011**:e203628. doi:10.1155/2011/203628
58. Sivori S, Vitale M, Morelli L, Sanseverino L, Augugliaro R, Bottino C, Moretta L, Moretta A. p46, a novel natural killer cell-specific surface molecule that mediates cell activation. *J Exp Med* (1997) **186**:1129–1136.

59. Pessino A, Sivori S, Bottino C, Malaspina A, Morelli L, Moretta L, Biassoni R, Moretta A. Molecular Cloning of NKp46: A Novel Member of the Immunoglobulin Superfamily Involved in Triggering of Natural Cytotoxicity. *J Exp Med* (1998) **188**:953–960.
60. Vitale M, Bottino C, Sivori S, Sanseverino L, Castriconi R, Marcenaro E, Augugliaro R, Moretta L, Moretta A. NKp44, a novel triggering surface molecule specifically expressed by activated natural killer cells, is involved in non-major histocompatibility complex-restricted tumor cell lysis. *J Exp Med* (1998) **187**:2065–2072.
61. Cantoni C, Bottino C, Vitale M, Pessino A, Augugliaro R, Malaspina A, Parolini S, Moretta L, Moretta A, Biassoni R. NKp44, a triggering receptor involved in tumor cell lysis by activated human natural killer cells, is a novel member of the immunoglobulin superfamily. *J Exp Med* (1999) **189**:787–796.
62. Pende D, Parolini S, Pessino A, Sivori S, Augugliaro R, Morelli L, Marcenaro E, Accame L, Malaspina A, Biassoni R, et al. Identification and molecular characterization of NKp30, a novel triggering receptor involved in natural cytotoxicity mediated by human natural killer cells. *J Exp Med* (1999) **190**:1505–1516.
63. Foster CE, Colonna M, Sun PD. Crystal Structure of the Human Natural Killer (NK) Cell Activating Receptor NKp46 Reveals Structural Relationship to Other Leukocyte Receptor Complex Immunoreceptors. *J Biol Chem* (2003) **278**:46081–46086. doi:10.1074/jbc.M308491200
64. Jaron-Mendelson M, Yossef R, Appel MY, Zilka A, Hadad U, Afergan F, Rosental B, Engel S, Nedvetzki S, Braiman A, et al. Dimerization of NKp46 receptor is essential for NKp46-mediated lysis: characterization of the dimerization site by epitope mapping. *J Immunol Baltim Md 1950* (2012) **188**:6165–6174. doi:10.4049/jimmunol.1102496
65. Cantoni C, Ponassi M, Biassoni R, Conte R, Spallarossa A, Moretta A, Moretta L, Bolognesi M, Bordo D. The three-dimensional structure of the human NK cell receptor NKp44, a triggering partner in natural cytotoxicity. *Struct Lond Engl 1993* (2003) **11**:725–734.
66. Joyce MG, Tran P, Zhuravleva MA, Jaw J, Colonna M, Sun PD. Crystal structure of human natural cytotoxicity receptor NKp30 and identification of its ligand binding site. *Proc Natl Acad Sci U S A* (2011) **108**:6223–6228. doi:10.1073/pnas.1100622108
67. Augugliaro R, Parolini S, Castriconi R, Marcenaro E, Cantoni C, Nanni M, Moretta L, Moretta A, Bottino C. Selective cross-talk among natural cytotoxicity receptors in human natural killer cells. *Eur J Immunol* (2003) **33**:1235–1241. doi:10.1002/eji.200323896
68. Falco M, Cantoni C, Bottino C, Moretta A, Biassoni R. Identification of the rat homologue of the human NKp46 triggering receptor. *Immunol Lett* (1999) **68**:411–414.
69. Walzer T, Jaeger S, Chaix J, Vivier E. Natural killer cells: from CD3(-)NKp46(+) to post-genomics meta-analyses. *Curr Opin Immunol* (2007) **19**:365–372. doi:10.1016/j.coi.2007.04.004
70. Tomasello E, Yessaad N, Gregoire E, Hudspeth K, Luci C, Mavilio D, Hardwigsen J, Vivier E. Mapping of NKp46(+) Cells in Healthy Human Lymphoid and Non-Lymphoid Tissues. *Front Immunol* (2012) **3**:344. doi:10.3389/fimmu.2012.00344
71. Vitale C, Chiossone L, Cantoni C, Morreale G, Cottalasso F, Moretti S, Pistorio A, Haupt R, Lanino E, Dini G, et al. The corticosteroid-induced inhibitory effect on NK cell function reflects down-regulation and/or dysfunction of triggering receptors involved in natural cytotoxicity. *Eur J Immunol* (2004) **34**:3028–3038. doi:10.1002/eji.200425418
72. Mavoungou E, Bouyou-Akotet MK, Kremsner PG. Effects of prolactin and cortisol on natural killer (NK) cell surface expression and function of human natural cytotoxicity receptors (NKp46, NKp44 and NKp30). *Clin Exp Immunol* (2005) **139**:287–296. doi:10.1111/j.1365-2249.2004.02686.x
73. Della Chiesa M, Carlomagno S, Frumento G, Balsamo M, Cantoni C, Conte R, Moretta L, Moretta A, Vitale M. The tryptophan catabolite L-kynurenine inhibits the surface expression of NKp46- and NKG2D-activating receptors and regulates NK-cell function. *Blood* (2006) **108**:4118–4125. doi:10.1182/blood-2006-03-006700

74. Memmer S, Weil S, Beyer S, Zöller T, Peters E, Hartmann J, Steinle A, Koch J. The Stalk Domain of NKp30 Contributes to Ligand Binding and Signaling of a Preassembled NKp30-CD3ζ Complex. *J Biol Chem* (2016) **291**:25427–25438. doi:10.1074/jbc.M116.742981
75. Delahaye NF, Rusakiewicz S, Martins I, Ménard C, Roux S, Lyonnet L, Paul P, Sarabi M, Chaput N, Semeraro M, et al. Alternatively spliced NKp30 isoforms affect the prognosis of gastrointestinal stromal tumors. *Nat Med* (2011) **17**:700–707. doi:10.1038/nm.2366
76. Siewiera J, Gouilly J, Hocine H-R, Cartron G, Levy C, Al-Daccak R, Jabrane-Ferrat N. Natural cytotoxicity receptor splice variants orchestrate the distinct functions of human natural killer cell subtypes. *Nat Commun* (2015) **6**:10183. doi:10.1038/ncomms10183
77. Shemesh A, Kugel A, Steiner N, Yezersky M, Tirosh D, Edri A, Teltsh O, Rosental B, Sheiner E, Rubin E, et al. NKp44 and NKp30 splice variant profiles in decidua and tumor tissues: a comparative viewpoint. *Oncotarget* (2016) **7**:70912–70923. doi:10.18632/oncotarget.12292
78. Messaoudene M, Fregni G, Enot D, Jacquelot N, Neves E, Germaud N, Garchon HJ, Boukouaci W, Tamouza R, Chanal J, et al. NKp30 isoforms and NKp46 transcripts in metastatic melanoma patients: Unique NKp30 pattern in rare melanoma patients with favorable evolution. *Oncoimmunology* (2016) **5**:e1154251. doi:10.1080/2162402X.2016.1154251
79. Tang Q, Grzywacz B, Wang H, Kataria N, Cao Q, Wagner JE, Blazar BR, Miller JS, Verneris MR. Umbilical cord blood T cells express multiple natural cytotoxicity receptors after IL-15 stimulation, but only NKp30 is functional. *J Immunol Baltim Md 1950* (2008) **181**:4507–4515.
80. Ponnampalam AP, Gargett CE, Rogers PAW. Identification and hormonal regulation of a novel form of NKp30 in human endometrial epithelium. *Eur J Immunol* (2008) **38**:216–226. doi:10.1002/eji.200636429
81. Correia DV, Fogli M, Hudspeth K, da Silva MG, Mavilio D, Silva-Santos B. Differentiation of human peripheral blood Vδ1+ T cells expressing the natural cytotoxicity receptor NKp30 for recognition of lymphoid leukemia cells. *Blood* (2011) **118**:992–1001. doi:10.1182/blood-2011-02-339135
82. Castriconi R, Cantoni C, Della Chiesa M, Vitale M, Marcenaro E, Conte R, Biassoni R, Bottino C, Moretta L, Moretta A. Transforming growth factor beta 1 inhibits expression of NKp30 and NKG2D receptors: consequences for the NK-mediated killing of dendritic cells. *Proc Natl Acad Sci U S A* (2003) **100**:4120–4125. doi:10.1073/pnas.0730640100
83. Allcock RJN, Barrow AD, Forbes S, Beck S, Trowsdale J. The human TREM gene cluster at 6p21.1 encodes both activating and inhibitory single IgV domain receptors and includes NKp44. *Eur J Immunol* (2003) **33**:567–577. doi:10.1002/immu.200310033
84. De Maria A, Ugolotti E, Rutjens E, Mazza S, Radic L, Faravelli A, Koopman G, Di Marco E, Costa P, Ensoli B, et al. NKp44 expression, phylogenesis and function in non-human primate NK cells. *Int Immunol* (2009) **21**:245–255. doi:10.1093/intimm/dxn144
85. Glatzer T, Killig M, Meisig J, Ommert I, Luetke-Eversloh M, Babic M, Paclik D, Blüthgen N, Seidl R, Seifarth C, et al. RORγt$^+$ innate lymphoid cells acquire a proinflammatory program upon engagement of the activating receptor NKp44. *Immunity* (2013) **38**:1223–1235. doi:10.1016/j.immuni.2013.05.013
86. Fuchs A, Cella M, Kondo T, Colonna M. Paradoxic inhibition of human natural interferon-producing cells by the activating receptor NKp44. *Blood* (2005) **106**:2076–2082. doi:10.1182/blood-2004-12-4802
87. Balsamo M, Scordamaglia F, Pietra G, Manzini C, Cantoni C, Boitano M, Queirolo P, Vermi W, Facchetti F, Moretta A, et al. Melanoma-associated fibroblasts modulate NK cell phenotype and antitumor cytotoxicity. *Proc Natl Acad Sci U S A* (2009) **106**:20847–20852. doi:10.1073/pnas.0906481106
88. Raulet DH. Roles of the NKG2D immunoreceptor and its ligands. *Nat Rev Immunol* (2003) **3**:781–790. doi:10.1038/nri1199
89. El-Gazzar A, Groh V, Spies T. Immunobiology and conflicting roles of the human NKG2D lymphocyte receptor and its ligands in cancer. *J Immunol Baltim Md 1950* (2013) **191**:1509–1515. doi:10.4049/jimmunol.1301071

90. Lanier LL. NKG2D Receptor and Its Ligands in Host Defense. *Cancer Immunol Res* (2015) **3**:575–582. doi:10.1158/2326-6066.CIR-15-0098
91. Pende D, Rivera P, Marcenaro S, Chang C-C, Biassoni R, Conte R, Kubin M, Cosman D, Ferrone S, Moretta L, et al. Major histocompatibility complex class I-related chain A and UL16-binding protein expression on tumor cell lines of different histotypes: analysis of tumor susceptibility to NKG2D-dependent natural killer cell cytotoxicity. *Cancer Res* (2002) **62**:6178–6186.
92. Sutherland CL, Chalupny NJ, Cosman D. The UL16-binding proteins, a novel family of MHC class I-related ligands for NKG2D, activate natural killer cell functions. *Immunol Rev* (2001) **181**:185–192. doi:10.1034/j.1600-065X.2001.1810115.x
93. Shibuya A, Campbell D, Hannum C, Yssel H, Franz-Bacon K, McClanahan T, Kitamura T, Nicholl J, Sutherland GR, Lanier LL, et al. DNAM-1, a novel adhesion molecule involved in the cytolytic function of T lymphocytes. *Immunity* (1996) **4**:573–581.
94. de Andrade LF, Smyth MJ, Martinet L. DNAM-1 control of natural killer cells functions through nectin and nectin-like proteins. *Immunol Cell Biol* (2014) **92**:237–244. doi:10.1038/icb.2013.95
95. Bottino C, Castriconi R, Pende D, Rivera P, Nanni M, Carnemolla B, Cantoni C, Grassi J, Marcenaro S, Reymond N, et al. Identification of PVR (CD155) and Nectin-2 (CD112) as cell surface ligands for the human DNAM-1 (CD226) activating molecule. *J Exp Med* (2003) **198**:557–567. doi:10.1084/jem.20030788
96. Bottino C, Castriconi R, Moretta L, Moretta A. Cellular ligands of activating NK receptors. *Trends Immunol* (2005) **26**:221–226. doi:10.1016/j.it.2005.02.007
97. Stanietsky N, Simic H, Arapovic J, Toporik A, Levy O, Novik A, Levine Z, Beiman M, Dassa L, Achdout H, et al. The interaction of TIGIT with PVR and PVRL2 inhibits human NK cell cytotoxicity. *Proc Natl Acad Sci U S A* (2009) **106**:17858–17863. doi:10.1073/pnas.0903474106
98. Chan CJ, Martinet L, Gilfillan S, Souza-Fonseca-Guimaraes F, Chow MT, Town L, Ritchie DS, Colonna M, Andrews DM, Smyth MJ. The receptors CD96 and CD226 oppose each other in the regulation of natural killer cell functions. *Nat Immunol* (2014) **15**:431–438. doi:10.1038/ni.2850
99. Green BJ, Clark GJ, Hart DN. The CMRF-35 mAb recognizes a second leukocyte membrane molecule with a domain similar to the poly Ig receptor. *Int Immunol* (1998) **10**:891–899.
100. Clark GJ, Cooper B, Fitzpatrick S, Green BJ, Hart DN. The gene encoding the immunoregulatory signaling molecule CMRF-35A localized to human chromosome 17 in close proximity to other members of the CMRF-35 family. *Tissue Antigens* (2001) **57**:415–423.
101. Simhadri VR, Andersen JF, Calvo E, Choi S-C, Coligan JE, Borrego F. Human CD300a binds to phosphatidylethanolamine and phosphatidylserine, and modulates the phagocytosis of dead cells. *Blood* (2012) **119**:2799–2809. doi:10.1182/blood-2011-08-372425
102. Lankry D, Rovis TL, Jonjic S, Mandelboim O. The interaction between CD300a and phosphatidylserine inhibits tumor cell killing by NK cells. *Eur J Immunol* (2013) **43**:2151–2161. doi:10.1002/eji.201343433
103. Binici J, Hartmann J, Herrmann J, Schreiber C, Beyer S, Güler G, Vogel V, Tumulka F, Abele R, Mäntele W, et al. A soluble fragment of the tumor antigen BCL2-associated athanogene 6 (BAG-6) is essential and sufficient for inhibition of NKp30 receptor-dependent cytotoxicity of natural killer cells. *J Biol Chem* (2013) **288**:34295–34303. doi:10.1074/jbc.M113.483602
104. Baychelier F, Sennepin A, Ermonval M, Dorgham K, Debré P, Vieillard V. Identification of a cellular ligand for the natural cytotoxicity receptor NKp44. *Blood* (2013) **122**:2935–2942. doi:10.1182/blood-2013-03-489054
105. Horton NC, Mathew PA. NKp44 and Natural Cytotoxicity Receptors as Damage-Associated Molecular Pattern Recognition Receptors. *Front Immunol* (2015) **6**: doi:10.3389/fimmu.2015.00031
106. Mandelboim O, Lieberman N, Lev M, Paul L, Arnon TI, Bushkin Y, Davis DM, Strominger JL, Yewdell JW, Porgador A. Recognition of haemagglutinins on virus-infected cells by NKp46 activates lysis by human NK cells. *Nature* (2001) **409**:1055–1060. doi:10.1038/35059110

107. Arnon TI, Achdout H, Lieberman N, Gazit R, Gonen-Gross T, Katz G, Bar-Ilan A, Bloushtain N, Lev M, Joseph A, et al. The mechanisms controlling the recognition of tumor- and virus-infected cells by NKp46. *Blood* (2004) **103**:664–672. doi:10.1182/blood-2003-05-1716
108. Jarahian M, Watzl C, Fournier P, Arnold A, Djandji D, Zahedi S, Cerwenka A, Paschen A, Schirrmacher V, Momburg F. Activation of Natural Killer Cells by Newcastle Disease Virus Hemagglutinin-Neuraminidase. *J Virol* (2009) **83**:8108–8121. doi:10.1128/JVI.00211-09
109. Jarahian M, Fiedler M, Cohnen A, Djandji D, Hämmerling GJ, Gati C, Cerwenka A, Turner PC, Moyer RW, Watzl C, et al. Modulation of NKp30- and NKp46-mediated natural killer cell responses by poxviral hemagglutinin. *PLoS Pathog* (2011) **7**:e1002195. doi:10.1371/journal.ppat.1002195
110. Mavoungou E, Held J, Mewono L, Kremsner PG. A Duffy binding-like domain is involved in the NKp30-mediated recognition of Plasmodium falciparum-parasitized erythrocytes by natural killer cells. *J Infect Dis* (2007) **195**:1521–1531. doi:10.1086/515579
111. Chaushu S, Wilensky A, Gur C, Shapira L, Elboim M, Halftek G, Polak D, Achdout H, Bachrach G, Mandelboim O. Direct recognition of Fusobacterium nucleatum by the NK cell natural cytotoxicity receptor NKp46 aggravates periodontal disease. *PLoS Pathog* (2012) **8**:e1002601. doi:10.1371/journal.ppat.1002601
112. Vitenshtein A, Charpak-Amikam Y, Yamin R, Bauman Y, Isaacson B, Stein N, Berhani O, Dassa L, Gamliel M, Gur C, et al. NK Cell Recognition of Candida glabrata through Binding of NKp46 and NCR1 to Fungal Ligands Epa1, Epa6, and Epa7. *Cell Host Microbe* (2016) **20**:527–534. doi:10.1016/j.chom.2016.09.008
113. Garg A, Barnes PF, Porgador A, Roy S, Wu S, Nanda JS, Griffith DE, Girard WM, Rawal N, Shetty S, et al. Vimentin expressed on Mycobacterium tuberculosis-infected human monocytes is involved in binding to the NKp46 receptor. *J Immunol Baltim Md 1950* (2006) **177**:6192–6198.
114. Gur C, Porgador A, Elboim M, Gazit R, Mizrahi S, Stern-Ginossar N, Achdout H, Ghadially H, Dor Y, Nir T, et al. The activating receptor NKp46 is essential for the development of type 1 diabetes. *Nat Immunol* (2010) **11**:121–128. doi:10.1038/ni.1834
115. Gur C, Enk J, Kassem SA, Suissa Y, Magenheim J, Stolovich-Rain M, Nir T, Achdout H, Glaser B, Shapiro J, et al. Recognition and killing of human and murine pancreatic beta cells by the NK receptor NKp46. *J Immunol Baltim Md 1950* (2011) **187**:3096–3103. doi:10.4049/jimmunol.1101269
116. Gur C, Doron S, Kfir-Erenfeld S, Horwitz E, Abu-Tair L, Safadi R, Mandelboim O. NKp46-mediated killing of human and mouse hepatic stellate cells attenuates liver fibrosis. *Gut* (2012) **61**:885–893. doi:10.1136/gutjnl-2011-301400
117. Narni-Mancinelli E, Gauthier L, Baratin M, Guia S, Fenis A, Deghmane A-E, Rossi B, Fourquet P, Escalière B, Kerdiles YM, et al. Complement factor P is a ligand for the natural killer cell-activating receptor NKp46. *Sci Immunol* (2017) **2**: doi:10.1126/sciimmunol.aam9628
118. Hecht M-L, Rosental B, Horlacher T, Hershkovitz O, De Paz JL, Noti C, Schauer S, Porgador A, Seeberger PH. Natural cytotoxicity receptors NKp30, NKp44 and NKp46 bind to different heparan sulfate/heparin sequences. *J Proteome Res* (2009) **8**:712–720. doi:10.1021/pr800747c
119. Arnon TI, Lev M, Katz G, Chernobrov Y, Porgador A, Mandelboim O. Recognition of viral hemagglutinins by NKp44 but not by NKp30. *Eur J Immunol* (2001) **31**:2680–2689. doi:10.1002/1521-4141(200109)31:9<2680::AID-IMMU2680>3.0.CO;2-A
120. Hershkovitz O, Rosental B, Rosenberg LA, Navarro-Sanchez ME, Jivov S, Zilka A, Gershoni-Yahalom O, Brient-Litzler E, Bedouelle H, Ho JW, et al. NKp44 receptor mediates interaction of the envelope glycoproteins from the West Nile and dengue viruses with NK cells. *J Immunol Baltim Md 1950* (2009) **183**:2610–2621. doi:10.4049/jimmunol.0802806
121. Esin S, Batoni G, Pardini M, Favilli F, Bottai D, Maisetta G, Florio W, Vanacore R, Wigzell H, Campa M. Functional characterization of human natural killer cells responding to Mycobacterium bovis bacille Calmette-Guérin. *Immunology* (2004) **112**:143–152. doi:10.1111/j.1365-2567.2004.01858.x

122. Esin S, Counoupas C, Aulicino A, Brancatisano FL, Maisetta G, Bottai D, Di Luca M, Florio W, Campa M, Batoni G. Interaction of Mycobacterium tuberculosis cell wall components with the human natural killer cell receptors NKp44 and Toll-like receptor 2. *Scand J Immunol* (2013) **77**:460–469. doi:10.1111/sji.12052
123. Esin S, Batoni G, Counoupas C, Stringaro A, Brancatisano FL, Colone M, Maisetta G, Florio W, Arancia G, Campa M. Direct Binding of Human NK Cell Natural Cytotoxicity Receptor NKp44 to the Surfaces of Mycobacteria and Other Bacteria. *Infect Immun* (2008) **76**:1719–1727. doi:10.1128/IAI.00870-07
124. Rosental B, Brusilovsky M, Hadad U, Oz D, Appel MY, Afergan F, Yossef R, Rosenberg LA, Aharoni A, Cerwenka A, et al. Proliferating cell nuclear antigen is a novel inhibitory ligand for the natural cytotoxicity receptor NKp44. *J Immunol Baltim Md 1950* (2011) **187**:5693–5702. doi:10.4049/jimmunol.1102267
125. Vieillard V, Strominger JL, Debré P. NK cytotoxicity against CD4+ T cells during HIV-1 infection: a gp41 peptide induces the expression of an NKp44 ligand. *Proc Natl Acad Sci U S A* (2005) **102**:10981–10986. doi:10.1073/pnas.0504315102
126. Brusilovsky M, Radinsky O, Cohen L, Yossef R, Shemesh A, Braiman A, Mandelboim O, Campbell KS, Porgador A. Regulation of natural cytotoxicity receptors by heparan sulfate proteoglycans in -cis: A lesson from NKp44. *Eur J Immunol* (2015) **45**:1180–1191. doi:10.1002/eji.201445177
127. Barrow AD, Edeling MA, Trifonov V, Luo J, Goyal P, Bohl B, Bando JK, Kim AH, Walker J, Andahazy M, et al. Natural Killer Cells Control Tumor Growth by Sensing a Growth Factor. *Cell* (2018) **172**:534-548.e19. doi:10.1016/j.cell.2017.11.037
128. Białoszewska A, Baychelier F, Niderla-Bielińska J, Czop A, Debré P, Vieillard V, Kieda C, Malejczyk J. Constitutive expression of ligand for natural killer cell NKp44 receptor (NKp44L) by normal human articular chondrocytes. *Cell Immunol* (2013) **285**:6–9. doi:10.1016/j.cellimm.2013.08.005
129. Bowen KE, Mathew SO, Borgmann K, Ghorpade A, Mathew PA. A novel ligand on astrocytes interacts with natural cytotoxicity receptor NKp44 regulating immune response mediated by NK cells. *PLOS ONE* (2018) **13**:e0193008. doi:10.1371/journal.pone.0193008
130. Arnon TI, Achdout H, Levi O, Markel G, Saleh N, Katz G, Gazit R, Gonen-Gross T, Hanna J, Nahari E, et al. Inhibition of the NKp30 activating receptor by pp65 of human cytomegalovirus. *Nat Immunol* (2005) **6**:515–523. doi:10.1038/ni1190
131. Pogge von Strandmann E, Simhadri VR, von Tresckow B, Sasse S, Reiners KS, Hansen HP, Rothe A, Böll B, Simhadri VL, Borchmann P, et al. Human leukocyte antigen-B-associated transcript 3 is released from tumor cells and engages the NKp30 receptor on natural killer cells. *Immunity* (2007) **27**:965–974. doi:10.1016/j.immuni.2007.10.010
132. Simhadri VR, Reiners KS, Hansen HP, Topolar D, Simhadri VL, Nohroudi K, Kufer TA, Engert A, Pogge von Strandmann E. Dendritic cells release HLA-B-associated transcript-3 positive exosomes to regulate natural killer function. *PloS One* (2008) **3**:e3377. doi:10.1371/journal.pone.0003377
133. Brandt CS, Baratin M, Yi EC, Kennedy J, Gao Z, Fox B, Haldeman B, Ostrander CD, Kaifu T, Chabannon C, et al. The B7 family member B7-H6 is a tumor cell ligand for the activating natural killer cell receptor NKp30 in humans. *J Exp Med* (2009) **206**:1495–1503. doi:10.1084/jem.20090681
134. Schlecker E, Fiegler N, Arnold A, Altevogt P, Rose-John S, Moldenhauer G, Sucker A, Paschen A, von Strandmann EP, Textor S, et al. Metalloprotease-mediated tumor cell shedding of B7-H6, the ligand of the natural killer cell-activating receptor NKp30. *Cancer Res* (2014) **74**:3429–3440. doi:10.1158/0008-5472.CAN-13-3017
135. Wang W, Guo H, Geng J, Zheng X, Wei H, Sun R, Tian Z. Tumor-released Galectin-3, a soluble inhibitory ligand of human NKp30, plays an important role in tumor escape from NK cell attack. *J Biol Chem* (2014) **289**:33311–33319. doi:10.1074/jbc.M114.603464
136. Matta J, Baratin M, Chiche L, Forel J-M, Cognet C, Thomas G, Farnarier C, Piperoglou C, Papazian L, Chaussabel D, et al. Induction of B7-H6, a ligand for the natural killer cell-activating receptor

NKp30, in inflammatory conditions. *Blood* (2013) **122**:394–404. doi:10.1182/blood-2013-01-481705

137. Fiegler N, Textor S, Arnold A, Rölle A, Oehme I, Breuhahn K, Moldenhauer G, Witzens-Harig M, Cerwenka A. Downregulation of the activating NKp30 ligand B7-H6 by HDAC inhibitors impairs tumor cell recognition by NK cells. *Blood* (2013) **122**:684–693. doi:10.1182/blood-2013-02-482513
138. Cao G, Wang J, Zheng X, Wei H, Tian Z, Sun R. Tumor Therapeutics Work as Stress Inducers to Enhance Tumor Sensitivity to Natural Killer (NK) Cell Cytolysis by Up-regulating NKp30 Ligand B7-H6. *J Biol Chem* (2015) **290**:29964–29973. doi:10.1074/jbc.M115.674010
139. Horton NC, Mathew SO, Mathew PA. Novel interaction between proliferating cell nuclear antigen and HLA I on the surface of tumor cells inhibits NK cell function through NKp44. *PloS One* (2013) **8**:e59552. doi:10.1371/journal.pone.0059552
140. Fausther-Bovendo H, Vieillard V, Sagan S, Bismuth G, Debré P. HIV gp41 engages gC1qR on CD4+ T cells to induce the expression of an NK ligand through the PIP3/H2O2 pathway. *PLoS Pathog* (2010) **6**:e1000975. doi:10.1371/journal.ppat.1000975
141. Sasisekharan R, Venkataraman G. Heparin and heparan sulfate: biosynthesis, structure and function. *Curr Opin Chem Biol* (2000) **4**:626–631.
142. Knelson EH, Nee JC, Blobe GC. Heparan sulfate signaling in cancer. *Trends Biochem Sci* (2014) **39**:277–288. doi:10.1016/j.tibs.2014.03.001
143. Hershkovitz O, Jivov S, Bloushtain N, Zilka A, Landau G, Bar-Ilan A, Lichtenstein RG, Campbell KS, van Kuppevelt TH, Porgador A. Characterization of the recognition of tumor cells by the natural cytotoxicity receptor, NKp44. *Biochemistry (Mosc)* (2007) **46**:7426–7436. doi:10.1021/bi7000455
144. Groh V, Wu J, Yee C, Spies T. Tumour-derived soluble MIC ligands impair expression of NKG2D and T-cell activation. *Nature* (2002) **419**:734–738. doi:10.1038/nature01112
145. Kaiser BK, Yim D, Chow I-T, Gonzalez S, Dai Z, Mann HH, Strong RK, Groh V, Spies T. Disulphide-isomerase-enabled shedding of tumour-associated NKG2D ligands. *Nature* (2007) **447**:482–486. doi:10.1038/nature05768
146. Waldhauer I, Goehlsdorf D, Gieseke F, Weinschenk T, Wittenbrink M, Ludwig A, Stevanovic S, Rammensee H-G, Steinle A. Tumor-associated MICA is shed by ADAM proteases. *Cancer Res* (2008) **68**:6368–6376. doi:10.1158/0008-5472.CAN-07-6768
147. Fernández-Messina L, Ashiru O, Boutet P, Agüera-González S, Skepper JN, Reyburn HT, Valés-Gómez M. Differential mechanisms of shedding of the glycosylphosphatidylinositol (GPI)-anchored NKG2D ligands. *J Biol Chem* (2010) **285**:8543–8551. doi:10.1074/jbc.M109.045906
148. López-Cobo S, Campos-Silva C, Valés-Gómez M. Glycosyl-Phosphatidyl-Inositol (GPI)-Anchors and Metalloproteases: Their Roles in the Regulation of Exosome Composition and NKG2D-Mediated Immune Recognition. *Front Cell Dev Biol* (2016) **4**:97. doi:10.3389/fcell.2016.00097
149. Koike S, Horie H, Ise I, Okitsu A, Yoshida M, Iizuka N, Takeuchi K, Takegami T, Nomoto A. The poliovirus receptor protein is produced both as membrane-bound and secreted forms. *EMBO J* (1990) **9**:3217–3224.
150. Baury B, Masson D, McDermott BM, Jarry A, Blottière HM, Blanchardie P, Laboisse CL, Lustenberger P, Racaniello VR, Denis MG. Identification of secreted CD155 isoforms. *Biochem Biophys Res Commun* (2003) **309**:175–182.
151. Iguchi-Manaka A, Okumura G, Kojima H, Cho Y, Hirochika R, Bando H, Sato T, Yoshikawa H, Hara H, Shibuya A, et al. Increased Soluble CD155 in the Serum of Cancer Patients. *PloS One* (2016) **11**:e0152982. doi:10.1371/journal.pone.0152982
152. Reiners KS, Topolar D, Henke A, Simhadri VR, Kessler J, Sauer M, Bessler M, Hansen HP, Tawadros S, Herling M, et al. Soluble ligands for NK cell receptors promote evasion of chronic lymphocytic leukemia cells from NK cell anti-tumor activity. *Blood* (2013) **121**:3658–3665. doi:10.1182/blood-2013-01-476606
153. Pesce S, Tabellini G, Cantoni C, Patrizi O, Coltrini D, Rampinelli F, Matta J, Vivier E, Moretta A, Parolini S, et al. B7-H6-mediated downregulation of NKp30 in NK cells contributes to ovarian

carcinoma immune escape. *Oncoimmunology* (2015) **4**:e1001224. doi:10.1080/2162402X.2014.1001224

154. Zingoni A, Fionda C, Borrelli C, Cippitelli M, Santoni A, Soriani A. Natural Killer Cell Response to Chemotherapy-Stressed Cancer Cells: Role in Tumor Immunosurveillance. *Front Immunol* (2017) **8**: doi:10.3389/fimmu.2017.01194
155. Malmberg K-J, Carlsten M, Björklund A, Sohlberg E, Bryceson YT, Ljunggren H-G. Natural killer cell-mediated immunosurveillance of human cancer. *Semin Immunol* (2017) **31**:20–29. doi:10.1016/j.smim.2017.08.002
156. Locatelli F, Pende D, Mingari MC, Bertaina A, Falco M, Moretta A, Moretta L. Cellular and molecular basis of haploidentical hematopoietic stem cell transplantation in the successful treatment of high-risk leukemias: role of alloreactive NK cells. *Front Immunol* (2013) **4**: doi:10.3389/fimmu.2013.00015
157. Knorr DA, Bachanova V, Verneris MR, Miller JS. Clinical utility of natural killer cells in cancer therapy and transplantation. *Semin Immunol* (2014) **26**:161–172. doi:10.1016/j.smim.2014.02.002
158. Mancusi A, Ruggeri L, Velardi A. Haploidentical hematopoietic transplantation for the cure of leukemia: from its biology to clinical translation. *Blood* (2016) **128**:2616–2623. doi:10.1182/blood-2016-07-730564
159. Simonetta F, Alvarez M, Negrin RS. Natural Killer Cells in Graft-versus-Host-Disease after Allogeneic Hematopoietic Cell Transplantation. *Front Immunol* (2017) **8**: doi:10.3389/fimmu.2017.00465
160. Rezvani K, Rouce RH. The Application of Natural Killer Cell Immunotherapy for the Treatment of Cancer. *Front Immunol* (2015) **6**: doi:10.3389/fimmu.2015.00578
161. Thielens A, Vivier E, Romagné F. NK cell MHC class I specific receptors (KIR): from biology to clinical intervention. *Curr Opin Immunol* (2012) **24**:239–245. doi:10.1016/j.coi.2012.01.001
162. Stojanovic A, Correia MP, Cerwenka A. Shaping of NK cell responses by the tumor microenvironment. *Cancer Microenviron Off J Int Cancer Microenviron Soc* (2013) **6**:135–146. doi:10.1007/s12307-012-0125-8
163. Baginska J, Viry E, Paggetti J, Medves S, Berchem G, Moussay E, Janji B. The Critical Role of the Tumor Microenvironment in Shaping Natural Killer Cell-Mediated Anti-Tumor Immunity. *Front Immunol* (2013) **4**: doi:10.3389/fimmu.2013.00490
164. Vitale M, Cantoni C, Pietra G, Mingari MC, Moretta L. Effect of tumor cells and tumor microenvironment on NK-cell function. *Eur J Immunol* (2014) **44**:1582–1592. doi:10.1002/eji.201344272
165. Poggi A, Varesano S, Zocchi MR. How to Hit Mesenchymal Stromal Cells and Make the Tumor Microenvironment Immunostimulant Rather Than Immunosuppressive. *Front Immunol* (2018) **9**:262. doi:10.3389/fimmu.2018.00262
166. Rouas-Freiss N, Moreau P, LeMaoult J, Carosella ED. The dual role of HLA-G in cancer. *J Immunol Res* (2014) **2014**:359748. doi:10.1155/2014/359748
167. Marcenaro E, Della Chiesa M, Bellora F, Parolini S, Millo R, Moretta L, Moretta A. IL-12 or IL-4 prime human NK cells to mediate functionally divergent interactions with dendritic cells or tumors. *J Immunol Baltim Md 1950* (2005) **174**:3992–3998.
168. Semeraro M, Rusakiewicz S, Minard-Colin V, Delahaye NF, Enot D, Vély F, Marabelle A, Papoular B, Piperoglou C, Ponzoni M, et al. Clinical impact of the NKp30/B7-H6 axis in high-risk neuroblastoma patients. *Sci Transl Med* (2015) **7**:283ra55. doi:10.1126/scitranslmed.aaa2327
169. Shemesh A, Brusilovsky M, Hadad U, Teltsh O, Edri A, Rubin E, Campbell KS, Rosental B, Porgador A, Shemesh A, et al. Survival in acute myeloid leukemia is associated with NKp44 splice variants. *Oncotarget* (2016) **7**:32933–32945. doi:10.18632/oncotarget.8782
170. Yáñez-Mó M, Siljander PR-M, Andreu Z, Zavec AB, Borràs FE, Buzas EI, Buzas K, Casal E, Cappello F, Carvalho J, et al. Biological properties of extracellular vesicles and their physiological functions. *J Extracell Vesicles* (2015) **4**:27066.

171. Greening DW, Xu R, Gopal SK, Rai A, Simpson RJ. Proteomic insights into extracellular vesicle biology - defining exosomes and shed microvesicles. *Expert Rev Proteomics* (2017) **14**:69–95. doi:10.1080/14789450.2017.1260450
172. Chen W, Jiang J, Xia W, Huang J. Tumor-Related Exosomes Contribute to Tumor-Promoting Microenvironment: An Immunological Perspective. *J Immunol Res* (2017) **2017**:1073947. doi:10.1155/2017/1073947
173. Balsamo M, Manzini C, Pietra G, Raggi F, Blengio F, Mingari MC, Varesio L, Moretta L, Bosco MC, Vitale M. Hypoxia downregulates the expression of activating receptors involved in NK-cell-mediated target cell killing without affecting ADCC. *Eur J Immunol* (2013) **43**:2756–2764. doi:10.1002/eji.201343448
174. Hasmim M, Messai Y, Ziani L, Thiery J, Bouhris J-H, Noman MZ, Chouaib S. Critical Role of Tumor Microenvironment in Shaping NK Cell Functions: Implication of Hypoxic Stress. *Front Immunol* (2015) **6**: doi:10.3389/fimmu.2015.00482
175. Olsen DR, Nagayoshi T, Fazio M, Mattei MG, Passage E, Weil D, Timpl R, Chu ML, Uitto J. Human nidogen: cDNA cloning, cellular expression, and mapping of the gene to chromosome Iq43. *Am J Hum Genet* (1989) **44**:876–885.
176. Ho MSP, Böse K, Mokkapati S, Nischt R, Smyth N. Nidogens-Extracellular matrix linker molecules. *Microsc Res Tech* (2008) **71**:387–395. doi:10.1002/jemt.20567
177. Nagayoshi T, Sanborn D, Hickok NJ, Olsen DR, Fazio MJ, Chu ML, Knowlton R, Mann K, Deutzmann R, Timpl R. Human nidogen: complete amino acid sequence and structural domains deduced from cDNAs, and evidence for polymorphism of the gene. *DNA Mary Ann Liebert Inc* (1989) **8**:581–594. doi:10.1089/dna.1989.8.581
178. Dedhar S, Jewell K, Rojiani M, Gray V. The receptor for the basement membrane glycoprotein entactin is the integrin alpha 3/beta 1. *J Biol Chem* (1992) **267**:18908–18914.
179. Senior RM, Gresham HD, Griffin GL, Brown EJ, Chung AE. Entactin stimulates neutrophil adhesion and chemotaxis through interactions between its Arg-Gly-Asp (RGD) domain and the leukocyte response integrin. *J Clin Invest* (1992) **90**:2251–2257. doi:10.1172/JCI116111
180. Yelian FD, Edgeworth NA, Dong LJ, Chung AE, Armant DR. Recombinant entactin promotes mouse primary trophoblast cell adhesion and migration through the Arg-Gly-Asp (RGD) recognition sequence. *J Cell Biol* (1993) **121**:923–929.
181. Dong LJ, Hsieh JC, Chung AE. Two distinct cell attachment sites in entactin are revealed by amino acid substitutions and deletion of the RGD sequence in the cysteine-rich epidermal growth factor repeat 2. *J Biol Chem* (1995) **270**:15838–15843.
182. Yang Y, Todt JC, Svinarich DM, Qureshi F, Jacques SM, Graham CH, Chung AE, Gonik B, Yelian FD. Human trophoblast cell adhesion to extracellular matrix protein, entactin. *Am J Reprod Immunol N Y N 1989* (1996) **36**:25–32.
183. Gresham HD, Graham IL, Griffin GL, Hsieh JC, Dong LJ, Chung AE, Senior RM. Domain-specific interactions between entactin and neutrophil integrins. G2 domain ligation of integrin alpha3beta1 and E domain ligation of the leukocyte response integrin signal for different responses. *J Biol Chem* (1996) **271**:30587–30594.
184. Kim S, Wadsworth WG. Positioning of longitudinal nerves in C. elegans by nidogen. *Science* (2000) **288**:150–154.
185. Lee HK, Seo IA, Park HK, Park YM, Ahn KJ, Yoo YH, Park HT. Nidogen is a prosurvival and promigratory factor for adult Schwann cells. *J Neurochem* (2007) **102**:686–698. doi:10.1111/j.1471-4159.2007.04580.x
186. Fox JW, Mayer U, Nischt R, Aumailley M, Reinhardt D, Wiedemann H, Mann K, Timpl R, Krieg T, Engel J. Recombinant nidogen consists of three globular domains and mediates binding of laminin to collagen type IV. *EMBO J* (1991) **10**:3137–3146.
187. Reinhardt D, Mann K, Nischt R, Fox JW, Chu ML, Krieg T, Timpl R. Mapping of nidogen binding sites for collagen type IV, heparan sulfate proteoglycan, and zinc. *J Biol Chem* (1993) **268**:10881–10887.

188. Lee HK, Seo IA, Park HK, Park HT. Identification of the basement membrane protein nidogen as a candidate ligand for tumor endothelial marker 7 in vitro and in vivo. *FEBS Lett* (2006) **580**:2253–2257. doi:10.1016/j.febslet.2006.03.033
189. Mayer U, Mann K, Timpl R, Murphy G. Sites of nidogen cleavage by proteases involved in tissue homeostasis and remodelling. *Eur J Biochem* (1993) **217**:877–884.
190. Sage J, Leblanc-Noblesse E, Nizard C, Sasaki T, Schnebert S, Perrier E, Kurfurst R, Brömme D, Lalmanach G, Lecaille F. Cleavage of nidogen-1 by cathepsin S impairs its binding to basement membrane partners. *PloS One* (2012) **7**:e43494. doi:10.1371/journal.pone.0043494
191. Willumsen N, Bager CL, Leeming DJ, Bay-Jensen A-C, Karsdal MA. Nidogen-1 Degraded by Cathepsin S can be Quantified in Serum and is Associated with Non-Small Cell Lung Cancer. *Neoplasia N Y N* (2017) **19**:271–278. doi:10.1016/j.neo.2017.01.008
192. Titz B, Dietrich S, Sadowski T, Beck C, Petersen A, Sedlacek R. Activity of MMP-19 inhibits capillary-like formation due to processing of nidogen-1. *Cell Mol Life Sci CMLS* (2004) **61**:1826–1833. doi:10.1007/s00018-004-4105-0
193. Martino-Echarri E, Fernández-Rodríguez R, Rodríguez-Baena FJ, Barrientos-Durán A, Torres-Collado AX, Plaza-Calonge M del C, Amador-Cubero S, Cortés J, Reynolds LE, Hodivala-Dilke KM, et al. Contribution of ADAMTS1 as a tumor suppressor gene in human breast carcinoma. Linking its tumor inhibitory properties to its proteolytic activity on nidogen-1 and nidogen-2. *Int J Cancer* (2013) **133**:2315–2324. doi:10.1002/ijc.28271
194. Gonzales PA, Pisitkun T, Hoffert JD, Tchapyjnikov D, Star RA, Kleta R, Wang NS, Knepper MA. Large-scale proteomics and phosphoproteomics of urinary exosomes. *J Am Soc Nephrol JASN* (2009) **20**:363–379. doi:10.1681/ASN.2008040406
195. Zhang Y, Xu B, Liu Y, Yao H, Lu N, Li B, Gao J, Guo S, Han N, Qi J, et al. The ovarian cancer-derived secretory/releasing proteome: A repertoire of tumor markers. *Proteomics* (2012) **12**:1883–1891. doi:10.1002/pmic.201100654
196. Lai RC, Yeo RWY, Tan SS, Zhang B, Yin Y, Sze NSK, Choo A, Lim SK. "Mesenchymal Stem Cell Exosomes: The Future MSC-Based Therapy?," in *Mesenchymal Stem Cell Therapy* Stem Cell Biology and Regenerative Medicine. (Humana Press, Totowa, NJ), 39–61. doi:10.1007/978-1-62703-200-1_3
197. Lazar I, Clement E, Ducoux-Petit M, Denat L, Soldan V, Dauvillier S, Balor S, Burlet-Schiltz O, Larue L, Muller C, et al. Proteome characterization of melanoma exosomes reveals a specific signature for metastatic cell lines. *Pigment Cell Melanoma Res* (2015) **28**:464–475. doi:10.1111/pcmr.12380
198. Chan Y-K, Zhang H, Liu P, Tsao S-W, Lung ML, Mak N-K, Ngok-Shun Wong R, Ying-Kit Yue P. Proteomic analysis of exosomes from nasopharyngeal carcinoma cell identifies intercellular transfer of angiogenic proteins. *Int J Cancer* (2015) **137**:1830–1841. doi:10.1002/ijc.29562
199. Li L, Zhang Y, Li N, Feng L, Yao H, Zhang R, Li B, Li X, Han N, Gao Y, et al. Nidogen-1: a candidate biomarker for ovarian serous cancer. *Jpn J Clin Oncol* (2015) **45**:176–182. doi:10.1093/jjco/hyu187
200. Alečković M, Wei Y, LeRoy G, Sidoli S, Liu DD, Garcia BA, Kang Y. Identification of Nidogen 1 as a lung metastasis protein through secretome analysis. *Genes Dev* (2017) **31**:1439–1455. doi:10.1101/gad.301937.117
201. Zhou Y, Zhu Y, Fan X, Zhang C, Wang Y, Zhang L, Zhang H, Wen T, Zhang K, Huo X, et al. NID1, a new regulator of EMT required for metastasis and chemoresistance of ovarian cancer cells. *Oncotarget* (2017) **8**:33110–33121. doi:10.18632/oncotarget.16145
202. Ulazzi L, Sabbioni S, Miotto E, Veronese A, Angusti A, Gafà R, Manfredini S, Farinati F, Sasaki T, Lanza G, et al. Nidogen 1 and 2 gene promoters are aberrantly methylated in human gastrointestinal cancer. *Mol Cancer* (2007) **6**:17. doi:10.1186/1476-4598-6-17
203. Pedrola N, Devis L, Llauradó M, Campoy I, Martinez-Garcia E, Garcia M, Muinelo-Romay L, Alonso-Alconada L, Abal M, Alameda F, et al. Nidogen 1 and Nuclear Protein 1: novel targets of ETV5 transcription factor involved in endometrial cancer invasion. *Clin Exp Metastasis* (2015) **32**:467–478. doi:10.1007/s10585-015-9720-7

204. Darbro BW, Mahajan VB, Gakhar L, Skeie JM, Campbell E, Wu S, Bing X, Millen KJ, Dobyns WB, Kessler JA, et al. Mutations in extracellular matrix genes NID1 and LAMC1 cause autosomal dominant Dandy-Walker malformation and occipital cephaloceles. *Hum Mutat* (2013) **34**:1075–1079. doi:10.1002/humu.22351
205. Kruegel J, Sadowski B, Miosge N. Nidogen-1 and nidogen-2 in healthy human cartilage and in late-stage osteoarthritis cartilage. *Arthritis Rheum* (2008) **58**:1422–1432. doi:10.1002/art.23480
206. Zhu D, Xie H, Li H, Cai P, Zhu H, Xu C, Chen P, Sharan A, Xia Y, Tang W. Nidogen-1 is a common target of microRNAs MiR-192/215 in the pathogenesis of Hirschsprung's disease. *J Neurochem* (2015) **134**:39–46. doi:10.1111/jnc.13118
207. Bruschi M, Musante L, Candiano G, Ghiggeri GM, Herbert B, Antonucci F, Righetti PG. Soft immobilized pH gradient gels in proteome analysis: a follow-up. *Proteomics* (2003) **3**:821–825. doi:10.1002/pmic.200300361
208. Candiano G, Bruschi M, Musante L, Santucci L, Ghiggeri GM, Carnemolla B, Orecchia P, Zardi L, Righetti PG. Blue silver: a very sensitive colloidal Coomassie G-250 staining for proteome analysis. *Electrophoresis* (2004) **25**:1327–1333. doi:10.1002/elps.200305844
209. Kulak NA, Pichler G, Paron I, Nagaraj N, Mann M. Minimal, encapsulated proteomic-sample processing applied to copy-number estimation in eukaryotic cells. *Nat Methods* (2014) **11**:319–324. doi:10.1038/nmeth.2834
210. Cox J, Mann M. MaxQuant enables high peptide identification rates, individualized p.p.b.-range mass accuracies and proteome-wide protein quantification. *Nat Biotechnol* (2008) **26**:1367–1372. doi:10.1038/nbt.1511
211. Benton G, Kleinman HK, George J, Arnaoutova I. Multiple uses of basement membrane-like matrix (BME/Matrigel) in vitro and in vivo with cancer cells. *Int J Cancer* (2011) **128**:1751–1757. doi:10.1002/ijc.25781
212. Labani-Motlagh A, Israelsson P, Ottander U, Lundin E, Nagaev I, Nagaeva O, Dehlin E, Baranov V, Mincheva-Nilsson L. Differential expression of ligands for NKG2D and DNAM-1 receptors by epithelial ovarian cancer-derived exosomes and its influence on NK cell cytotoxicity. *Tumour Biol J Int Soc Oncodevelopmental Biol Med* (2016) **37**:5455–5466. doi:10.1007/s13277-015-4313-2
213. Nandakumar V, Chou Y, Zang L, Huang XF, Chen S-Y. Epigenetic control of natural killer cell maturation by histone H2A deubiquitinase, MYSM1. *Proc Natl Acad Sci U S A* (2013) **110**:E3927-3936. doi:10.1073/pnas.1308888110
214. Alsultan A, Shamseldin HE, Osman ME, Aljabri M, Alkuraya FS. MYSM1 is mutated in a family with transient transfusion-dependent anemia, mild thrombocytopenia, and low NK- and B-cell counts. *Blood* (2013) **122**:3844–3845. doi:10.1182/blood-2013-09-527127
215. Montaldo E, Zotto GD, Chiesa MD, Mingari MC, Moretta A, Maria AD, Moretta L. Human NK cell receptors/markers: A tool to analyze NK cell development, subsets and function. *Cytometry A* (2013) **83A**:702–713. doi:10.1002/cyto.a.22302
216. Carrega P, Loiacono F, Di Carlo E, Scaramuccia A, Mora M, Conte R, Benelli R, Spaggiari GM, Cantoni C, Campana S, et al. NCR(+)ILC3 concentrate in human lung cancer and associate with intratumoral lymphoid structures. *Nat Commun* (2015) **6**:8280. doi:10.1038/ncomms9280

7. ACKNOWLEDGMENTS

I would like to thank my supervisor Prof. Claudia Cantoni for her invaluable help and the head of Laboratorio di Immunologia Clinica e Sperimentale (Ist. Gaslini, Genoa) Prof. Cristina Bottino. I also would like to thank all the people who worked on this project: most of the data described in this thesis are in press in Oncoimmunology (Nidogen-1 is a novel extracellular ligand for the NKp44 natural cytotoxicity receptor. Gaggero, S., Bruschi, M., Petretto, A., Parodi, M., Del Zotto, G., Lavarello, C., Prato, C., Santucci, L., Barbuto, A., Bottino, C., Candiano, G., Moretta, A., Vitale, M., Moretta, L., Cantoni, C.).